Institut für Biochemie und Biologie

Functional characterisation of NIC2, a member of the MATE family from *Arabidopsis thaliana* (L.) Heynh.

Dissertation
zur Erlangung des akademischen Grades
"doctor rerum naturalium"
(Dr. rer. nat.)
in der Wissenschaftsdisziplin "Molekularbiologie"

eingereicht an der
Mathematisch-Naturwissenschaftlichen Fakultät
der Universität Potsdam

von
Blazej Dolniak

Potsdam, den 28.02.2005.

najblizszym mi osobom

Abbreviations

2,4-D	2,4- dichlorophenoxyacetic acid
A	adenine
aa	amino acid residue
A. thaliana	*Arabidopsis thaliana*
ATP	adenosine triphosphate
A. tumefaciens	*Agrobacterium tumefaciens*
BASTA	gluphosinate ammonium
bp	base pair
C	cytosine
cRNA	complementary RNA
DAG	day after germination
cDNA	complementary DNA
DNA	deoxyribonucleic acid
dsRED	Red Fluorescent Protein
E. coli	*Escherichia coli*
EST	expressed sequence tag
F-IAA	5-fluoro-indole-3-acetic acid
Fig.	Figure
g	gravitropic stimulus
G	guanine
GFP	Green Fluorescence Protein
GUS	β-glucuronidase gene
h	hour
IAA	indole-3-acetic acid
IBA	indole-3-butyric acid
IPTG	isopropyl-ß-D-thiogalaktopyranosid
MATE	multidrug and toxic compounds extrusion family
MICs	minimum inhibitory concentrations
min	minutes
NAA	naphthalene-1-acetic acid
NIC	Novel Ion Carrier family
OD	optical density
PCR	polymerase chain reaction
PEG	polyethylenglykole
Real time RT-PCR	real time reverse transcriptase PCR
RNA	ribonucleic acid
RNAi	RNA interference
S. cerevisiae	*Saccharomyces cerevisiae*
sec	second
SDS	sodium dodecylsulfate
ssDNA	salmon sperm DNA
T	thymine
$T_{1/2}$	time required to reach half-maximal optical density
TEACl	Tetraethylammonium chloride
TMACl	Tetramethylammonium chloride
U	uracile
UTR	untranslated region
WT	wild-type
X. laevis	*Xenopus laevis*

According to the instructions for authors from the Plant Cell (http://www.plantcell.org/misc/ifora.shtml) the names of genes are written using italic type of capital letters, e.g *NIC2*, the names of proteins are written using capital letters, e.g NIC2, and the mutant strains and mutant lines using italic type of small letters, e.g *erc1* or *axr1*.

Introduction

Living organisms synthesise and accumulate a diverse range of natural products, which can have many functions, including defense or attraction to various insects and microbes in their environment. On the other hand, they have also developed various ways to resist the exogenous toxin effects, including toxic compounds secreted by other organisms or pathogenic microbes. Disposal and detoxification of toxic compounds of both endogenous and exogenous origin are very important processes for organism survival and development. There are several possible mechanisms of detoxification. They incude the modification of toxic compounds by endogenous enzymes (Davies, 1994; Dixon *et al*., 1998), target alteration (Weisblum, 1995), inhibition of toxin entry into the cell (Nikaido and Vaara, 1985; Nikaido, 1989) as well as sequestration into the vacuole (Yelin *et al*., 1999; Liu *et al*., 2000) and efflux, that is transport outside of the cell (Putman *et al*., 2000; Zgurskaya and Nikaido, 2000).

1. The Multidrug efflux pumps

The transmembrane-protein-catalysed extrusion of noxious compounds from the cell is one of the most frequently used strategies for resistance to cytotoxic drugs in both prokaryotes and eukaryotes. These efflux proteins act like pumps (**Fig. 1**), reducing the intracellular concentration of an enormous number of various, hydrophobic endogenous or exogenous compounds to subtoxic level (Borges-Walmsley and Walmsley, 2001; Borges-Walmsley *et al*., 2003).

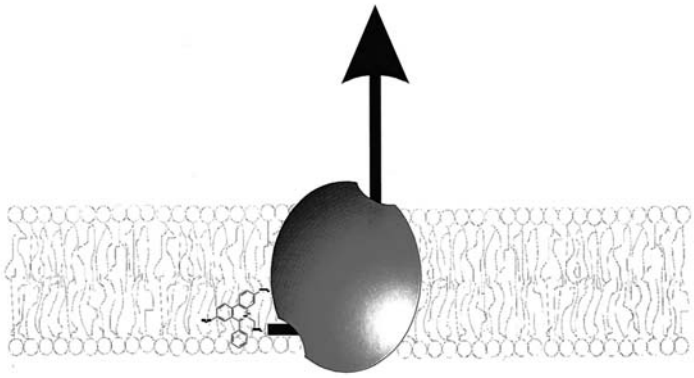

Figure 1. Schematic representation of hydrophobic compounds extrusion by multidrug efflux pumps. Cytotoxic compounds are expelled from the cytoplasmic leaflet of the membrane to the external medium (adapted from Putman *et al*., 2000).

Extensive analyses of the genome of both prokaryotic and eukaryotic organisms revealed that membrane transport proteins which mediate the efflux fall into two major classes (http://www.membranetransport.org): **a**denosine **t**ri**p**hosphate (**ATP**) binding cassette (ABC) transporters (**Fig. 2*A***) that couple the hydrolysis of ATP to substrate transport across the cell membrane, and secondary transporters (**Fig. 2*B***), which use chemiosmotic gradients to facilitate an antiporter mechanism (Higgins, 1992; Paulsen *et al.*, 2002).

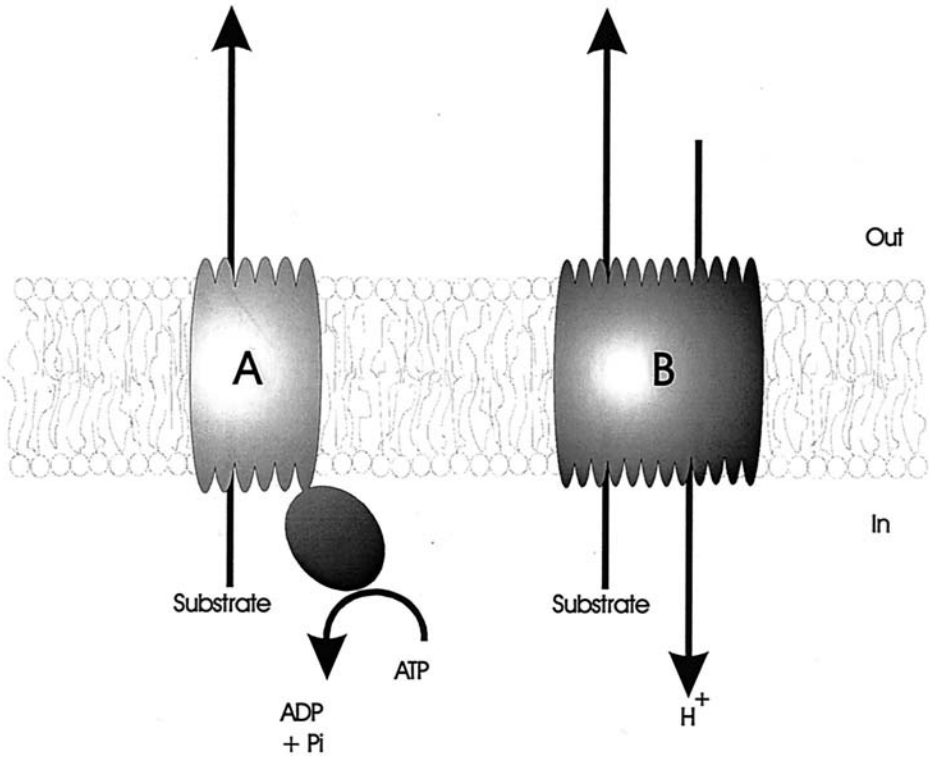

Figure 2. Schematic representation of the two major classes of multidrug transporters. *A*, ABC-type multidrug transporters utilize the free energy of ATP hydrolysis to pump drugs out of the cell. ***B***, Secondary multidrug transporters mediate the extrusion of structurally unrelated drugs in a coupled exchange with proton ions (adapted from Putman *et al.*, 2000).

The ABC superfamily, present in prokaryotic as well as eukaryotic organisms, is a very large, ancient family of ATP-dependent transporters. The general structure of an ABC transporter usually consists of the following components: two integral membrane domains each having six putative transmembrane α-helices, two peripheral domains that bind and hydrolyse ATP, and one periplasmic (or lipoprotein) substrate-binding domain. The ATP-binding domain component is the most conserved, the transmembrane region is less conserved, and the substrate-binding component is most divergent (Tam and Saier 1993; Saurin and Dassa

1994). ATP-dependent transporters include uptake and efflux systems for a range of substrates including drugs, sugars, amino acids, carboxylates, metal ions, peptides, and others (Paulsen *et al*., 2002).

The second group of mutlidrug efflux system, secondary transporters, is sensitive to agents that dissipate the proton motive force (PMF), indicating that they mediate the extrusion of toxic compounds from the cells in a coupled exchange with protons (Paulsen *et al*., 1996 and 2002). On the basis of size and similarities in the primary and secondary structure, these transporters are devided into several distinct families; the major facilitator superfamily (MSF) (Pao *et al*., 1998; Saier *et al*., 2000), the small multidrug resistance (SMR) family (Paulsen *et al*., 1996; Chung and Saier, 2001), the resistance-nodulation-cell division (RND) family (Saier *et al*., 1994; Tseng *et al*., 1999), and the multidrug endosomal transporter (MET) family (Hogue *et al*., 1999). The MFS is an evolutionary old, large and diverse superfamily that includes over a thousand sequenced members found ubiquitously in all three kingdoms of living organisms. These 12-14 transmembrane transporters are single-polypeptide secondary carriers, which are capable only of transporting small solutes in response to chemiosmotic ion gradients. Using uniport, symport or antiport mechnisms, they can transport sugars, polyols, drugs, neurotransmitters, Krebs cycle metabolites, phosphorylated glycolytic intermediates, amino acids, peptides, osmolites, iron-siderophores, nucleosides, organic anions and inorganic anions (Pao *et al*., 1998; Paulsen *et al*., 2002). Multidrug transporters of the SMR and the RND families consist only of bacterial proteins. The SMR family includes carriers with only four transmembane domains, which transport sugars, purines and other metabolites (Paulsen *et al*., 1996; Chung and Saier, 2001), whereas to the RND family belong to 12 transmembrane transporters, which encompass efflux systems for drugs, metal ions, lipooligosaccharides, proteins and glycolipids (Tseng *et al*., 1999). Interestingly, some members of the bacterial ABC, MSF and RND families function additionally with accessory proteins belonging to the membrane fusion protein (MFP) and outer membrane factor (OMF) families to enable efflux across both membranes of the Gram-negative bacterial cell envelope (Dinh *et al*., 1994). Members of the MET family are exclusively found in animals,

typically located in late endosomal, Golgi and lysosomal membranes, and have four transmembrane domains. The only characterised protein, the mouse MTP, is able to transport a wide range of various compounds, like thymidine, nucleobase and nuclosides analogues, antibiotics, anthracyclines, ionophores and steroid hormones into intracellular compartments (Hogue *et al*., 1999).

Although proton-driven uniport, symport or antiport are the major mechnisms of drug efflux in secondary transporters, other important mechanisms have recently been described (Brown *et al*., 1999). This novel group of transport proteins share the common theme, that multidrug and toxin efflux is coupled to Na^+ influx (Morita *et al.*, 1998 and 2000).

2. Multidrug and toxic compounds extrusion family

The extistance of a new energy-dependent efflux system, designated as NORM, in cells of *Vibrio parahaemolyticus* was found during Norfloxacin accumulation experiments (Morita *et al.*, 1998). NORM and its homologue from *Escherichia coli*, YDHE/NORE, mediate the efflux of dyes, hydrophilic fluoroquinolones and aminoglycosides. Based on hydrophobicity plots which revealed that NORM and YDHE/NORE possess 12 transmembrane spaning regions, the proteins were initially classified to be membres of the MFS. Brown *et al*. (1999), however, demonstrated that neither NORM nor YDHE/NORE shared significant sequence similiarities with any member of the MFS. They found that both proteins were members of a previoulsy unidentified family which contained more than 30 proteins, including represenatives from three kingdoms of life (Eukarya, Archaea and Eubacteria). Phylogenetic analysis of this family revealed the presence of three distinct clusters. The first cluster included bacterial NORM, YDHE/NORE and hypothetical proteins from *Haemophilus*, *Bacillus* and *Synechocystis*. The constituents of the second cluster were exclusively eukaryotic proteins with one functionally characterised protein from *Saccharomyces cerevisiae*, ERC1 (Shiomi *et al*., 1991). The third cluster included the DINF proteins from *Escherichia coli* and *Streptococcus pneumoniae*, which functions are still unknown. Based on the extensive phylogenetic studies with NORM as a prototype, the new family was established and termed

the multidrug and toxic compounds extrusion (MATE) family (Brown *et al*., 1999). Currently, the MATE family contains 203 sequenced genes and most of the members are about 450-550 amino acid residues in length and possess 12 putative transmembrane spaning regions (**Fig. 3**). The yeast proteins are, however, larger, with up to 700 amino acid residues, whereas the archaeal proteins are generally smaller (Hvorup *et al.*, 2003).

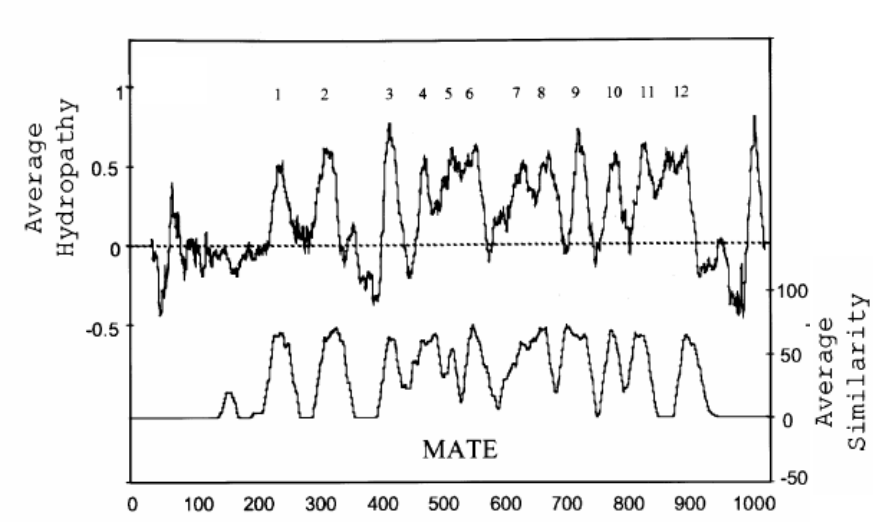

Figure 3. Avarage hydropathy plot (top) and avarage similarity plot (bottom) for the MATE family. The numbers above the hydropathy plot indicate the numbers of the putative transmembrane spaning regions (adapted from Hvorup *et al*., 2003).

To date, only very few proteins of the MATE family were functionally characterised. These proteins include examples from bacteria, yeast and plants.

2.1. Bacterial multidrug and toxic compound extrusion family

According to the name of the family, the MATE proteins function in bacterial cells as multidrug efflux pumps which cause multidrug resistance, a serious clinical problem. These proteins mediate the resistance to a wide range of cationic dyes, fluoroquinolones, aminoglycosides and other structurally diverse antibiotics and drugs (**Tab. 1**). While cationic dyes are generally amphipathic and positively charged, aminoglycosides are strongly hydrophobic, and Norfloxacin, the most common substrate for the MATE proteins, is amphiphilic. Thus, the bacterial MATE family transporter substrates seem to be very diverse in nature (Hvorup *et al*., 2003).

Table 1. Functionally characterised members of the bacterial MATE family

Organism	Gene name	Substrates (drug class)	References
Vibrio parahaemolyticus	*NORM*	Norfloxacin[a], Ciprofloxacin[a], Ethidium bromide, Berberine, Kanamycin[b]	Morita *et al*., 1998, 2000
	VMRA	Acriflavine, Ethidium bromide, DAPI, TPPCl	Chen *et al*., 2002
Escherichia coli	*YDHE/NORE*	Norfloxacin, Ciprofloxacin, Acriflavine, Berberine	Morita *et al*., 1998, 2000
Vibrio cholerae non-O1	*VCMA*	Norfloxacin, Ciprofloxacin, Ethidium bromide, Acriflavine, Kanamycin, Streptomycin[b]	Huda *et al*., 2001
Bacteroides thetaiotaomicron	*BEXA*	Norfloxacin, Ciprofloxacin, Ethidium bromide	Miyamae *et al*., 2001
Brucella melitensis	*NORMI*	Norfloxacin, Ciprofloxacin, Acriflavine, Berberine	Braibant *et al*., 2002
Pseudomonas aeruginosa	*PMPM*	Norfloxacin, Ciprofloxacin, Ethidium bromide, Acriflavine	He *et al*., 2004

[a] Quinolones and fluoroquinolones; [b] aminoglycosides

The first evidence which highlighted the extrusion mechanism used by the proteins of the MATE family was given by Morita *et al*. (2000). The prototype of the MATE family, NORM multidrug efflux protein from *Vibrio parahaemolyticus*, has been shown to function as an antiporter by a Na^+/drug mechanism (**Fig. 4**). The antiport mediated by NORM exhibited an influx of Ethidium bromide, one of its substrates, which was elicited by an efflux of Na^+ from the bacterial cells. YDHE/NORE (Morita *et al.*, 2000), VCMA (Huda *et al.*, 2001), and VMRA (Chen *et al.*, 2002) were also characterised as Na^+/drug antiporters and other proteins, BEXA (Miyamae *et al.*, 2001) and NORMI (Braibant *et al.*, 2002), may also function by Na^+/drug antiport mechanism. In this sense, the mechanism in the bacterial MATE family seemed to be ubiquitous and rather unique, because these pumps utilised an electrochemical potential of Na^+ across the cytoplasmic membrane as driving force. Recently, He *at al*. (2004) reported a multidrug efflux pump, PMPM, from *Pseudomonas aeruginosa* which belonged to the MATE family and utilised H^+, but not Na^+, as the coupling ion for drug extrusion (**Fig. 4**). This

evidence clearly showed that more than one multidrug extrusion mechanism exist in bacterial cells.

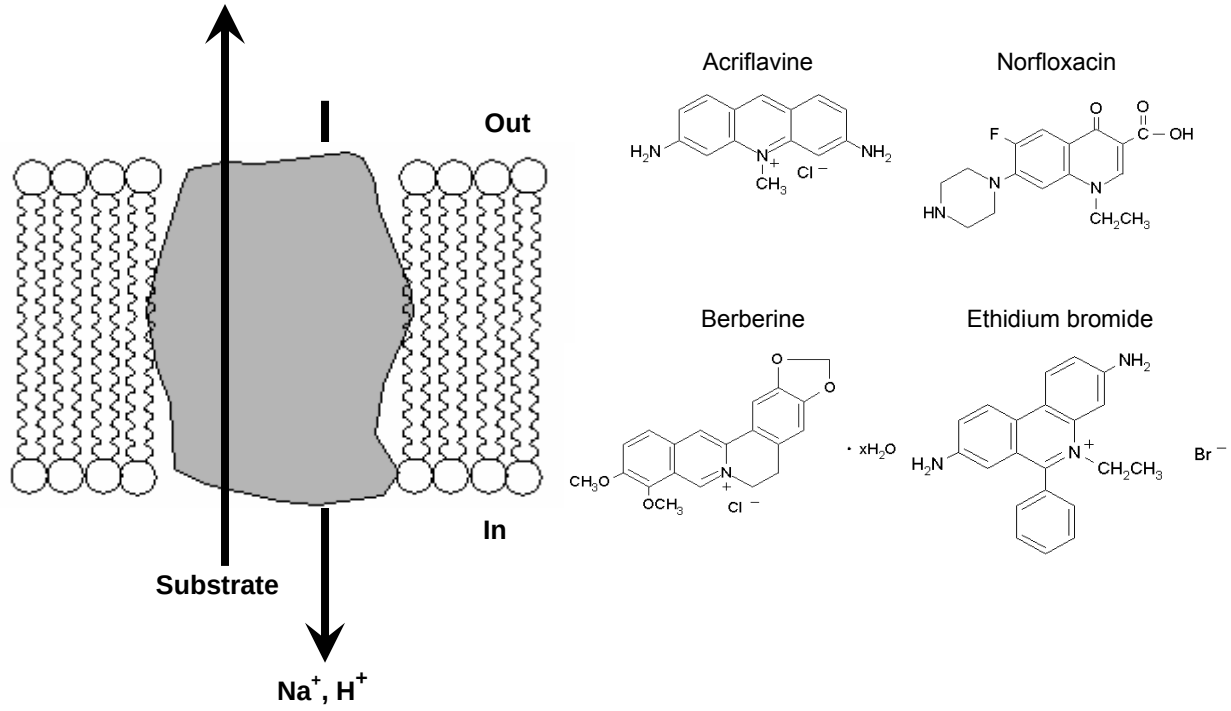

Figure 4. Putative transport reaction catalyzed by proteins of the bacterial MATE family. The prototype of the MATE family, NORM, and possibly other proteins of the bacterial MATE family function by a substrate:Na^+or a substrate:H^+ antiport mechanism to expell structurally diverse drug and toxic compounds such as Acriflavine, Norfloxacin, Berberine and Ethidium bromide from the cell.

The expression of the described genes and the subsequent functional characterisations were performed in *E. coli* mutant cells as a host. It has been reported that *E. coli* cells possess many multidrug efflux pumps (Putman *et al*., 2000) among which the AcrAB system is the major one (Ma *et al*., 1995). To use them as a useful tool for the cloning of multidrug efflux pumps from other bacteria, a mutant strain of *E. coli*, termed KAM3, has been constructed (Morita *et al*., 1998). The KAM3 mutant strain lacks the AcrAB multidrug efflux pump system and is therefore very sensitive towards various drug and toxic compounds, including a wide range of cationic dyes (Ethidium bromide), fluoroquinolones (Norfloxacin, Ciprofloxacin), aminoglycosides (Kanamycin, Streptomycin), plant antimicrobial alkaloids (Acriflavine, Berberine), and other structurally diverse antibiotis and drugs which were used for multidrug efflux pump discovery and characterisation (Morita *et al*., 1998 and 2000; Huda *et al*., 2001). Recently, a new *E. coli* mutant strain, termed KAM32, was also constructed and used for the

same purpose (Chen *et al*., 2002). This mutant strain lacks the AcrAB major multidrug efflux pump system as well as YDHE/NORE, the multidrug efflux protein which is a homologue of NorM from *V. parahaemolyticus* and which represents the only MATE protein in *E. coli*. The disruption of both the *AcrAB* operon and *YDHE*/*NORE* created the drug-hypersusceptible *E. coli* mutant KAM32, which was successfully used in the characterisation of several multidrug efflux pumps thereafter (Miyamae *et al*., 2001; Braibant *et al*., 2002; Chen *et al*., 2002; He *et al*., 2004).

2.2. Yeast multidrug and toxic compound extrusion family

The complete sequencing of the genome of the yeast *Saccharomyces cerevisiae* allowed to search for the yeast members of the MATE family. Untill now, only two proteins, ERC1 (termed YHR032w in the *Saccharomyces* Genome Database; http://www.yeastgenome.org/) and YDR338c, were classified as MATE proteins among all known and predicted yeast proteins. The first protein, ERC1, was discovered earlier without any classification but was characterised by Shiomi *et al.* (1991). When the nucleotide sequence of the gene (1852 bp) was present on a multi-copy plasmid in yeast cells, its protein caused a high accumulation of S-adenosyl-L-methionine (SAM) and conferred resistance to ethionine, a toxic analogue of methionine. Hence, the gene was termed *Ethionine Resistance Conferring* 1 (*ERC1*). A hydrophobic plot determined by the method of Kyte and Doolittle indicated that ERC1 is a transmembrane protein (Shiomi *et al*., 1991), however the subcellular localisation still remains unknown. The second member, YDR338c, was identified in the genome of yeast *S. cerevisiae* using the nucleotide sequence of *ERC1* as a bait without any further functional characterisation. To the best of the knowledge, neither *ERC1* nor *YDR338c* were shown to mediate the resistance to a wide range of cationic dyes, fluoroquinolones, aminoglycosides or other structurally diverse antibiotics and drugs previously used to characterise the members of the bacterial MATE family.

Compared with bacteria, yeast cells combine the advantages of eukaryotes with the easy handling of prokaryotes (Bill, 2001). As in the case of bacteria, they grow rapidly, are easy to

culture and can be easily genetically manipulated (Cregg *et al*., 2000). They contain very similar secretory pathway to other eukaryotes and many of the second-messenger signaling pathways that exist in higher eukaryotes (Kron and Gow, 1995). They can also perform eukaryotic-specific, post-translational modifications such as proteolytic processing, protein folding, disulfide-bond formation and certain types of glycosylation (Eckart and Bussineau, 1996). Since bacteria lack many of these features, eukaryotic proteins can be more often misfolded or inactivated when produced in prokaryotic than in eukaryotic hosts. Therefore, yeasts like e.g. *Saccharomyces cerevisiae*, are used as a suitable alternative host system for functional characterisation of homologous and heterologous proteins. This aim is elegantly achieved using the technique of 'functional complementation' of the relevant yeast deletion mutants. For the functional characterisation of MATE genes, the yeast *erc1* and *ydr338c* deletion mutants colud be very useful.

2.3. Plant multidrug and toxic compounds extrusion family

The complete sequencing of the *Arabidopsis thaliana* genome revealed the existance of 56 genes belonging to the MATE family (Arabidopsis Genome Initiative, 2000). To date five *Arabidopsis* genes, i.e. *TRANSPARENT TESTA 12* (*TT12*), *ABERRANT LATERAL ROOT FORMATION 5* (*ALF5*), *ENHANCED DISEASE SUSCEPTIBILITY 5* (*EDS5*), *Arabidopsis thaliana DETOXIFICATION 1* (*AtDTX1*) and *FERRIC REDUCTASE DEFECTIVE* 3 (*FRD3*), have been functionally characterised (Debeaujon *et al*., 2001, Diener *et al*., 2001, Nawrath *et al*., 2002, Li *et al*., 2002, Rogers and Guerinot, 2002). The MATE transporters encoded by these genes may generally cover a diverse range of functions in plant growth and development, in particular in the transport of important and cytotoxic (TT12, EDS5 and FRD3) as well as xenobiotic compounds (ALF5 and AtDTX1).

Debeaujon *et al*. (2001) reported that TT12 appears to control the vacuolar sequestration of flavonoids in the seed coat (testa) endothelium. Due to their high chemical reactivity, flavonoids are toxic endogenous compounds that must be removed from the cytoplasm after their synthesis and sequestered in the vacuole or cell wall. There, they function as protectans

against damage by UV light, oxidative stress and pathogen attack. The mutant seeds, lacking the function of TT12, are therefore pale in color and show reduced seed dormancy due to an inefficient transport and accumulation of flavonoids. This observation supports the idea that TT12, together with flavonoids, plays an important role in seed biology (Winkel-Shirley, 1998; Debeaujon *et al*., 2001).

The discovery and characterisation of the *Arabidopsis* mutant, *eds5* (allelic to *sid1*; Rogers and Ausubel, 1997), shows that plants can recruit MATE transporters in the network of defence against pathogens (Nawrath *et al*., 2002). The *EDS5* transcript is rapidly induced by pathogens (like e.g. *Pseudomonas syringae*) and abiotic stresses, such as UV-C light, which induce the accumulation of salicylic acid (SA). SA was found to be essential for gene-for-gene resistance, systemic (affecting the entire plant) acquired resistance and reduction of disease development after inoculation with virulent pathogens (Delaney *et al*., 1995; Nawrath and Metraux, 1999). Although the subcellular localisation and nature of substrates transported by EDS5 still remain unknown, it is possible that this protein may transport phenolic compounds that are precursors for the biosynthesis of SA, therefore functioning in the SA-dependent pathway of plant defence against pathogens (Nawrath *et al*., 2002).

The correct iron localisation in the root and shoot of *Arabidopsis thaliana* required the functional MATE gene, *FRD3* (Rogers and Guerinot, 2002), although the encoded protein function is root-specific. Green and Rogers (2004) based on the given *FRD3*'s expression in cells surrounding the root vascular tissues and the further analysis of the *frd3* mutant, hypothesized that FRD3 may control efflux into the xylem of low M_r compounds, like iron chelators or other factors, but not iron itself. These FRD3-specific and still uncharacterised iron chelators or factors may be necessary for correct iron unloading from the xylem in the shoot, giving a role for FRD3 in the delivery of iron to the shoot in a useable form (Green and Rogers, 2004).

Although a biochemical function for the next *Arabidopsis* MATE gene, *ALF5*, has not been demonstrated, the *alf5* mutant phenotype is consistent with the involvment of this gene in transporting small, organic molecules. Diener *et al.* (2001) suggested that ALF5 plays a

direct role in either the vacuolar sequestration or the cellular efflux of small, organic molecules and in that way, it protects roots from growth inhibiton by a number of compounds contaminating commercial agar and the tested toxic cation, tetramethylammonium. The mechanism of *ALF5*-mediated toxin resistance is still unresolved, however, the spatial expression of the gene in *Arabidopsis* roots, which come into immediate contact with soil and the various soluble substances in it, suggested that ALF5 function may be required for the protection of the roots from naturally occurring toxic compounds as well as exogenous chemicals, such as pesticides (Diener *et al.,* 2001).

The first plant MATE protein, that has been shown to function as a detoxifying efflux carrier, is AtDTX1 (Li *et al*., 2002). Using the *E. coli* KAM3 mutant, Li *et al*. (2002) presented clear evidence that AtDTX1 mediates the extrusion of lipophilic cations such as Ethidium bromide, the plant alkaloid Berberine, and the fluoroquinolone Norfloxacin. AtDTX1 also mediates cadmium resistance. Regarding the mechanism underlying the efflux, it has been shown that a proton-motive force, but not sodium gradient that is a characteristic feature of the bacterial MATE proteins, is required for AtDTX1-mediated extrusion. The location in the plasma membrane, especially in roots, is consistent with the functional properties of AtDTX1 as a detoxifying effflux carrier, which may be required there for the protection of the roots from naturally occurring toxic compounds. *AtDTX1*'s expression in above-ground organs also suggests the function as an efflux carrier, but probably for secondary metabolites synthesised in plant cells (Li *et al*., 2002).

- *Arabidopsis thaliana Novel Ion Carrier* (*NIC*)-family

Before the MATE family was created from the 56 selected genes, eight of them were earlier classified into one family. The prototype of this family was identified and functionally characterised using expression systems such as *Xenopus laevis* oocytes and yeast *Saccharomyces cerevisae* (Klaus Pellengahr, PhD thesis, 2004). Based on preliminary results, which indicated a putative function as an ion carrier, this protein was termed Novel Ion Carrier 1 (NIC1). Accordingly, the family of the eight homologous genes was called the

NIC family. After subsequent identification and isolation of the remaining members of the NIC family (*NIC2*-*NIC8*), three of them, *NIC2* (Blazej Dolniak, Master thesis, 2001), *NIC3* (Fabien Poree, PhD thesis, 2004) and *NIC4* (Mandy Kursawe, unpublished data), have partly been characterised. The preliminary results suggest that *NIC2* can increase the LiCl and likely NaCl tolerance in *Saccharomyces cerevisiae*. *In planta*, *NIC2* is expressed in the vascular tissue of all organs, but its overexpression in transgenic *Arabidopsis* plants showed no changes in the plant phenotype. It was casued by the use of the wrong construct, where *NIC2* was fused with its C-terminus to *GFP*. No differences were also observed in transgenic *Arabidopsis* plants transformed by a construct with *NIC2* in the antisense orientation in order to silence the gene (Blazej Dolniak, Master thesis, 2001). Other experimental data show that *NIC3* also increases the LiCl and NaCl tolerance in *S. cerevisiae*, however, its overexpression in transgenic *Arabidopsis* plants leads to major changes in plant architecture, indicating an important role in development, but the precise function *in planta* is still unclear (Fabien Poree, PhD thesis, 2004). The expression of *NIC4* in *S. cerevisiae* indicates that the protein encoded by this gene is able to transport the LICl and NaCl as well, similar to NIC2 and NIC3. Moreover, the overexpression of *NIC4* in transgenic *Arabidopsis* plants also casues extreme phenotypic changes suggesting its role in the distribution of a substrate or substrates, which regulate the growth and development of *Arabidopsis*, however, the precise function of *NIC4* is being elucidated at the moment (Mandy Kursawe, unpublished data).

- Identification of MATE genes in other plant species

The complete sequencing of the 12 chromosomes from *Oryza sativa* (cultivar Nipponbare) allowed to search for rice genes of the MATE family (The International Rice Genome Sequencing Project; http://rgp.dna.affrc.go.jp/, 2005). *In silico* analysis using Aramemnon, a membrane protein database (http://aramemnon.botanik.uni-koeln.de/), revealed the existance of 49 genes belonging to the MATE family. To the best of the knowledge, none of the genes was functionally characterised to date. According to the Maize Genetics and Genomics Database (http://www.maizegdb.org/), and the TIGR Wheat Genome Database

(http://www.tigr.org/tdb/e2k1/tae1/) none of the currently identified genes encode MATE carriers in both plant species. However, the full sequencing of both genomes will certainly reveal genes which will be classified into the MATE family.

The great number of various multidrug transporters indicate that plant cells are capable of removing a large number of cytotoxic compounds from the cytoplasm. A question which can be asked about plant MATE carriers concerns their 'real' function. Are these proteins functioning solely to protect the plant against toxic compounds like the exampled bacterial or yeast MATE carriers, or do they have more specific functions like plant ABC- and other secondary transporters, and just accidentally, they happen to be also polyspecific? The answer seems to be complex, because based on the characterised plant MATE proteins, it appears that they have evolved to perform very specific functions in transporting a wide range of natural substrates as well as in multidrug resistance to toxic compounds. Substrate specificities, structural diversities, gene expression patterns and subcellular localisations lead to functional variations among plant MATE genes and proteins. These functional diversities suggest unique functions *in planta*, and at the moment await further exploration.

Aim of work

The identification of 56 genes belonging to the *Arabidopsis thaliana* multidrug and toxic compounds extrusion (MATE) family has caused an interest, which aim is to figure out their functions *in planta*. One of these genes, *NIC2*, which belongs to the subgroup of the *Arabidopsis* MATE family, the NIC family, was partly characterised in the past (Blazej Dolniak, Master thesis, 2001). To complete its characterisation and to discover the physiological role in *Arabidopsis*, *NIC2* was functionally characterised in detail using various heterologous and homologous expression systems in the light of the previously characterised MATE genes.

Materials and methods

1. General materials and methods

Unless otherwise indicated, standard molecular and biological techniques were performed according to Sambrook *et al*. (1989). Restriction enzymes were purchased from New England Bioloabs (Frankfurt am Main, Germany), oligonucleotides from TibMolbiol (Berlin, Germany) and Invitrogen (Karlsruhe, Germany). DNA sequencing was done by SeqLab (Göttingen, Germany). Chemicals were obtained from Roche (Grenzach-Wyhlen, Germany), Merck (Darmstadt, Germany), SIGMA (Deisenhofen, Germany), Fluka (Deisenhofen, Germany) and Duchefa Biochemie (Haarlem, The Netherlands). General *E. coli* strains XL-1 Blue (Stratagene, Helidelberg, Germany) and DH5α (Invitrogen, Karlsruhe, Germany) were used for general DNA work. For analysis of sequences, the tools provided by the National Center for Biotechnology Information (http://www.ncbi.nlm.nih.gov/), the ExPASy Proteomics Server (http://us.expasy.org), The Arabidopsis Information Resource (TAIR; http://www.arabidopsis.org/), Aramemnon, a membrane protein database, (http://aramemnon.botanik.uni-koeln.de/) and the Plant CARE, Plant Cis-Acting Regulatory Element database (http://sphinx.rug.ac.be:8080/PlantCARE/) were utilised. In addition, the multiple sequence alignment was performed using the BCM Search Launcher server (http://searchlauncher.bcm.tmc.edu/).

2. *Escherichia coli*-expression host system

Bacterial strains

E. coli TG1 [Δ(lac-pro) supE thi hsdΔ5/F'traD36 proA$^+$B$^+$ lacI^q lacZΔM15] (Zymo Research Corporation, Orange, CA), and a derivative of TG1, KAM3 [Δ(lac-pro) supE thi hsdΔ 5/F'traD36 proA$^+$B$^+$ lacI^q lacZΔM15 ΔacrAB], a gift from Tomofusa Tsuchiya (Japan), were used for protein expression. *E. coli* XL1-blue (supE44 hsdR17 recA1 endA1 gyrA46 thi relA1 lac-F' [proAB$^-$ lacI^q lacZ Δ M15 Tn10(tet^t)] was used for plasmid propagation.

Cloning of NIC2 and YDHE/NORE

The cDNA of *NIC2* (1533 bp) was TA-cloned into plasmid pCR®2.1 (Invitrogen, Karlsruhe, Germany) from a pool of first-strand cDNAs of 45-day-old *Arabidopsis thaliana* (L.) Heynh. C24 wild-type plants using PCR with the high-fidelity DNA polymerase HF2 polymerase (BD Biosciences Clontech, Heidelberg, Germany) and the primers *NIC2*for*Bam*HI (5'-GGATCCATGGAAGACAATCCAGTCAGAT-3') and *NIC2*rev*Pst*I (5'-CTGCAGTTACAAAAC-ATCACCCAACTTCTC-3'). *NIC2* was then subcloned into the pQE30 expression vector (QIAGEN, Hilden, Germany) using the underlined restriction sites for *Bam*HI and *Pst*I. The bacterial *YDHE*/*NORE* gene (1374 bp) was cloned from *Escherichia coli* TG1 cells as follows. Chromosomal DNA was prepared from *E. coli* cells by the CTAB method (Sambrook *et al.*, 1989) and the gene was TA-cloned into pCR®2.1 using PCR with HF2 polymerase and the primers *YdhE*for*Bam*HI (5'-GGATCCGTGCAGAAGTATATCAGTGAAGCG-3') and *YdhE*rev*Hin*dIII (5'-AAGCTTTTAGCGGGATGCTCGTTGCAGAAT-3'). *YDHE/NORE* was then subcloned into pQE30 expression vector (QIAGEN) using the underlined restriction sites for *Bam*HI and *Hin*dIII. Competent cells of *E. coli* KAM3 were transformed by the heat shock method (Sambrook *et al.*, 1989) with the plasmids pQE30::*NIC2* and pQE30::*YDHE/NORE* and were used in the first bacterial expression system (**IPTG-induced expression system**). For the second bacterial expression system (**host-induced expression system**), plasmids containing *NIC2* and *YDHE/NORE* coding regions were prepared as follows. The cDNA of *NIC2* was isolated from a pool of first-strand cDNAs of 45-day-old *Arabidopsis thaliana* (L.) Heynh. C24 wild-type plant using PCR with HF2 polymerase and the primers *NIC2*for (5'-ATGGAAGACAAAATCCAGTCAGA-TGATTTC-3') and *NIC2*rev (5'-TTACAAAACATCACCC-AACTTCTCATCATC-3') and then TA-cloned into pGem®–T Easy vector (Promega, Mannheim, Germany). From the chromosomal DNA of *E. coli* TG1 cells the 858 bp upstream flanking fragment of *YDHE/NORE* was isolated using PCR with HF2 polymerase and the primers 5flankfor*Nco*I (5'-CATGCCATGGCAGATCAGG-

CTTCTGTGCCT-3') and 5flankrev*Nco*I (5'-CATGCCATGGGTGAACACCTTTTATTTGTA-3'). The fragment was then digested with *Nco*I and subcloned as a promoter-like sequence upstream of the ATG start codon of *NIC2*. *YDHE/NORE* together with a 858 bp upstream flanking sequence and 662 bp downstream flanking sequence was cloned from chromosomal DNA of *E. coli* TG1 cells by PCR with HF2 polymerase and the primers 5flankfor (5'-CAGATCAGGCTTCTGTTGCCTGGTTGATTCA-3') and 3flankrev (5'-CATTTATCGTCTGGGGACGGATGGCCTTCA-3') and TA-cloned into pGem®–T Easy vector as a sequence of 2896 bp. Competent cells of *E. coli* KAM3 were transformed by the heat shock method with the plasmids pGem®–T Easy::*NIC2* and pGem®–T Easy::*YDHE/NORE* and then used in the second bacterial expression system.

Media and growth conditions

E. coli TG1 and KAM3 cells were grown in YT-medium containing 1.6 % bacto-tryptone, 1 % bacto-yeast extract, 0.5 % NaCl, pH 7.0 with or without 0.8 % phytagar. KAM3 cells transformed with the plasmids pQE30::*NIC2*, pQE30::YDHE/NORE, pGem®–T Easy::*NIC2* and pGem®–T Easy::YDHE/NORE grew on the same medium that was additionally supplemented with 25 µg/ml of Ampicillin. Where indicated, 1 mM of isopropyl-thio-β-D-galactopyranoside (IPTG) and various drug and toxic compounds were added to the medium. All *E. coli* strains were grown under aerobic conditions at either 30°C or 37°C.

Drug susceptibility assays

The following compound stock solutions were prepared in water unless indicated otherwise and were used in drug susceptibility assays: Acriflavine (Sigma) at 10 mg/ml; Berberine (Sigma) at 20 mg/ml in methanol; Ciprofloxacin (Sigma) at 1 mg/ml in ethanol; DL-Ethionine (Sigma) at 110 mM in water with pH 3.0 adjusted with 1 M HCl; Fluoro-3-indolyl-acetic acid (Sigma) at 100 mM in ethanol; Norfloxacin (Sigma) at 1 mg/ml in ethanol; Tetraethylammonium chloride (Sigma) at 4 M and Tetramethylammonium chloride (Sigma) at

5 M. The minimum inhibitory concentrations (MICs) of drugs for *E. coli* TG1 and KAM3 cells were determined in the drop test experiments with a decrasing amount of cells (0.1, 0.01 and 0.001 in 1 ml) measured by optical density at 600 nm (OD_{600nm}) using SmartSpec™3000 spectrophotometer (Bio-Rad Laboratories Muenchen, Germany). Cells were grown at 37°C for 24 h on YT-agar plates containing various drug and toxic compounds at various cocentrations, and the size of colonies was subsequently photographed.

In the frist bacterial expression system (**IPTG-induced expression system**), KAM3 cells transformed with pQE30::*NIC2* and pQE30::*YDHE/NORE* were grown at 30°C from 24 to 48 h on YT-agar plates containing 1 mM IPTG, 25 µg/ml Ampicillin and various concentrations of drug and toxic compounds. TG1 and non-transformed KAM3 cells grew on the same YT-media, but without Ampicillin. The size of colonies was photographed.

In the second bacterial expression system (**host-induced expression system**), to examine the growth of KAM3 cells transformed with pGem®–T Easy::*NIC2* and pGem®–T Easy::*YDHE/NORE*, a filter-based growth assay was peformed. Cells were grown overnight at 37°C in YT-medium supplemented with 25 µg/ml Ampicillin. Afterwards, the cells were washed twice with sterile water and 250 µl of each bacterial strain (OD_{600nm} 0.5) were plated onto YT-agar plates containing 25 µg/ml Ampicillin. Various drug and toxic compounds were spotted on SS-033 (Wescor, Utah) paper discs which were already transferred onto bacterial plates, and then incubated at 30°C for 24 h. TG1 and non-transformed KAM3 cells were grown on the same media, but without Ampicillin. After incubation, the size of bacterial colonies was photographed.

3. *Saccharomyces cerevisiae*-expression host system

Bacterial and yeast strains

E. coli XL1-blue (*supE44 hsdR17 recA1 endA1 gyrA46 thi relA1 lac-F' [proAB⁻ lacI^q lacZ Δ M15 Tn10(tet^r)]* was used for plasmid propagation. The following haploid yeast strains were obtained from the European Saccharomyces Cerevisiae Archive for Functional Analysis

(EUROSCARF) stock centre (Oberursel, Germany) the following haploid yeast strains were obtained: the parental strain BY4741 (MAT a; his3Δ1; leu2Δ0; met15Δ0; ura3Δ0), the single mutant strains *ydr338c* (MAT a; his3Δ1; leu2Δ0; l met15Δ0; ura3Δ0; YDR338c::kanMX4), and *erc1* (*yhr032w*) (MAT a; his3Δ1; leu2Δ0; met15Δ0; ura3Δ0; YHR032w::kanMX4), and the double mutant strain *ydr338c erc1* (MAT a; his3Δ1; leu2Δ0; met15Δ0; ura3Δ0; YDR338c::kanMX4; Yhr032w::kanMX4) which were thereafter used in the experiments described in this work. All mutant strains were constructed using the parental strain BY4741 as a background.

Cloning of NIC2 and APOAEQUORIN

The cDNA of *NIC2* (1533 bp) was TA-cloned into plasmid pCR®2.1 from a pool of first-strand cDNAs of 45-day-old *Arabidopsis thaliana* (L.) Heynh. C24 wild-type plants using PCR with HF2 polymerase and the primers *NIC2*for*Eco*RI (5'- GAATTCATGGAAGACAAAATCCAGTC-AGAT-3') and *NIC2*rev*Xba*I (5'-TCTAGATTACAAAACATCACCCAACTTCTC-3'). *NIC2* was then subcloned into yeast expression vector pYES2 (Invitrogen) using the underlined restriction sites for *Eco*RI and *Xba*I. The cDNA of *APOAEQUORIN*, which was a gift from Marc Knight (University of Oxford, UK), was subcloned from the pRTL2 plasmid into pYES3/CT yeast expression vector (Invitrogen) using the restriction sites for *Sph*I.

Basic media and growth conditions

Non-transformed yeast strains were grown in the yeast minimal medium (SC) containing Yeast Nitrogen Base without Amino Acids and Ammonium Sulfate (DIFCO, Sigma-Aldrich Chemie Muenchen, Germany), CSM (BIO101 distributed by Qbiogene, Heidelberg, Germany), 2 % galactose (Sigma) and, where indicated, 0.8 % select yeast agar (Gibco BRL, distributed by Invitrogen). Plasmid-transformed yeast cells were grown in the same yeast minimal medium, that was supplemented with CSM-URA, CSM-TRP or CSM-URA-TRP (BIO101, distributed by Qbiogene). In addition, 1 % of raffinose (Sigma) and the

prostetic group coelenterazine (Nanolight Technology, Pinetop, AZ) with its final concentration of 0.5 µM were added during the growth of yeasts transformed with pYES3/CT::*APOAEQUORIN*. All yeasts strains were grown at 30°C.

Yeast transformation

For the transformation of the plasmids pYES2::*NIC2* and the empty pYES2 vector, the parental strain BY4741 was grown overnight at 28°C in YPD-medium (1 % [w/v] yeast extract, 2 % [w/v] bacto-peptone, 2 % [w/v] glucose) with vigorous shaking (190 rpm). The competent yeast cells were thereafter transformed according to the LiAc/SS-DNA/PEG procedure (Gietz *et al*., 1995). Indepenedent transformants carrying the plasmids were selected on SC-medium without uracil. The plasmids pYES3/CT::*APOAEQUORIN* and pYES2::*NIC2* were jointly transformated into the competent yeast expression strain INVSc1 (Invitrogen) according to the LiAc/SS-DNA/PEG procedure (Gietz *et al*., 1995). As a control, the INVSc1 cells were solely transformed with pYES3/CT::*APOAEQUORIN*. The transformants carrying the pYES3/CT::*APOAEQUORIN* were selected on the SC-medium without tryptophane, while the transformants carrying pYES3/CT::*APOAEQUORIN* and pYES2::*NIC2* grew on the SC-medium without tryptophane and uracil.

Extraction of yeast RNA and Northern blot analysis

To confirm the expression of *NIC2*, total yeast RNA from two independent transformants were extracted according to the procedure of Rivas *et al*. (2001). As a negative control, total RNA was extracted from yeast cells transformed with the empty pYES2 vector. After blotting on a Nylon membrane Nucleobond AX (Macherey-Nagel, Düren, Germany), Northern blot analysis was performed using cDNA of *NIC2* as a probe labelled with Rediprime II random prime labeling system (Amersham Biosciences Europe, Freiburg, Germany).

Drug susceptibility assays and drop test experiments

The following compound stock solutions were prepared in water unless otherwise indicated, and then used in drug susceptibility assays: Acriflavine at 10 mg/ml; Berberine at 20 mg/ml in methanol; Ciprofloxacin at 1 mg/ml in ethanol; DL-Ethionine at 110 mM in water with pH 3.0 adjusted with 1 M HCl; Norfloxacin at 1 mg/ml in ethanol; Tetraethylammonium chloride at 4 M; Tetramethylammonium chloride at 5 M. To characterise the single and double mutants, growth experiments with DL-Ethionine were performed. Equal amounts of yeast cells (0.001) determined by optical density measurements at 600 nm (OD_{600}) were added to SC-medium containing 0 mM, 0.25 mM, 0.5 mM, 1 mM, 1.2 mM or 1.5 mM DL-Ethionine, and after 24 h of vigorous shaking at 30°C the percentage of surviving yeasts cells was calculated. As control references the growth of yeast cells to which no DL-Ethionine was added was used.

Drop test experiments were performed with the parental strain BY4741 as well as with the single and double mutants as follows. Decreasing amounts of yeast cells (0.1, 0.01 and 0.001) determined at OD_{600} were spotted as a drop of 20 µl on agar plates containing Yeast Nitrogen Base without Amino Acids and Ammonium Sulfate, CSM, 2 % galactose, 0.8 % select yeast agar and different concentrations of various drug and toxic compounds (shown in **Table 3**) and were grown at 30°C. The size of yeast colonies was photographed afterwards. For the BY4741 yeast cells transformed with pYES2::*NIC2* and the empty pYE2 vector, drop test experiments were performed in the similar way, but CSM-URA and various concentrations of salts like LiCl, KCl, NaCl and $CaCl_2$ were added. The cells were grown at 30°C from 24 h to 10 days and the the size of yeast colonies was photographed thereafter.

Lithium and sodium liquid growth experiments

Cultures containing liquid SC-medium without uracil, but with 0 mM LiCl, 300 mM LiCl, 600 mM LiCl or 900 mM NaCl, or 1600 mM NaCl, were inoculated with the same amount of cells (OD_{600nm} 0.001) from 5 independent yeast transformants carrying either pYES2::*NIC2* or the

empty pYES2 vector. The cultures were grown at 30°C with vigorous shaking (190 rpm) and their growth was monitored by the measurement of the optical density at 600 nm.

Aequorin luminescence measurements and $[Ca^{2+}]_{cyt}$ quantification

Aequorin luminescence was determined with a custom-built luminometer following the procedures used to quantify $[Ca^{2+}]_{cyt}$ in yeast cells (Matsumoto *et al*., 2002). Cells were transformed with either the plasmid pYES3/CT::*APOAEQUORIN,* or the plasmids pYES3/CT:: *APOAEQUORIN* and pYES2::*NIC2*. At stationary phase, after overnight growth in the presense of 0.5 µM of coelenterazine, the cells were harvested by centrifugation and resuspended in a fresh SC-medium without tryptophane and uracil to an OD_{600} of ~ 0.1-0.2. Cells were then grown to an OD_{600} of ~ 0.6-0.8. Hypertonic shock was administered to yeast cells by diluting the suspension 1:1 with SC medium without tryptophane and uracil containing LiCl, NaCl, or Sorbitol at 2x final concentration. Inhibitory compounds were diluted and added to the yeast cultures as indicated. $GdCl_3$ and $LaCl_3$ (Sigma) were dissolved in water to concentrations of 1 mM and then diluted with SC medium without tryptophane and uracil to 0.5 µM and 5 µM, respectively. The inhibiotors were added to the yeast cultures 10 min before the measurements. The chemical agents like NaCl, LiCl and sorbitol were added to yeast cells immediately after the acquisition of the basal luminescence reading. Luminescence from aequorin that remained in cells at the end of an experiment was determined after treating cells with 70 % ethanol, 1 M $CaCl_2$ and 0.01 % Triton X-100. These data were used to calculate the $[Ca^{2+}]_{cyt}$ using the following equation:

$$[Ca^{+2}] = \{(L/L_{max})^{1/3} + [118(L/L_{max})^{1/3}] - 1)/(7 \times 10^6 - [7 \times 10^6(L/L_{max})^{1/3}])$$

where L is the luminescence intensity at any time point and L_{max} is the integrated luminescence intensity (Matsumoto *at el*., 2002).

4. *Xenopus laevis* oocytes-expression host system

Bacterial strain and Xenopus laevis oocytes

E. coli XL1-blue (*supE44 hsdR17 recA1 endA1 gyrA46 thi relA1 lac-F' [proAB$^-$ lacI^q lacZ Δ M15 Tn10(tet^t)]* was used for plasmid propagation. The adult female toad *Xenopus laevis* was supplied by the Köhler company, Hamburg, Germany. *Xenopus laevis* oocytes were used for protein expression and uptake assays.

Cloning of NIC2, in vitro transcription and protein expression

The cDNA of *NIC2* was subcloned from pCR®2.1::*NIC2* into the pGEMHE vector using the restriction sites for *Bam*HI and *Xba*I. The pGEMHE vector based on the pGEM 3Z vector (Promega) possesses promoter sequences for the T7 and SP6 RNA polymerases as well as the 5' and 3' UTR from a *Xenopus β-GLOBIN* (Liman *et al*., 1992). *In vitro* transcription of pGEMHE::*NIC2* was performed with the T7 mMESSAGE mMACHINE-kit (Ambion Europe, Huntingdon, Cambridgeshire, UK) according to the manufacturer's instruction. To stop the reaction and precipitate the *NIC2* cRNA, 30 µl nuclease-free H_2O, 25 µl LiCl (4 M) and 75 µl ethanol (100 %) were added. Further purification was made using a phenol:chloroform (1:1) mixture and from an aqueous phase the cRNA was precipitated with an equal volume of isopropanol at 4°C. After centrifugation, the cRNA pellet was resuspended in DEPC-H_2O and utilised for injections into *Xenopus laevis* oocytes. The injection of *NIC2* cRNA (approximately 40 nl, *i.e.* 40 ng of cRNA per oocyte) was made using a glass micropipette (tip diameter: 10-15 µm) and the manipulated oocytes were stored at 18-20°C in the modified ND96 solution (88 mM NaCl, 1 mM KCl, 2,4 mM $NaHCO_3$, 10 mM HEPES dissolved in NaOH, 0,33 mM $Ca(NO_3)_2$ x 4 H_2O, 0,41 mM $CaCl_2$ x 2 H_20, 0,82 mM $MgSO_2$ x 7 H_20, pH 7,4 and 50 µg/ml of Gentamycin). After 3 days, when the expression of cRNA has been at maximum (Buchanan *et al*., 2000), oocytes expressing *NIC2* were used for the uptake assay. As a control non-manipulated oocytes were taken.

[^{3}H]-IAA uptake assay

Control and *NIC2*-expressing oocytes were placed into small wells of the microtiter plate filled with 100 µl of the modified ND96 solution containing 100 nM of non-labeled IAA (Sigma) and incubated at room temperature for 10 min with vigorous shaking (200 rpm). To measure the [^{3}H]-IAA uptake, 20 µl of the modified ND96 solution including 100 nM of non-labeled IAA and 37 kBq of ^{3}H-labeled IAA (Amersham Biosciences) per assay were added to oocytes and incubated at room temperature with vigorous shaking (200 rpm). After a certain time of incubation (10 min, 20 min, 30 min, 40 min, 50 min and 60 min) 10 control and 10 *NIC2* expressing oocytes were removed from the incubation solution and then three times gently washed with 1 ml of the modified ND96 solution containing 100 nM of non-labeled IAA before transferring to the scitillation vials. 100 µl of the NCS Tissue Solubilizer (Amersham Biosciences) were thereafter added and the oocytes were incubated at 60°C for 24 h with vigorous shaking (200 rpm). Uptake of labeled IAA into control and *NIC2*-expressing oocytes was determined by using 5 ml of OCS scintillation coctail (Amersham Biosciences) and a scintillation counter.

5. *Arabidopsis thaliana*-expression host system

Plant material and growth conditions

Arabidopsis thaliana (L.) Heynh. C24 wild-type plants were grown on Murashige and Skoog medium (Murashige and Skoog, 1962), supplemented with 2% (w/v) sucrose and solidified with 0.8 % phytagar, at 22°C under a 16 h day (200 µmol m^{-2} sec^{-1}) and 8 h night regime. After 20 days, seedlings were transferred in a 1:1 (v/v) mixture of soil (GS90; Gebr. Patzer, Sinntal Jossa, Germany) and vermiculite (German/Deuschte Vermiculite Daemmstoff, Sprockhoevel, Germany) and grown in the greenhouse with an irradiance of 150 µmol m^{-2} sec^{-1} at 20/18°C (day/night) temperature regime and a photoperiod of 16 h, until harvesting. Plant material was frozen in liquid nitrogen before storage at -80°C, unless otherwise indicated.

Real-time reverse transcription PCR

Total RNA was isolated either from 7-to 14- day- old seedlings or from roots, rosette leaves, inflorescence stems and flowers of mature plants (35- to 45-day-old) using TRIZOL reagent (Invitrogen). RNA concentration was measured using SmartSpec™3000 spectrophotometer (Bio-Rad Laboratories), and RNA integrity was determined on a 1.5 % (w/v) agarose gel. 20-50 µg of total RNA was digested with RNAse-free Turbo DNaseI (Ambion, Huntingdon, Cambridgeshire, UK) according to the manufacturer's instructions. Absence of genomic DNA was subsequently confirmed by PCR using control primers that amplified on cDNA of a gene (At3g18780) a short fragment of 200 bp, instead of 600 bp, which corresponds to the amplification on genomic DNA. Reverse transcription was performed using the SuperScript™ III reverse transcriptase kit (Invitrogen). The effciency of cDNA synthesis was assessed by real-time PCR amplification of control cDNAs encoding *actin2* (primers: At3g18780for, 5'-TCCCTCAGCACATTCCAGCAGAT-3'; At3g18780rev, 5'-AACGATTCCGGACCTGCCCATC-3'), and *UBQ10* (primers: At4g05329for, 5'-CACACTCCACTTGGTCTTGCGT-3'; At4g05329rev, 5'-TGGTCTTTCCGGTGAGAGTCTTCA-3'). To determine the *NIC2* transcript, the primers RT-*NIC2*for (5'-TCTCCTTCAGCCGTTACGTGTT-3') and RT-*NIC2*rev (5'-CCACATCATCGGTTTCGTCAC-3') were designed using the PRIME program of the GCG® Wisconsin Package™, version 10.2 (Madison, WI). Polymerase chain reactions were performed in an optical 96-well plate with the Applied Biosystem 5700 detection system (Applied Biosystems, Darmstadt, Germany) using SYBR® Green to monitor dsDNA synthesis. Reactions contained 2x SYBR®Green Master Mix reagent (Applied Biosystems), cDNA and gene-specific primers in a final volume of 20µl. The following standard thermal profile was used for PCR: 50°C for 2 min; 95°C for 10 min; 40 cycles of 95°C for 15 sec and 60°C for 1 min. Data were analysed according to Czechowski *et al*. (2004). *NIC2* gene expression was normalised against that of *UBQ10* by subtracting the C_T value of *UBQ10* from the C_T value of the *NIC2* gene, and the value (ΔC_T) was calculated in the following

formula: $2^{-\Delta C_T}$. The calculated values from $2^{-\Delta C_T}$ reflected the level of *NIC2* expression in investigated organs or tissues.

To quantify the *NIC2* transcript level in the transgenic plants in comparison with the wild-type plants, the values of *NIC2* expression ($2^{-\Delta C_T}$) obtained from the wild-type plants were used as basic references which were subtracted from values of *NIC2* expression ($2^{-\Delta C_T}$) obtained from the transgenic plants.

Pro_{NIC2} :GUS fusion

A 1483 bp 5' genomic fragment upstream of the ATG start codon of *NIC2* was amplified using the Advantage-HF2 PCR kit with primers Prom*NIC2*for (5'-CCACGACTCTTCATCACTAGTTCACCATTA-3') and Prom*NIC2*rev (5'-TGAAAATGGTGGA-TTTTTAGTTTACTGAGT-3'). *Arabidopsis thaliana* (L.) Heynh. C24 genomic DNA was used as a template. The amplified promoter fragment was inserted into plasmid pCR®2.1 and subsequently fused to the β-glucuronidase (*GUS*) reporter gene in plasmid pBI101 (Clontech, PaloAlto, CA). The final construct was transformed into *Agrobacterium tumefaciens* strain GV3101 with virulent plasmid pMP90RK, which was grown on YEB-medium (0.2 % yeast extract, 0.5 % beef extract, 0.5 % peptone, 0.5 % sucrose, 2 mM $MgSO_4$, pH 6.8-7.0) supplemented with Rifampicin (50 µg/ml), Gentamycin (200 µg/ml) and Kanamycin (50 µg/ml) at 30°C for 72 h. Transgenic *Arabidopsis* plants were obtained by the floral dip method (Clough and Bent, 1998). Transgenic plants were selected on sterile MS medium supplemented with 50 µg/ml Kanamycin and after 20 days transferred into soli and grown as described above. GUS activty was determined in vacuum-infiltrated seedlings and mature plants using a GUS staining solution containing 50 mM sodium phosphate (pH 7.2), 10 mM EDTA, 0.33 mg/ml $K_3[Fe(CN)_6]$, 0.1 % Triton X100 and 2 mM X-Gluc (5-bromo-4-chloro-3-indolyl-β-D-glucuronic acid; Duchefa Biochemie, Haarlem, The Netherlands) utilised as a substrate. The infiltrated seedlings were incubated in GUS staining solution for 2-4 hours at 37°C. The infiltrated plants were stained overnight at 37°C. GUS staining patterns

were viewed with an Olympus SZX12 binocular microscope and under a Nikon Eclipse E600 (Nikon, Duesseldorf, Germany) microscope. For tissue cross-sections, the stained plant organs were fixed in hydroxyethylmethacrylate (HEMA) Technovit 7100 (Heraeus Kulzer, Wehrheim, Germany) according to the manufacturer's instructions, and subsequently they were cut with a Leica RM 2155 microtome (Leica Instruments, Nussloch, Germany). Tissue sections (15 µm) were stained with 0.02 % (w/v) Ruthenium Red, washed and examined under a Nikon Eclipse E600 microscope.

Cloning of NIC2 cDNA

Amplification of *NIC2* cDNA was carried out by polymerase chain reaction (PCR) using the Advantage-HF2 PCR kit (Clontech). As template, a mixture of cDNAs from primary and secondary roots, rosette leaves, inflorescence stems and flowers of *Arabidopsis* was used. Primer sequences were as follows: *NIC2*for (5'-ATGGAAGACAAAATCCAGTCAGATGATTT-C-3') and *NIC2*rev (5'- TTACAAAACATCACCCAACTTCTCATCATC-3'). The PCR product was purified using the QIAquick PCR purification kit (Qiagen), and subcloned into either plasmid pCR®2.1 or pGem®–T Easy. The sequence of the entire 1533 bp long *NIC2* cDNA was determined and deposited at GenBank under accession number AF489857.

NIC2-overexpression and NIC2-silenced lines

To overexpress *NIC2* in *Arabidopsis thaliana*, the cDNA was subcloned from the pCR®2.1 into a pGreen0229 35S vector (http://www.pgreen.ac.uk/) downstream of the Cauliflower Mosaic Virus (CaMV) 35S promoter using restriction sites for *Eco*RI. The final construct was propagated in *E. coli* DH5α strain grown in YT-medium with 50 µg/ml Kanamycin and co-transformed into *Agrobacterium tumefaciens* strain GV3101 (pMP90) together with pSoup vector (http://www.pgreen.ac.uk). The cells were thereafter selected on YEB-agar plates supplemented with Gentamycin (200 µg/ml), Kanamycin (50 µg/ml), Rifampicin (50 µg/ml), and Tetracyclin (25 µg/ml) at 30°C for 72 h. Transgenic *Arabidopsis* plants were obtained by

the floral dip method and the F1, F2 and F3 generations of transgenic plants were selected in soil by spraying with a herbicide solution containing gluphosinate ammonium (BASTA) at a final concentration of 240 µg/ml. For gene silencing, the intron-spliced hairpin RNA technology (RNA interference) was used (Smith *et al.*, 2000; Waterhouse and Helliwell, 2003). A *NIC2*-specific 156 bp PCR fragment (encompassing nucleotide positions 220 bp to 375 bp of the *NIC2* cDNA) was recombined into a modified Gateway® pDONR™201 vector, pSpectre, which carries a Spectinomycin resistance cassette replacing the Ampicillin resistance cassette (modified by B. Trevaskis, Max-Planck Institute of Molecular Plant Physiology, Golm, Germany), *via* the Gateway® Technology (Invitrogen). The *NIC2*-fragment was subsequently recombined in two different orientations into the Gateway Compatible Binary Plant Gene Silencing Vector pJawohl8-RNAi (a gift from Bekir Ulker and Imre Somssich, Max-Planck Institute for Plant Breeding, Koeln, Germany). The intermediate and the final construct were propagated in the Library Efficiency® DH5α Competent *E. coli* (Invitrogen) grown on YT-medium supplemented with either 100 µg/ml Spectinomycin or 25 µg/ml Ampicillin and then transformed into *Agrobacterium tumefaciens* strain GV3101 carrying the pMP90 RK vector. *Agrobacterium* cells were selected on YMB-agar plates (0.3 % yeast extract, 0.3 % maltose extract, 0.5 % proteose peptone No. 3, 1 % glucose and 0.8 % phytagar) supplemented with Carbenicillin (100 µg/ml), Kanamycin (50 µg/ml) and Rifampicin (50 µg/ml) at 30°C for 72 h. Transgenic *Arabidopsis* plants were obtained by the floral dip method and the F1, F2 and F3 generations of transgenic plants were identified through BASTA selection.

Growth analysis of NIC2-overexpression and NIC2-silenced plants

NIC2-overexpression and *NIC2*-silenced transgenic *Arabidopsis thaliana* seedlings were grown vertically for 8 and 11 days, respectively, on sterile MS-medium and the root growth was photographed thereafter. To investigate the gravitropic response, *NIC2*-overexpression seedlings were grown horizontally for 3 days on sterile MS-medium, then transferred onto

new medium and grown vertically for another 4 days. At day 7, seedlings were turned by 90° for 0 h, 1 h, 2 h, 4 h and 23 h, respectively. At each time point their growth was photographed. To assess root responses to the excess of various auxins, *NIC2*-overexpression seedlings were vertically grown for 17 days on MS-medium supplemented with either 5 µM IAA or 50 µM IBA and their growth was analysed.

Auxins, flavonoids, salts and gravitropism assays

Transgenic *Arabidopsis thaliana* seedlings transformed with the Pro_{NIC2}:*GUS* construct were grown horizontally for 5 or 6 days on sterile MS-medium containing either various auxins (100 nM 2,4D; 300 nM IAA; 100 nM NAA, 300 nM IBA), flavonoids (1 nM Naringenin; 10 nM Kaempferol; 1 nM Quercetin) or salts (5 mM LiCl; 20 mM NaCl) provided by Sigma. Seedlings were collected, incubated with GUS staining solution for 2-4 h at 37°C and cleared with 8.3 M Chloral Hydrate (Fluka). Gravitropism assays were performed by growing seedlings vertically for 5 days and then turning them by 90° for 0 min, 60 min and 120 min. Seedlings were then collected, incubated with GUS staining solution for 2h at 37°C, and cleared with 8.3 M Chloral Hydrate. All GUS staining patterns were viewed with a Olympus SZX12 binocular microscope and a Nikon Eclipse E600 microscope.

Subcellular localisation of NIC2-GFP fusion proteins

Nicotiana tabacum BY2 protoplasts were used for subcellular localisation of NIC2-GFP fusion proteins. BY2 protoplasts were treated according to Dreyer *et al*. (2004) and transiently transformed or co-transformed with control plasmids pA7-*35S-GFP* (created by K. Czempinski, University of Potsdam, Golm, Germany) to label the cytoplasm and the nucleus, or pOL-*35S-SKL-DsRED* (kindly provided by Hélène Barbier-Brygoo, Gif-sur-Yvette, France) to label peroxisomes, as well as with one of three *NIC2-GFP* constructs. To create the first construct, pA7-*35S-NIC2-GFP*, the full-length *NIC2* cDNA was subcloned from pGem®–T Easy::*NIC2* into pA7-*35S-GFP* using the restriction sites for *Nco*I in order to fuse the 3' end

of *NIC2* to *GFP*. In the second construct, pA7-*35S*-(174 bp)-*NIC2*-*GFP*, *NIC2*, already cloned into pA7-*35S*-*GFP*, was shortened by a fragment of 174 bp at the 5' end using the restriction sites for *Xho*I and re-ligated. To generate the third construct, pA7-*35S*-(1089 bp)-*NIC2*-*GFP*, *NIC2* in pGem®–T Easy::*NIC2* was digested for 2 h with *Xho*I and *Ava*I. Restriction enzymes cut out the 1089 bp long central part of *NIC2*, while the remainig parts of 174 bp at the 5' end and 363 bp at the 3' end of the gene were re-ligated. The truncated form of *NIC2* was then subcloned into pA7-*35S*-*GFP* using the restriction sites for *Nco*I, where the 3' end of *NIC2* was fused to *GFP*. After 40 h of incubation, BY2 protoplasts were viewed under a Nikon Eclipse E600 microscope equipped with a Super High Pressure Mercury Lamp Power Supply. For detection of GFP protein and NIC2-GFP fusion protein, green fluorescence filter settings (excitation 460-500 nm, emission 510-560 nm) were used. Rhodamine filter settings (excitation 540 nm, emission 605-655 nm) were used to detect SKL-DsRED protein.

Results

1.1. Identification and *in silico* characterisation of *NIC2*, a new member of the MATE family

The *NIC2* was identified in the *Arabidopsis thaliana* genome using the nucleotide sequence of *NIC1* as bait and the BLAST-N program (http://www.ncbi.nlm.nih.gov/). *NIC1* was the first characterised member of the Novel Ion Carrier (NIC) family and the object of previous research (Klaus Pellengahr, PhD thesis, 2004). The *NIC2*, representative the second member of the *NIC* family, is localised on chromosome 1 of *Arabidopsis thaliana* at the locus At1g71870. Referring to the predicted start (ATG) and stop (TAA) codons, the gene possesses two putative exons (548 bp, 983 bp) and one intron (908 bp) as shown in **Fig. 5*A***. To isolate the coding sequence of *NIC2*, pools of mRNA from four different plant parts (root, stem, rosette leaf and flower) were reverse transcribed into cDNA. Subsequently they were used as templates for PCR using the primers designed according to the predicted coding sequence of the gene. Sequencing of the PCR product revealed that the splicing of two predicted exons results in an expected open reading frame of 1533 bp, which encodes a putative protein of 510 amino acid residues (**Fig. 5*B***), and a molecular weight of 56.1 kDa (Blazej Dolniak, Master thesis, 2001). Further *in silico* analysis using Aramemnon (a membrane protein database; http://aramemnon.botanik.uni-koeln.de/), showed that NIC2 contains 11 potential transmembrane domains with the N- and C-terminii located extracellularly (**Fig. 5*C***). Analysis using subcellular localisation prediction programs, PSORT and TargetP (http://www.expasy.org/tools/) revealed no clear evidence of NIC2 localisation within the cell. Howerver, the outcome suggested that NIC2 might be localised in the plasma membrane. No signal peptide at either the N- or C-terminus of NIC2 was detected and also post-translational modifications of the protein were not detected (the ExPASy Proteomics Server).

A

ATGGAAGACAAAATCCAGTCAGATGATTTCACTTCCCATAAAAACCCAACTCTTCCTCAAGTCATTGAAGAGCTAAAAGAGCTCTGGG
CTATGGTTTTACCAATCACAGCAATGAACTGTCTTGTCTACGTGCGCGCCGTCGTGTCTGTTCTCTTCCTCGGCCGTCTCGGTAGCCT
CGAGTTAGCCGGAGGAGCTCTCTCCATCGGATTCACCAACATCACAGGATACTCTGTTATGGTTGGACTCGCCTCGGGTCTCGAGCCA
GTGTGTAGCCAAGCCTACGGTAGCAAAAACTGGGATCTCCTCACGCTCTCTCTTCACCGTATGGTCGTGATTCTCTTAATGGCCTCTC
TGCCCATAAGCCTCCTTTGGATCAACCTTGGACCCATCATGCTTTTCATGGGTCAAAACCCGGAGATAACCGCTACAGCGGCTGAATA
TTGTCTCTACGCGCTTCCTGATCTTTTGACCAATACTCTCCTTCAGCCGTTACGTGTTTATCTAAGGTCGCAGCGAGTGACGAAACCG
ATGATGTGGTGTACGCTAGCAGCAGTGGCGTTCCATGTGCCATTGAATTATTGGCTTGTGATGGTGAAGCATTGGGGTGTTCCTGGTG
TGGCTATTGCGTCTGTTGTGACGAATTTGATCATGGTTGTGCTTTTGGTTGGTTATGTTTGGGTTAGTGGGATGTTGCAGAAGAGAGT
GAGTGGTGATGGTGATGGTGGGTCTACTACGATGGTGGCGGTGGTGGCTCAGTCGTCGTCTGTGATGGAGTTGGTTGGAGGGTTGGGA
CCGTTGATGAGAGTGGCGGTTCCGAGTTGTTTGGGGATATGTTTGGAATGGTGGTGGTATGAGATTGTGATTGTGATGGGTGGTTACT
TGGAGAATCCTAAGCTTGCTGTGGCTGCCACTGGGATTTTGATTCAGACTACTAGTCTTATGTATACGGTTCCTATGGCTTTAGCTGG
ATGCGTCTCTGCTC**GG**gtatgtatctttatactttctgttatgtgaatgtaaatggtcaaaattatagttaaattaaagatgattaag
Tggtcaaaatttgagtcaaagctacaaagttgatttgagtcatgattagactaatgattagtgattaagtggtgaagatttaagtcta
Gaaaactatttgactaagttgatttgggttttgcatttgaaggttcaaaatcatgaaacttttgaatattaatttcgttttttttaaa
Aatgaattatgtggtgtttatgattgatattggaaagagtggaagtaattatattaaattaaagactaaaaagacaaaagtcttggaa
Cttgaaggtaccaaaacatttcagtagatgcaagaatgttttattcaagaaagatatgaacttttgttcttgtaattgacataagttc
Tttttctgtgtgtgtttttcgaggaccttattatgtgtttagaaggttctctgtttcctagtgattagtattttgttcgagaaaatt
Ttgaattttgttcttgtatctaattatggatttactcaagggaagttcttagaaggctctttgtttcctagttgttgttttttcttt
Ataagtttcttaacgctttttcgaaaagaagaaaagagatgataaaaaacgtgcaatgtaatgggaaaatgttacatcaacttccatt
Aataggtcactccgtggtatgtgattggacgttaacatacctaaaaataaaaatatataaaaaagtggttgaaaagagagtagtcaag
Tgtggtctatttattgttgccaatctcatgatactgttcaacctcattgatgtccttatctttccttacacgtgacaaaagtttgg
Cttcaataacttttttaagatttggtttcattgattttctc**ag**GTTGGGAACGAGCTCGGTGCAGGTAGACCTTACAAGGCCAGACTA
GCCGCGAACGTGGCTCTAGCTTGCGCGTTTGTAGTAGGAGCATTGAATGTGGCTTGGACGGTTATTCTAAAAGAGCGTTGGGCTGGAC
TATTCACTGGCTATGAGCCACTCAAGGTCTTGGTTGCTTCGGTTATGCCAATTGTCGGGCTATGCGAGCTAGGGAATTGTCCACAGAC
CACGGGCTGCGGGATTCTTAGAGGGACAGGTCGGCCTGCGGTTGGGGCACATGTGAATCTCGGGTCGTTTTATTTCGTTGGGACTCCC
GTGGCAGTTGGACTAGCGTTTTGGTTGAAAATTGGGTTTAGTGGGTTGTGGTTTGGGTTGCTTTCAGCTCAAGCGGCTTGCGTGGTTT
CGATATTGTATGCGGTTTTGGCGAGGACGGATTGGGAAGGGGAAGCCGTGAAGGCAATGAGACTGACGAGTTTGGAGATGAGGAAAGT
TGGACAAGATGAAGAGTCTTCATTGTTATTGTTGGATGATGAGAAGTTGGGTGATGTTTTG***TAA***

B

MEDKIQSDDFTSHKNPTLPQVIEELKELWAMVLPITAMNCLVYVRAVVSVLFLGRLGSLELAGGALSIGFTNITGY
SVMVGLASGLEPVCSQAYGSKNWDLLTLSLHRMVVILLMASLPISLLWINLGPIMLFMGQNPEITATAAEYCLYAL
PDLLTNTLLQPLRVYLRSQRVTKPMMWCTLAAVAFHVPLNYWLVMVKHWGVPGVAIASVVTNLIMVVLLVGYVWVS
GMLQKRVSGDGDGGSTTMVAVVAQSSSVMELVGGLGPLMRVAVPSCLGICLEWWWYEIVIVMGGYLENPKLAVAAT
GILIQTTSLMYTVPMALAGCVSARVGNELGAGRPYKARLAANVALACAFVVGALNVAWTVILKERWAGLFTGYEPL
KVLVASVMPIVGLCELGNCPQTTGCGILRGTGRPAVGAHVNLGSFYFVGTPVAVGLAFWLKIGFSGLWFGLLSAQA
ACVVSILYAVLART DWEGEAVKAMRLTSLEMRKVGQDEESSLLLLDDEKLGDVL

C

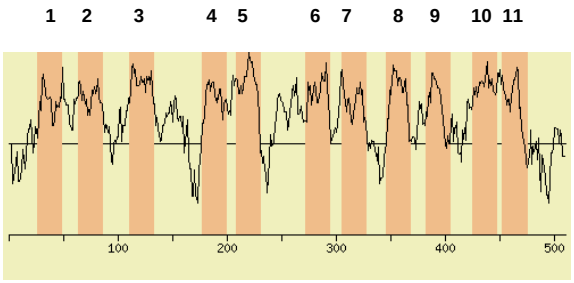

Figure 5. Sequence analysis of *NIC2*. *A*, 2440 bp genomic DNA of *NIC2*, spanning the coding region of the gene, revealed the presence of two exons; 548 bp and 983 bp, and one intron (908 bp) shown by capital and lowercase letters, respectively. The start and stop codons in exons are italicised and the spilcing sites are underlined. ***B***, The predicted protein consists of 510 amino acid residues. ***C***, A Kyte-Doolittle hydrophobicity plot of 11 potential transmembrane domains of NIC2 with N- and C-termini, which were predicted to be located extracellularly. The hydrophobicity plot was obtained from Aramemnon (http://aramemnon.botanik.uni-koeln.de/).

To classify NIC2 into known protein families, NIC2 was queried against all proteins in the NCBI database using the BLAST-P program. First, the results clearly indicated a homology

of NIC2 with the bacterial proteins NorM from *Vibrio parahaemolyticus* and YhdE/NorE from *Escherichia coli*. NorM and YdhE/NorE were the first biochemically characterised members of the multidrug and toxic compounds extrusion (MATE) family, and they have been found to pump antimicrobial agents out of bacterial cells in exchange for sodium (Morita *et al.*, 1998 and 2000). Second, NIC2 also showed homology with two MATE proteins from *Saccharomyces cerevisiae*. ERC1 effected the resistance against ethionine when the protein was overexpressed in yeast cells (Shiomi *et al.*, 1991). YDR338C, a putative protein which is a homolog of ERC1, has no known function to date. The multiple sequence alignment of NIC2, NORM, YDHE/NORE, ERC1 and YDR338C generated by the BCM Search Launcher server (http://searchlauncher.bcm.tmc.edu/) revealed that all proteins share sequence homology (**Fig. 6**). They exhibited between 23 % and 25.2 % identical and between 27 % and 35 % similar amino acid residues in overlapping regions. Based on the similarities with bacterial and yeast MATE proteins, NIC2 was also classified as a multidrug and toxic compounds extrusion protein.

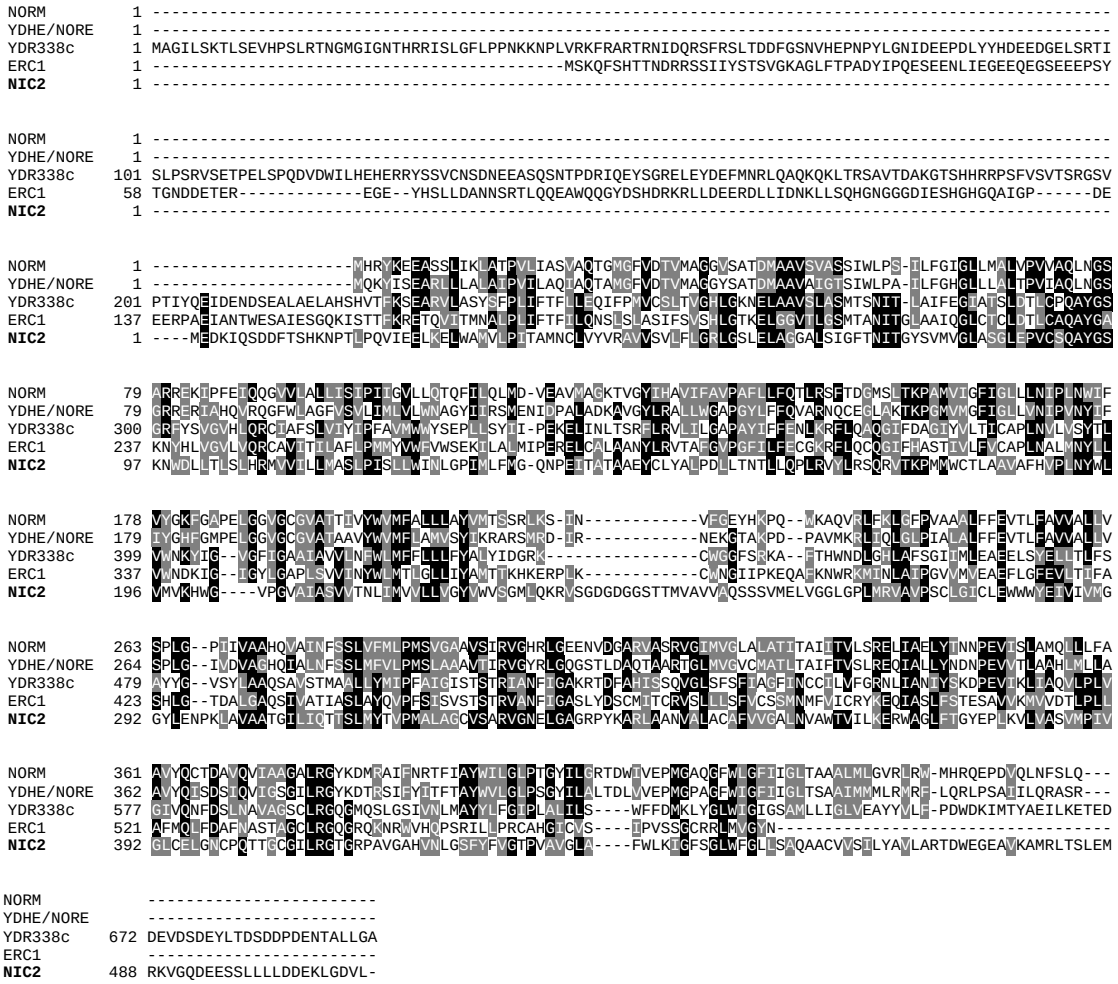

Figure 6. Alignment of the deduced amino acid sequence of NIC2 with amino acid sequences of bacterial and yeast MATE proteins. NIC2 shares a homology of 23 to 25.2% identity and 27 to 35% similarity with bacterial (*Vibrio parahaemolyticus* NORM and *Escherichia coli* YDHE/NORE) and yeast (*Saccharomyces cerevisiae* ERC1 and YDR338c) proteins. Identical amino acid residues are boxed and shown in black. Grey boxes represent positions where amino acid residue exchanges are conservative (L,I,V,M; A,S,T; F,W,Y; N,Q; D,E; and K,R) and shared by NIC2 and at least two other proteins. Numbers indicate amino acid positions.

The existance of an *Arabidopsis thaliana* MATE family was confirmed after the complete sequencing of the *Arabidopsis* genome, which revealed that there are 56 MATE family members, which is 10 times more than found in any other non-plant sequenced organism (Arabidopsis Genome Initiative, 2000). As shown in **Fig. 7**, all 56 *Arabidopsis* MATE family members can be grouped into five clusters and NIC2 was located in cluster number four. Until now, only five MATE family members, TT12 (Debeaujon *et al*., 2001), ALF5 (Diener *et al*., 2001), EDS5 (Nawrath *et al*., 2002), AtDTX1 (Li *et al*., 2002) and FRD3 (Rogers and Guerinot, 2002) were partially characterised, but only ALF5 and AtDTX1 exhibit multidrug and toxic extrusion functions.

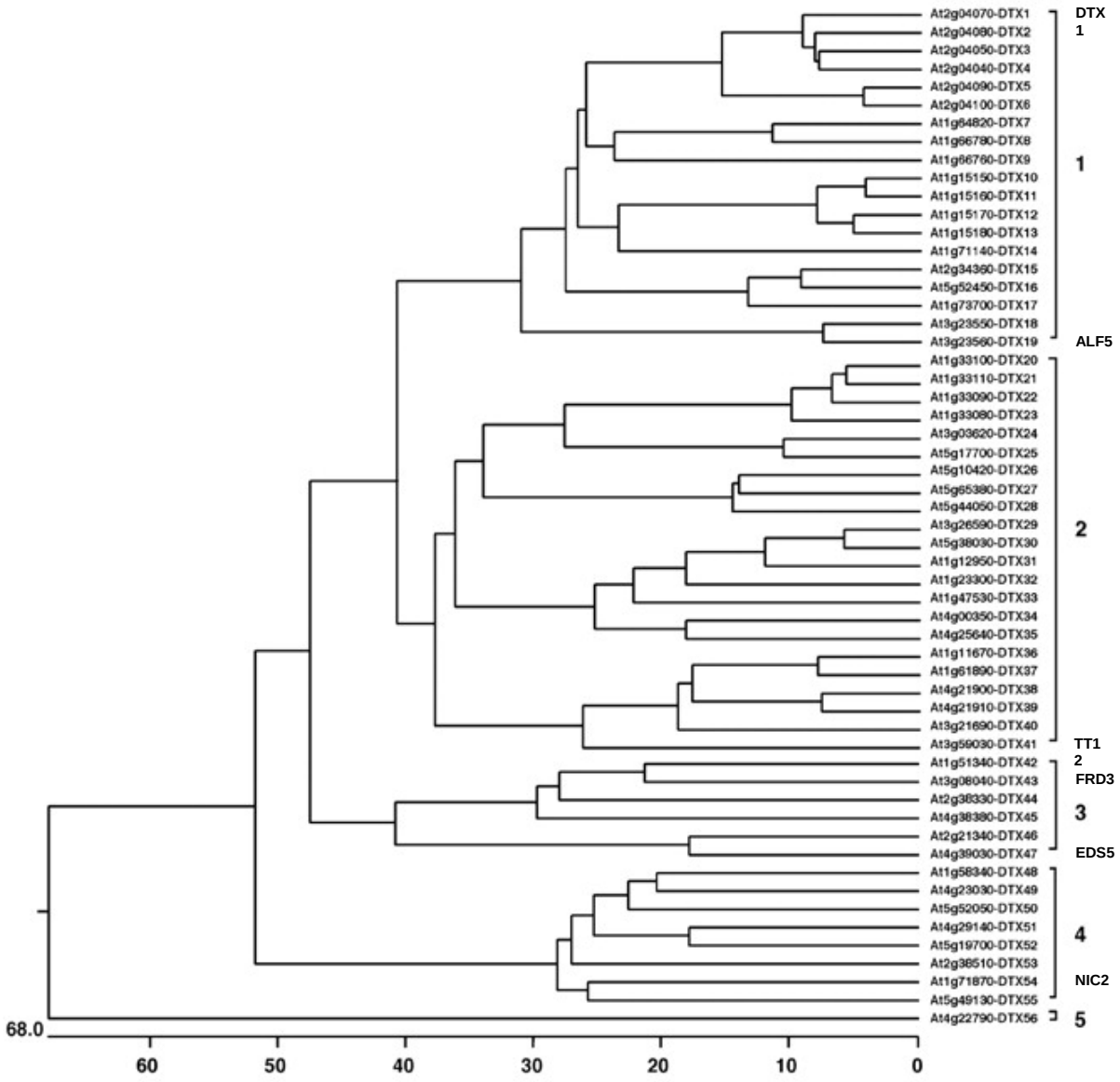

Figure 7. Phylogenetic tree of *Arabidopsis thaliana* MATE family members. The phylogenetic tree presents the relationship among NIC2 and other members of MATE family, including also the characterised proteins DTX1, ALF5, TT12, FRD3 and EDS5. The five clusters are indicated and numbered. The horizontal scale indicates the probability (%) of substitution of amino acid positions. (adapted from Li *et al*., 2002).

In order to search for motives and significant homologies among TT12, ALF5, EDS5, AtDTX1, FRD3 and NIC2, a multiple sequence alignment was performed. Although only a limited number of similar amino acid motives were found (**Fig. 8*A***), the outcome still demonstrated that NIC2 shared a meaningful sequence homology with TT12, ALF5, EDS5, AtDTX1 and FRD3, having between 21.7 % and 29.8 % identical and between 28 % and 38 % similar amino acid residues in overlapping regions. Kyte-Doolittle hydrophobicity plots

obtained from the Aramemnon database showed that all aligned proteins possess between 10 and 12 transmembrane spanning regions (**Fig. 8*B***).

A

```
ALF5      1 ------------------------------MADPATSSPLLDDHVGGEDERGRRSRSSTLVQKVID------------------------VEEAK
AtDTX1    1 ------------------------------------------MEPFLPQDEQLVPCKATWKSGQLN--------------------------VELK
TT12      1 ----------------------MSSTETYEPLLIRLHSDSQLTERSSPEIEEFLRRRGSTVTPRWWLKLA--------------------VWESK
NIC2      1 ------------------------------------------MEDKIQSDDFTSHKNPTLPQV----------------------------IEELK
FRD3      1 -------METEGDDLATVKKPIPFLVIFKDLRHVFSRDTTGREILGIAFPAALALAADPIASLIDTAFVGRLG---------------AVQLAAVGVSI
EDS5      1 MLIKSQRLTLFSPLLSKTRRIPVNSHQTLVAESVIIRRTLGAITATPSFHKNPVVIRRRIKLERVTRNCVRLDREIDEEEEEEEKERGDLVKQSIWEQMK

ALF5     42 AQMIYSLPMILTNVFYYCIPTISVMEASHLGQLELAGATLANSWATVSGFAFMVGLSG--------------SLETLCGQGFGAKRYRMLGVHLQSSCI
AtDTX1   30 KVSRLAVPMATVTIAQYLLPVISVMVAGHNGELQLSGVALATSFTNVSGFSIMFGLVG--------------SLETLSGQAYGAKQYEKMGTYTYSAIS
TT12     54 LLWTLSGASIVVSVLNYMLSFVIVMFTGHLGSLQLAGASIATVGIQGLAYGIMLGMAS---------------AVQTVCGQAYGARQYSSMGIICQRAMV
NIC2     27 ELAAVLPITAMNCLVYVRAVVSVLFLGRLGSLELAGGALSIGFTNITGYSVMVGLAS--------------GLEFVCSQAYGSKNWDLLTLSLHRMVV
FRD3     78 AIFNQASRITIFPLVSLTTSFVAEEDTMEKMKEEANKANLVHAETILVQDSLEKGISSPTSNDTNQPQQPPAPDTKSNSSNKSNKKEKRTIRTASTAMIL
EDS5    101 ELVKFTGPAYGWICGPLMSLIDTVVIGQGSSIELAALCPGTVLCDHMSYVFMFLSVA---------------TSNMVATSLAKQDKKEAQHQISVLLFI

ALF5    127 VSLVFSILITIFMFFTESIFGLIRQDPSISKQAALYMKYQAPGLLAYGFLQNILRFCQTQ--SMIAPLVIFSFVPLVINHIATAYVLVYMAGLGFIGAPIA
AtDTX1  115 SNIPICVLISILWIYMEKLLISLGQDPDISRVAGSYALRLIPTLFAHAIVLPLTRFLLAQ--GLVLPLLYFALTTLLFHIAVCWTLVSALGLGSNGAALA
TT12    139 LHLAAAVFLTFLYWYSGPILKTMGQSVAIAHIEQQIAFRGMIPQIYAFALACPMQRFLQAQ--NIVNPLAYMSLGVFLLHTLLTWLVTNVLDFGLLGAALI
NIC2    112 ILLTASLPISLLWINLGPIMLFMGQNPEITATAAEYCLYALPDLLTNTLLQPLRVYLRSQ--RVTKPMMCTLLAAVAFHVPLNYWLVMVKHWGVPGVAIA
FRD3    178 GLILGLVQAIFLIFSSKLLGVMGVKPNSPMLSPAHKYLSIRALGAPALLLSLAMQGIFRGFKDTKTPLFATVVADVINIVLDPIFIFVFRLGIIGAAIA
EDS5    186 GLVCGLMMLLLTRLFGPWAVTAFTRGKNHEIVPAANKYIQIRGLAWPFILVGLVAQSASLGMKNSWGPLKALAAATIINGLGDTILCLFLGQGIAGAAWA

ALF5    225 TSISLWHAFILGTYVMCSEKFKETWTG----------------FSLESFRYIVINLTLSLPSAAMVCLEYWAFEILVFLAGVMPNPEINTSLVAICVN
AtDTX1  213 ISVSFWFFAWTLSCYVRFSSSCEKTRRF----------------VSQDFLSSVKQFFRYGVPSAAMLCLEWWLFEILIICSGLLQNPKLETSVLSICLT
TT12    237 LSFSWWLLVAVNGMYILMSPNCKETWTG----------------FSTRAFRGIWPYFKLTVASAVMLCLEIWYNQGLVIISGLLSNPTISLDAISICMY
NIC2    210 SVVTNLIMVVLLVGYWVSGMLQKRVSGDGDGGSTTMVAVVAQSSSVMELVGGLGPLMRVAVPSCLGICLEWWYEIVIVMGGYLENPKLAVAATGILIQ
FRD3    278 HVISQYFMTLILFVFLAKKVNLIPPNFG----------------DLQFGRFLKNGLLLLARTIAVTFCQTLAAAWAARLGTTP-----WAAFQICLQ
EDS5    286 TTASQIYSAYMMDSLNKEGYNAYSFAIP----------------SPQELWKISALAAPVFISIFSKIAFYSFIIYCATSVGTHVLAAHQVMAQTY

ALF5    308 TEATSYMLTYGLSAAASTRVSNELGAGNVKGAKKATSVSKISLVLALGVVIVLLVGIDGVGLFSDSYVIKEEFASLRFFLAASITLDSIQGVLSGVAR
AtDTX1  296 TATLHYVIPVGVAAAISTRVSNKLGAGIPQVARVSVLAGLCLWLVESSFFSILLFAFRNIIGYAFSNSKEVVDYVADLSPLLCLSFVLDGFTAVLNGVAR
TT12    320 YLNWDMQFMLGLSAAISVRVSNELGAGNPRVAMLSVVVNITTVLISSVLCVIVLVFRVGLSKAFTSDAEVIAAVSDLFPLLAVSIFLNGIQPILSGVAI
NIC2    310 TTSLMYTVPMALAGCVSARVGNELGAGRPYKARLAANVALACAFVVGALNVAWTVILKERWAGLFTGYEPLKVLVASVMPIVGLCELGNCPQTTGCGILR
FRD3    354 VWLTSSLLNDGLAVAGQAILACSFAEKDYNKVTAVASRVLQMGFVLGLGLSVFVGLGLYFGAGVFSKDPAVIHLMAIGIPFIAATQPINSLAFVLDGVNF
EDS5    366 RMCNVMGEPLSQTAQSFMPEMLYGANRNLPKARTLLKSLMIIGATLGLVLGVIGTAVPGLFPGVYTHDKVIISEMHRLLIPFFMALSALPMTVSLEGTLL

ALF5    408 GCGWQRLVTVINLATFYLIGMPIAAFCGFKLKFYAKGLWIGLICGIFCQSS--SLLLMTIFRKVTKLNVATV----------------------------
AtDTX1  396 GCGWQHIGALNNVVAYYLVGAPVGIYLAFSCELNGKGLWCGVVVGSAVQAT--ILAIVTASMNWKEQVRAYYNTFFFFNSLK-----------------
TT12    420 GSGWQALVAYVNLVTYYVIGLPIGCVLGFKTSLGVAGIWWGMIAGVILQTL--TLIVLTLKTNWTSEVENAAQRVKTSATENQEMANAGV----------
NIC2    410 GTGRPAVGAHVNLGSFYFVGTPVAVGLAFWLKIGFSGLWFGLLSAQAACVVS-ILYALARIDWEGEAVKAMRLTSLEMRKVGQDEESSLLLLDDEKLGD
FRD3    454 G---ASDFAYTAYSMVGVAAISIAAVIYMAKTNGFIGIWIALTIYMALRAITGIARMATGTGPWRFLRGRSSSSSS----------------------
EDS5    466 AG--RDLKFYSSVMSSFFIGCLTLMFVTRSGYGLLGCWFVLVGFQWGRFG---LYLRRLLSPGGILNSDGPSPYTVEKIKSI----------------

ALF5        --
AtDTX1      --
TT12        --
NIC2    509 VL
FRD3        --
EDS5        --
```

B

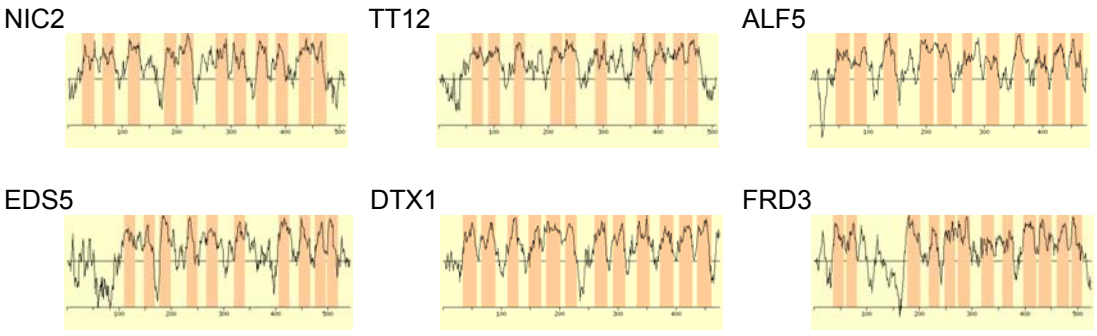

Figure 8. Sequence analysis of NIC2 and characterised *Arabidopsis* MATE family members. *A*, Amino acid alignment of NIC2 and selected *Arabidopsis* MATE family members identifies motives that share between 21.7 % and 29.8 % identical amino acid residues in overlapping regions. Identical amino acid residues are boxed and shown in black. Grey boxes represent positions where amino acid residue exchanges are conservative (L,I,V,M; A,S,T; F,W,Y; N,Q; D,E; and K,R) and shared by NIC2 and at least two other proteins. ***B***, Kyte-Doolittle hydrophobicity plots of NIC2, TT12, ALF5, EDS5, DTX1 and FRD3 presenting that all proteins share between 10 and 12 potential transmembrane domains which are indicated by pale orange bars. The hydrophobicity plots were obtained from Aramemnon (http://aramemnon.botanik.uni-koeln.de/).

1.2. Isolation of *NIC2* cDNA

As mentioned above, the expression of *NIC2* was initially unknown, and to isolate the *NIC2* cDNA by PCR, the primers *NIC2*for and *NIC2*rev, and a pool of first-strand cDNAs from primary and secondary roots, rosette leaves, inflorescence stems and flowers of 45-day-old *Arabidopsis thaliana* (L.) Heynh. C24 wild-type were used as a template. This approach produced the spliced coding sequence of *NIC2* without the intron. The subsequent sequencing in comparison with the expression sequence tag (EST), found recently in the NCBI database (last update 23.02.2004), confirmed that the splicing of *NIC2* coding sequences was correct.

NIC2 cDNA was TA-cloned into either pCR®2.1 or pGem®–T Easy vectors. The pCR®2.1::*NIC2* and pGem®–T Easy::*NIC2* constructs were then used for further subclonings into various vectors in order to characterise *NIC2* in heterologous and homologous expression systems.

Functional characterisation of *NIC2* in various heterologous systems

To investigate the function of *NIC2*, which based on sequence homology, is classified as a putative multidrug and toxic compounds extrusion protein, three various heterologous expression systems were used: the prokaryotic organism *Escherichia coli*, and two eukaryotic organisms, yeast *Saccharomyces cerevisae* and oocytes from *Xenopus laevis*.

2.1. *Escherichia coli* KAM3 as an expression host system

Up to date several multidrug efflux transporters from different bacteria and one from *Arabidopsis thaliana* (AtDTX1) were functionally characterised using the TG1 *E. coli* mutant, KAM3 (Morita *et al*., 1998 and 2000; Miyamae *et al*., 2001; Chen *et al*., 2002; Braibant *et al*., 2002; Li *et al*., 2002; Xu *et al*., 2003). KAM3 had a deletion in the *acrAB* region, which encodes the major multidrug efflux system of *E. coli* (Ma *et al*., 1995; Nikaido and Zgurskaya, 2001) The cells were therefore sensitive to many toxins and drugs which are known to be substrates of the AcrAB system. Based on the drug and toxin sensitivity, the expression of a

putative multidrug efflux transporter might be able to complement the growth of the KAM3 cells compared to the parental TG1 cells. Such complementation depends on drugs or toxins applied to the medium. Therefore, before the functional characterisation of NIC2 in KAM3 cells was performed, the drug and toxic susceptibilities of the parental TG1 and the KAM3 cells were examined in detail in drop test experiments. Both bacterial strains with the same amount of cells (0.1 at OD_{600}) were grown for 24 to 48 h at 37°C on YT-agar plates supplemented with various concentrations of different toxic compounds. It was found that the KAM3 cells, in contrast to the parental TG1 cells, exhibited high sensitvities to all substances tested (**Fig. 9**) which was consistent with the published reports (Nikaido, 1996; Yang *et al.*, 2003). They showed elevated susceptibilities to Norfloxacin (**Fig. 9.*1***), Berberine (**Fig. 9.*2***), Acriflavine (**Fig. 9.*3***), Ethidium bromide (**Fig. 9.*4***), Tetraethylammonium chloride (TEACl) (**Fig. 9.*5***) and Tetramethylammonium chloride (TMACl) (**Fig. 9.*6***). The parental TG1 cells were resistant to all drugs tested. In addition, growth of both bacterial strains were also examined in the presence of Ciprofloxacin, DL-Ethionine and Fluoro-3-indolyl-acetic acid (F-IAA). When TG1 and KAM3 cells were compared, no differential growth was observed (data not shown), indcating that both bacterial strains were sensitive to these toxins.

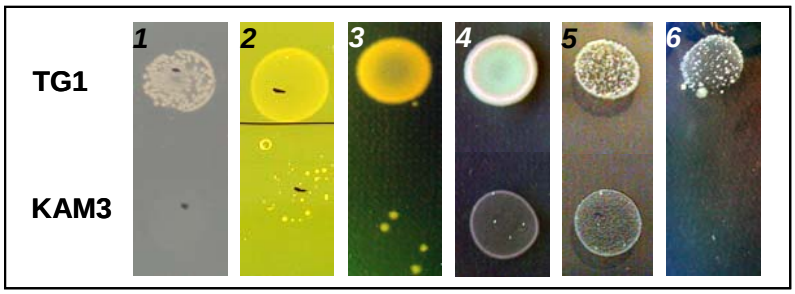

Figure 9. Susceptibilities of TG1 and KAM3 cells to different toxic compounds. Growth of TG1 and KAM3 strains on YT-medium supplemented with *(**1**)*, 0.1 µg/ml Norfloxacin, (***2***), 25 µg/ml Acriflavine, *(**3**),* 200 µg/ml Berberine, *(**4**)*, 15 µg/ml Ethidium bromide, *(**5**)*, 0.6 M TEACl and *(**6**),* 0.75 M TMACl. Equal amount of TG1 and KAM3 cells were grown for 48 h at 37°C. Growth of TG1 and KAM3 strains on medium with 1 µg/ml Ciprofloxacin, 1.2 mM DL-Ethionine and 3 mM Fluoro-3-indolyl-acetic acid is not shown.

The minimum inhibitory concentrations (MICs) for the all tested substances were also measured and are summarised in **Table 2**. The MICs were determined as the lowest concentrations of antimicrobial agents at which bacterial cells were almost unable to grow.

Table 2. Susceptibilities of *Escherichia coli* TG1 and KAM3 towards different toxic compounds

Compound	MIC (µg/ml)*	
	TG1	**KAM3**
Norfloxacin	0.1	0.025
Ciprofloxacin	1	1
Acriflavine	35	12
Berberine	300	100
Ethidium bromide	25	15
Tetraethylammonium chloride	2485 (0.6 M)	1670 (0.4 M)
Tetramethylammonium chloride	2100 (0.75 M)	1640 (0.6 M)
DL-Ethionine	4.9 (1.2 mM)	4.9 (1.2 mM)
Fluoro-3-indolyl-acetic acid	14.5 (3 mM)	14.5 (3 mM)

* MIC is the lowest concentration of antimicrobial agent at which bacterial cells are almost unable to grow.

2.2. Expression and functional characterisation of *NIC2* in *E. coli* KAM3

The differential drug susceptibilities of the parental *E. coli* TG1 and KAM3 cells were used for the functional characterisation of *NIC2*. The cDNA of *NIC2* was subcloned into an expression vector and then transformed into KAM3 cells. The cells were grown on YT-medium supplemented with drugs and toxins in order to search for the complemenation in comparison with the parental cells TG1. Additionally, the open reading frame of *Escherichia coli* MATE protein, *YDHE/NORE*, was cloned from chromosomal DNA into an expression vector *via* a TA-cloning plasmid. According to the literature (Morita *et al*., 1998 and 2000; Yang *et al.*, 2003) *YDHE/NORE* (1374 bp), encodes a 12 transmembrane spanning integral inner membrane protein, which is a Na^+-driven multidrug efflux pump able to complement the growth of KAM3 cell on media containing toxic compounds like Norfloxacin, Ethidium bromide, Acriflavine and Berberine. In the following experiments, KAM3 cells transformed with *YDHE/NORE* were therefore used as a positive control. In order to search for novel extrusion toxic compounds, new drugs such as TEACl, TMACl and F-IAA were also tested.

- **IPTG-induced expression system**

The cDNA of *NIC2* and the open reading frame of *YDHE*/*NORE* were subcloned into the QIA*express* pQE30 vector which were then transformed into KAM3 cells. The pQE30 vector contains an optimised T5 promoter and two *lac* operator sequences which allow for a high expression of NIC2 and YDHE/NORE after induction with 1 mM IPTG. To perform the experiment, parental TG1 cells, non-transformed KAM3, and KAM3 transformed with either pQE30::*NIC2* or pQE30::*YDHE*/*NORE* were grown overnight on YT-agar plates containing various toxins and 1 mM IPTG. In parallel, for KAM3 transformed with pQE30::*NIC2* and with pQE30::*YDHE*/*NORE*, the experiment was also performed without IPTG. As shown in **Fig. 10**, in the presence of IPTG and the toxins Norfloxacin (**Fig. 10*A***), Acriflavine (**Fig. 10*C***), Ethidium bromide (**Fig. 10*E***), or Berberine (**Fig. 10*G***) the parental TG1 and KAM3 cells grew as expected from previous experiments (see above; **Fig. 9**). However, growth in the presence of TEACl (**Fig. 10*J***) and TMACl (**Fig. 10*M***) was different.

KAM3 cells carrying *YDHE*/*NORE* did not grow on YT-media supplemented with Norfloxacin (**Fig. 10*B***), Acriflavine (**Fig. 10*D***) and Ethidium bromide (**Fig. 10*F***) in the presence or absence of IPTG (depicted in **Fig. 10** as ***+/-***). These toxic compounds completely inhibited growth of the cells. The cells grew much better on YT-medium supplemented with Berberine, TEACl and TMACl, but their growth was dependent on the application of IPTG. The presence of 1 mM IPTG (**Fig. 10*H***, **10*K*** and **10*N***) significantly retarded their growth indicating that expression of *YDHE*/*NORE* itself had an adverse effect when encoded by the plasmid, while the lack of IPTG in the medium caused better growth (**Fig. 10*I***, **10*L*** and **10*O***). KAM3 cells carrying *NIC2* showed no growth in the presence of all tested drug and toxic compounds, which were additionally supplemented with or without IPTG (**Fig. 10*B***, **10*D***, **10*F***, **10*H*** and **10*I***, **10*K*** and **10*L***, **10*N*** and **10*O***).

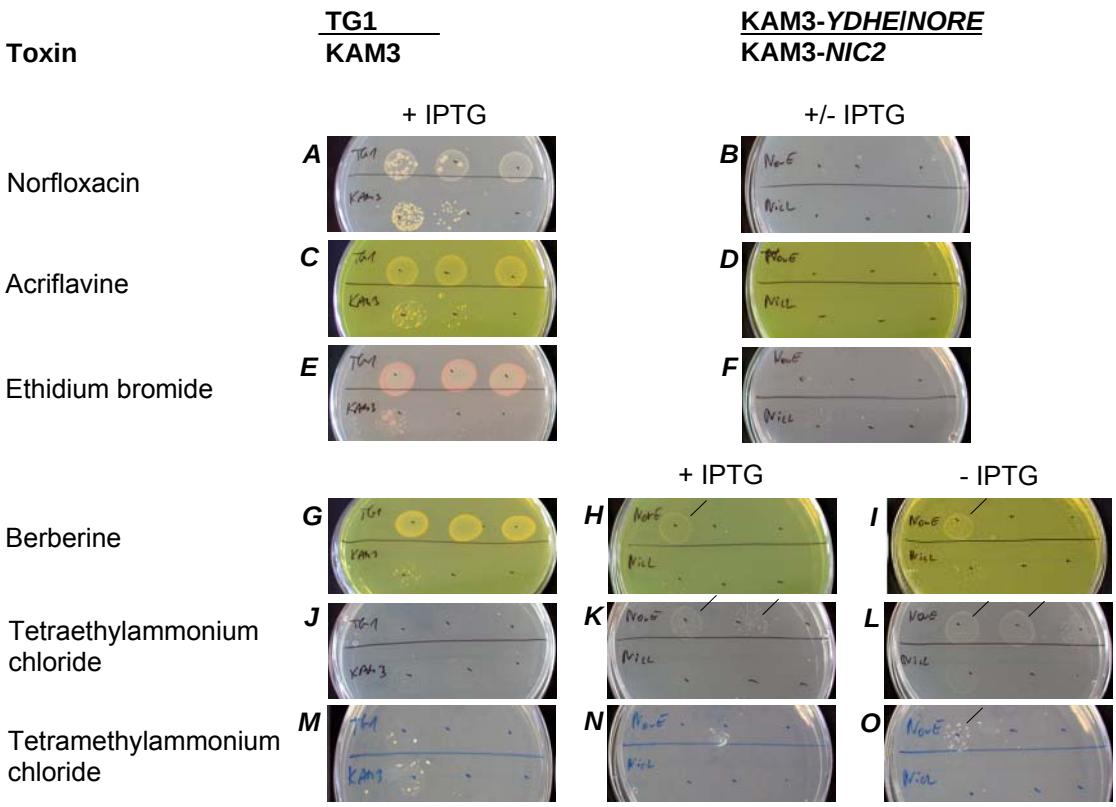

Figure 10. Susceptibilities of TG1, KAM3, KAM3-*YDHE/NORE* and KAM3-*NIC2* cells towards different toxic compounds in the presence or absence of 1 mM IPTG. The growth of serial dilutions of TG1 and KAM3 strains on YT-medium containing 1 mM IPTG and 0.1 µg/ml Norfloxacin (***A***), 25 µg/ml Acriflavine (***C***), 15 µg/ml Ethidium bromide (***E***), 200µg/ml Berberine (***G***), 0.6 M TEACl (***J***) and 0.75 M TMACl (***M***). The growth of serial dilutions of KAM3-*YDHE/NORE* and KAM3-*NIC2* strains on YT-medium supplemented with 0.1 µg/ml Norfloxacin (***B***), 25 µg/ml Acriflavine (***D***), 15 µg/ml Ethidium bromide (***F***) with or without 1 mM IPTG depicted as ***+/-*** IPTG. KAM3-*YDHE/NORE* and KAM3-*NIC2* growth on 200 µg/ml Berberine, 0.6 M TEACl and 0.75 M TMACl in the presence (***H***, ***K*** and ***N***) or absence (***I***, ***L*** and ***O***) of 1 mM IPTG, respectively. Arrow heads point at differential growth of the KAM3-*YDHE/NORE* strain in the presence or absence of 1 mM IPTG.

The results showed that the IPTG-induced expression of *NIC2* did not complement the growth of KAM3 cells on YT-agar plates supplemented with Norfloxacin, Acriflavine, Ethidium bromide, Berberine, TEACl or TMACl. The growth of KAM3 cells was partly complemented by YDHE/NORE expression when grown in the presence of Berberine, TEACl and TMACl, but was completely inhibited by Norfloxacin, Acriflavine and Ethidium bromide.

- **Host-induced expression system**

To further investigate the function of *NIC2* using KAM3 cells, a new expression system was established. The cDNA of *NIC2* was TA-cloned into pGem®–T Easy vector. As a promoter-sequence, the 858 bp upstream flanking sequence of *YDHE/NORE* was subcloned upstream of the ATG start codon of *NIC2*. In addition, a bacterial DNA consisting of the *YDHE*/*NORE*, the 858 bp upstream flanking sequence and the 662 bp downstream flanking sequence was also cloned into pGem®–T Easy vector and after transformation of KAM3 cells used as a positive control. The time and level of *NIC2* and *YDHE*/*NORE* expression was dependent on the 856 bp upstream flanking sequence of the latter and on the toxins specific for YDHE/NORE (Morita *et al.*, 1998 and 2000; Yang *et al.*, 2003). TG1, KAM3, KAM3 transformed with pGem®–T Easy::*NIC2* and pGem®–T Easy::*YDHE/NORE* were grown overnight at 30°C in the presence of various toxic compounds which were spotted on the filter discs. The concentrations of the applied toxins in the filter growth assays were either similar or higher than already tested. The drug and toxic compound susceptibilites of the parental TG1 and KAM3 cells were still very similar to the results shown in **Fig. 9** and in **Table 2**. Again, KAM3 cells (**Fig. 11*A2*** to **11*G2***), in contrast to the parental TG1 cells (**Fig. 11*A1*** to **11*G1***), were more susceptible to the toxic compounds (40 µg/ml Acriflavine, 200 µg/ml Berberine, 100 µg/ml Ethidium bromide, 0.05 µg/ml Norfloxacin, 4 M TEACl, 4 M TMACl, and 2 mM F-IAA spotted on the filter discs). KAM3 cells transformed with pGem®–T Easy::*NIC2* showed elevated growth resistance towards TEACl (**Fig. 11*E4***), TMACl (**Fig. 11*F4***) and F-IAA (**Fig. 11*G4***) which was similar to the resistance of the parental TG1 cells (**Fig. 11*E1***, **11*F1*** and **11*G1***). KAM3 cells carrying pGem®–T Easy::*NIC2* additionally exhibited growth sensitivities similar to those of non-transformed KAM3 cells to Acriflavine, Berberine, Ethidium bromide and Norfloxacin (**Fig. 11*A4*** to **11*D4***). KAM3 cells carrying pGem®–T Easy::*YDHE/NORE* showed an elevated growth resistance only for Norfloxacin (**Fig. 11*D3***) compared to non-transformed KAM3 and parental TG1 cells. Moreover, these cells grew like non-transformed KAM3 cells in the presence of Acriflavine, Berberine,

Ethidium bromide, TEACl, TMACl and F-IAA (**Fig. 11*A3*** to **11*C3*** and **11*E3*** to **11*F3***, respectively), showing no elevated resistance to the applied toxins.

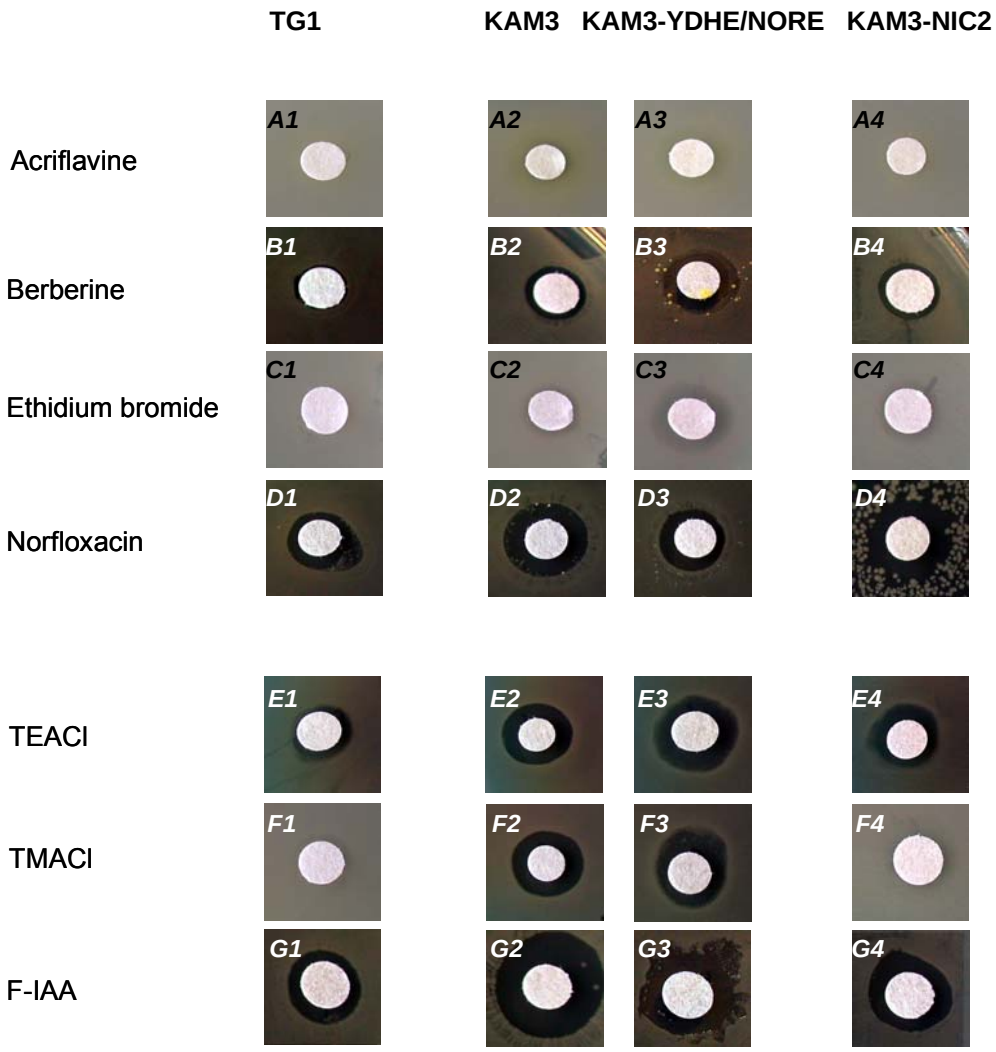

Figure 11. Filter growth assay for TG1, KAM3, KAM3 transformed with pGem®–T Easy*::YDHE/NORE* and KAM3 transformed with pGem®–T Easy::*NIC2*. The growth of parental TG1 cells (***A1*** to ***G1***), KAM3 mutant cells (***A2*** to ***G2***), KAM3 with pGem®–T Easy*::YDHE/NORE* (***A3*** to ***G3***) and KAM3 with pGem®–T Easy::*NIC2* (***A4*** to ***G4***) on agar plates in the presence of 40 µg/ml Acriflavine (***A*** series), 200 µg/ml Berberine (***B*** series), 100 µg/ml Ethidium bromide (***C*** series), 0.05 µg/ml Norfloxacin (***D*** series), 4 M TEACl (***E*** series), 4 M TMACl (***F*** series) and 2 mM F-IAA (***G*** series) spotted on filter discs. The growth of bacterial cells was performed at 30°C for 24 h.

This data demonstrated that in the presence of TEACl, TMACl and F-IAA the growth of KAM3 cells was complemented by *NIC2*, while YDHE/NORE complemented growth of KAM3 cells only in the presence of Norfloxacin accodringly to the published data (Morita *et al*., 1998).

3.1. *Saccharomyces cerevisiae* as an expression host system

Among all proteins (~ 6300) from the yeast *Saccharomyces cerevisiae*, only two, ERC1 and its homologue - YDR338c, were classified as members of the MATE family (Brown *et al*., 1999 and *Saccharomyces* Genome Database). To create a sensitive tool similar to *E. coli* KAM3 cells, three different yeast mutant strains *ydr338c*, *erc1* and *ydr338c erc1* generated by EUROSCARF were functionally characterised. Based on the procedure of Shiomi *et al*. (1991 and 1995), the mutant strains, as well as the parental strain BY4741, were grown for 20 h at 30°C in SC-medium supplemented with 2 % galactose and increasing concentrations of DL-Ethionine (0 mM to 1.5 mM). After inoculation with OD_{600} 0.01, the growth of cells in various concentrations of DL-Ethionine was calculated and given as a percentage of surviving cells. As shown in **Fig. 12**, the *erc1* strain exhibited a slightly elevated resistance to DL-Ethionine, compared with the parental strain BY4741 and other mutant strains. To confirm these results, decreasing amounts of cells (0.1 and 0.01 at OD_{600}) of the parental strain BY4741 and the mutant strains were spotted as drops on SC-agar plates containing 0.6 mM, 1 mM, 1.2 mM and 1.25 mM of DL-Ethionine and were grown for 24 h. Although the experiment was repeated three times, no differential growth was observed (data not shown). These results were in contrast to those shown in **Fig. 12**, especially with respect to the *erc1* strain.

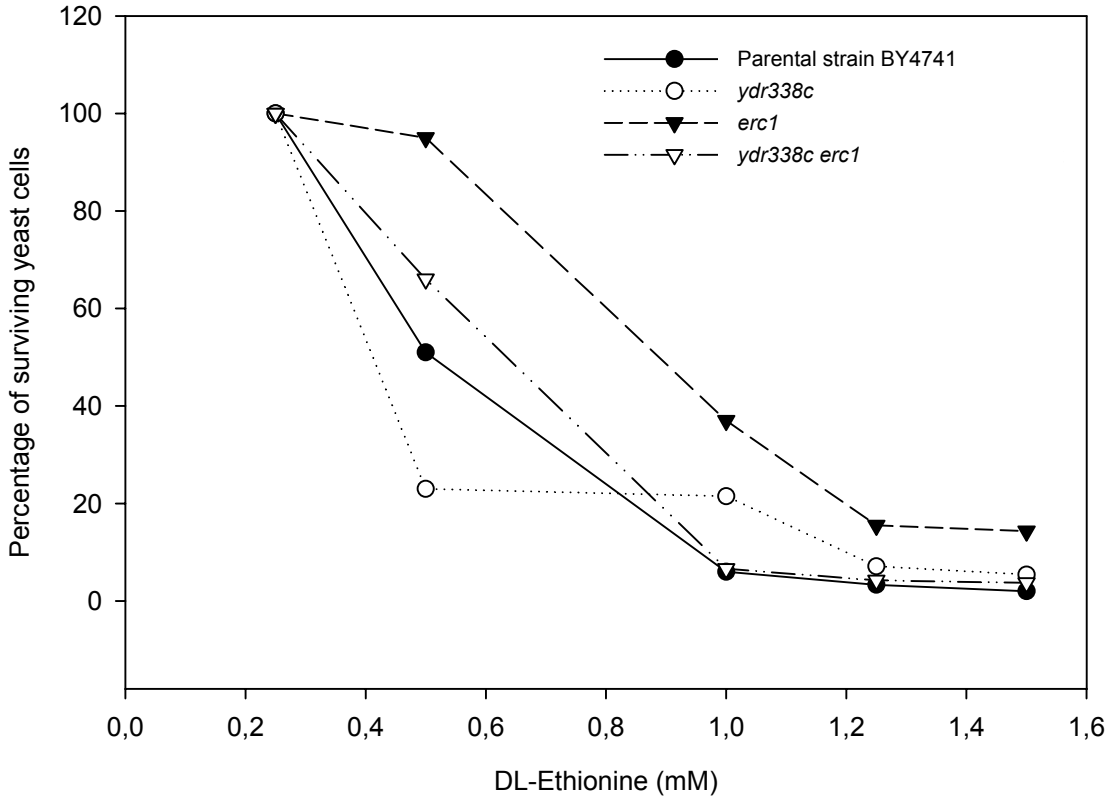

Figure 12. Percentage of surviving yeast cells after growth with DL-Ethionine. Percentage of surviving cells of the parental strain BY4741 and the mutant strains (*ydr338c*, *erc1* and *ydr338c erc1*) after 20 h at 30°C in the presence of 0.25 mM, 0.5 mM, 1 mM, 1.25 mM and 1.5 mM of DL-Ethionine. Growth of yeast cells in the absence of DL-Ethionine was taken as 100 %.

Due to the classification of YDR338c and ERC1 as MATE transporters, the single and double mutant strains as well as the parental strain BY4741 were also tested for susceptibilities to the drug and toxic compounds previously described. All yeast strains were grown on SC-agar plates supplemented with various concentrations of drug and toxic compounds, which are summarised in **Table 3**. Although the cells were grown as drops with three different concentrations (0.1, 0.01 and 0.001 at OD_{600}), no differential growth was observed after 24 h at 30°C (data not shown).

Because the MATE mutant strains exhibited no detectable susceptibilties to any of the drugs and toxic compounds tested when grown on plates, the functional characterisation of *NIC2* was performed only in the parental strain BY4741 of *S. cerevisiae*.

Table 3. Concentrations of drug and toxic compounds used to characterise the mutant yeast strains *ydr338c*, *erc1* and *ydr338c erc1*

Drug/Toxic Compound	Concentration
Acriflavine	4–250 µg/ml
Berberine	0.2-1 mg/ml
Ciprofloxacin	10-100 µg/ml
Chloramphenicol	1-5 µg/ml
Ethidium bromide	10-100 µg/ml
Norfloxacin	0.05-100 µg/ml
SDS	5-7.5 %
TEACl	0.25-0.8 M
TMACl	0.5-1 M

3.2. Expression and functional characterisation of *NIC2* in *S. cerevisiae* strain BY4741

The cDNA of *NIC2* was subcloned from the pCR®2.1 plasmid into the pYES2 vector using *Eco*RI and *Xba*I restriction sites. The construct pYES2::*NIC2* was then transformed into the *S. cerevisiae* yeast strain BY4741 and as a control the yeast cells were transformed with the empty pYES2 vector. After transformation, total RNA was extracted and tested using Northern blot experiments for the presence of *NIC2* transcript. The RNA from yeast cells transformed by the empty pYES2 vector served as a negative control (**Fig. 13**).

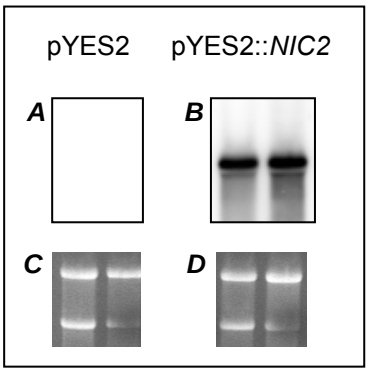

Figure 13. Detection of *NIC2* transcript by Northern blot analysis. Hybridisation signals of radiolabeled *NIC2* cDNA (visualised by autoradiography) from the RNAs extracted from two independent yeast cultures transformed with the empty pYES2 vector (***A***) or with pYES2::*NIC2* (***B***). The quality and quantity of RNA before blotting and hybridisation is shown in ***C*** and ***D***, where ***C*** corresponds to ***A***, and ***D*** to ***B***, respectively.

- **Drop test experiments**

Multidrug efflux pumps of the MATE family use either a Na^+ or a H^+ gradient across a membrane as a driving force. To test whether NIC2 functions in a smiliar way, which may confer tolerance to high, hence toxic, concentration of ions, yeast cells were grown in various concentrations of different salts. Monovalent and divalent inorganic cations including lithium, potassium, sodium and calcium were used. The growth experiments were performed as drop tests using decreasing cell concentrations (0.1, 0.01 and 0.001 at OD_{600}) of yeast cells transformed with empty pYES2 vector or pYES2::*NIC2*. The cells were grown at 30°C on SC-agar plates containing different salts (**Fig. 14**).

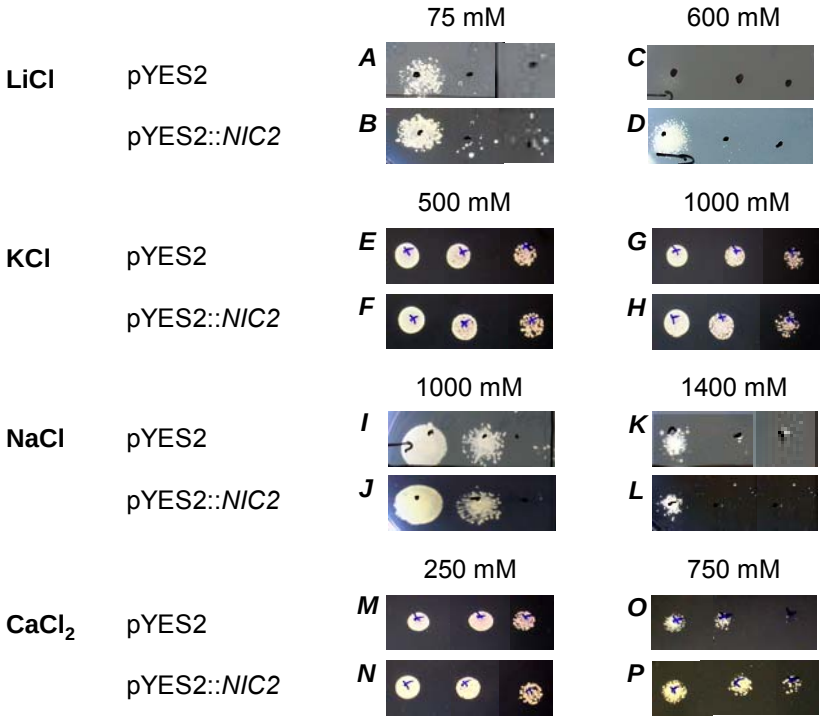

Figure 14. Drop test experiments of yeast cells transformed with pYES2 or pYES2::*NIC2*. The growth of serial dilutions (OD_{600nm} 0.1, 0.01 and 0.001) of yeast cells on SC-agar plates with 2 % galactose in the presence of two different concentrations of LiCl (75 mM and 600 mM; ***A*** to ***D***), KCl (500 mM and 1000 mM; ***E*** to ***H***), NaCl (1000 mM and 1400 mM; ***I*** to ***L***) and $CaCl_2$ (250 mM and 750 mM; ***M*** to ***P***). The yeast grew at 30°C from 1 to 10 days, depending on the applied concentrations of salts.

Very similar growth behaviour of yeast cells carrying pYES2 and pYES2::*NIC2* was observed at 500 mM (**Fig. 14*E*** and **14*F***) and 1000 mM KCl (**Fig. 14*G*** and **14*H***), at 1000 mM (**Fig. 14*I*** and **14*J***) and 1400 mM NaCl (**Fig. 14*K*** and **14*L***), and at 250 mM (**Fig. 14*M*** and **14*N***) and 750 mM $CaCl_2$ (**Fig. 14*O*** and **14*P***). Additionally, several intermediate concentrations of the

salts were also tested, but no differencies in growth was observed (data not shown). Although a similar growth phenotype was observed at 75 mM of LiCl (**Fig. 14*A*** and **14*B***), in the presence of highly increased LiCl, e.g. 600 mM (**Fig. 14*C*** and **14*D***), the yeast carrying pYES2::*NIC2* was able to grow, whereas control cells did not. Again, several intermediate concentrations of LiCl (150 mM, 300 mM and 450 mM) were tested. The differential growth of yeast carrying pYES2 or pYES2::*NIC2* became apparent at 150 mM of LiCl, while at 300 mM and 450 mM LiCl only the *NIC2* expressing yeast could grow (data not shown). To further confirm the results, the yeast cells were also grown in liquid SC-medium supplemented with various concentrations of LiCl. Although no difference of yeast growth was detected in the presence of NaCl, this salt was also tested in the following experiments, because Na^+ is a less toxic analogue of Li^+.

- **Lithium and sodium chloride growth experiments**

For every experiment the growth of five independent yeast transformants containing the empty pYES2 vector or pYES2::*NIC2* was monitored by measurement of the optical density of the cell culture at 600nm. The growth curves of the pYES2 containing strains were taken as references. The first growth experiments were done in media containing increasing amounts of lithium chloride. In the media where no LiCl was added (**Fig. 15*A***), the yeast cells showed the same indistinguishable growth behaviour. This was irrespective of whether or not *NIC2* cDNA was expressed in yeast and also indicated that its expression did not affect yeast viability. When concentration of LiCl in the growth medium was increased to 300 mM (**Fig. 15*B***) and then 600 mM (**Fig. 15*C***), the yeast strain expressing *NIC2* exhibited growth phenotypes significantly different from those observed in the yeast transformed with the empty pYES2 vector. The results indicated that the expression of *NIC2* in yeast cells, conferred tolerance to LiCl.

Following the lithium experiments, yeast cell tolerance was also tested in media containing increasing amounts of NaCl. Because sodium ions are less toxic than lithium ions, their concentrations were increased up to 1600 mM in the experiments. The growth of five

independent yeast transformants containing the empty pYES2 vector or pYES2::*NIC2* was recorded by OD_{600} measurements. The growth in media where no NaCl was added was examined and no differences were detected between the strains (**Fig. 16*A***). By increasing the NaCl concentrations to 900 mM (**Fig. 16*B***) and then to 1600 mM (**Fig. 16*C***), it was possible to detect a slight increase in the NaCl tolerance for *NIC2* expressing yeast compared to yeast carrying the empty pYES2 vector. A NaCl concentration higher than 1600 mM entirely inhibited the growth of all yeast strains. The results indicate that the expression of *NIC2* in yeast cells slightly increases tolerance to NaCl.

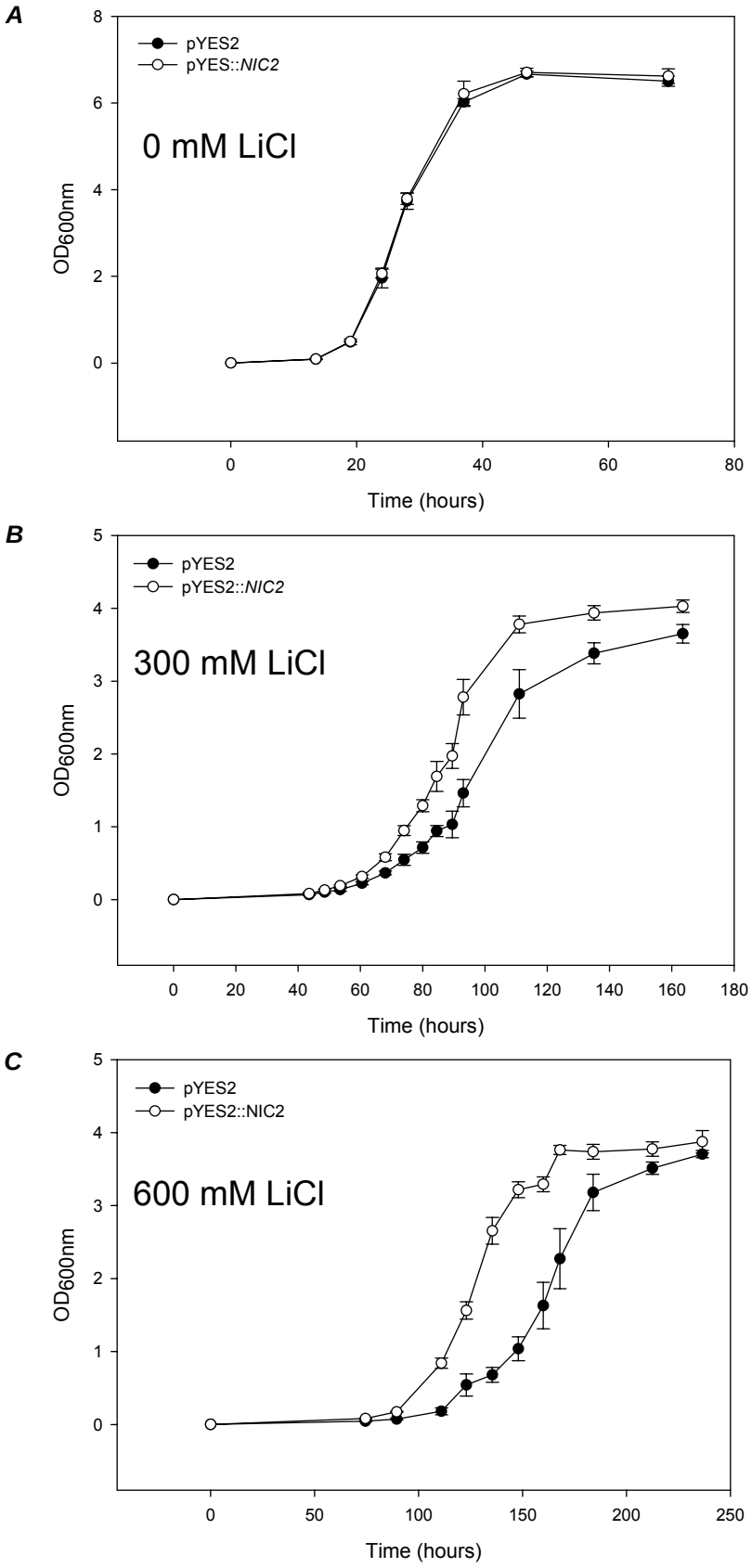

Figure 15. Yeast growth at increasing concentrations of LiCl. Growth responses to LiCl at concentrations of 0 mM (***A***), 300 mM (***B***) and 600 mM (***C***) of the yeast cells transformed with the empty pYES2 vector or the vector pYES2::*NIC2*. Yeast cultures grew in SC-medium without uracil at 30°C. Each OD_{600nm} value was calculated from five independent measurements. Error bars represent means ± SD.

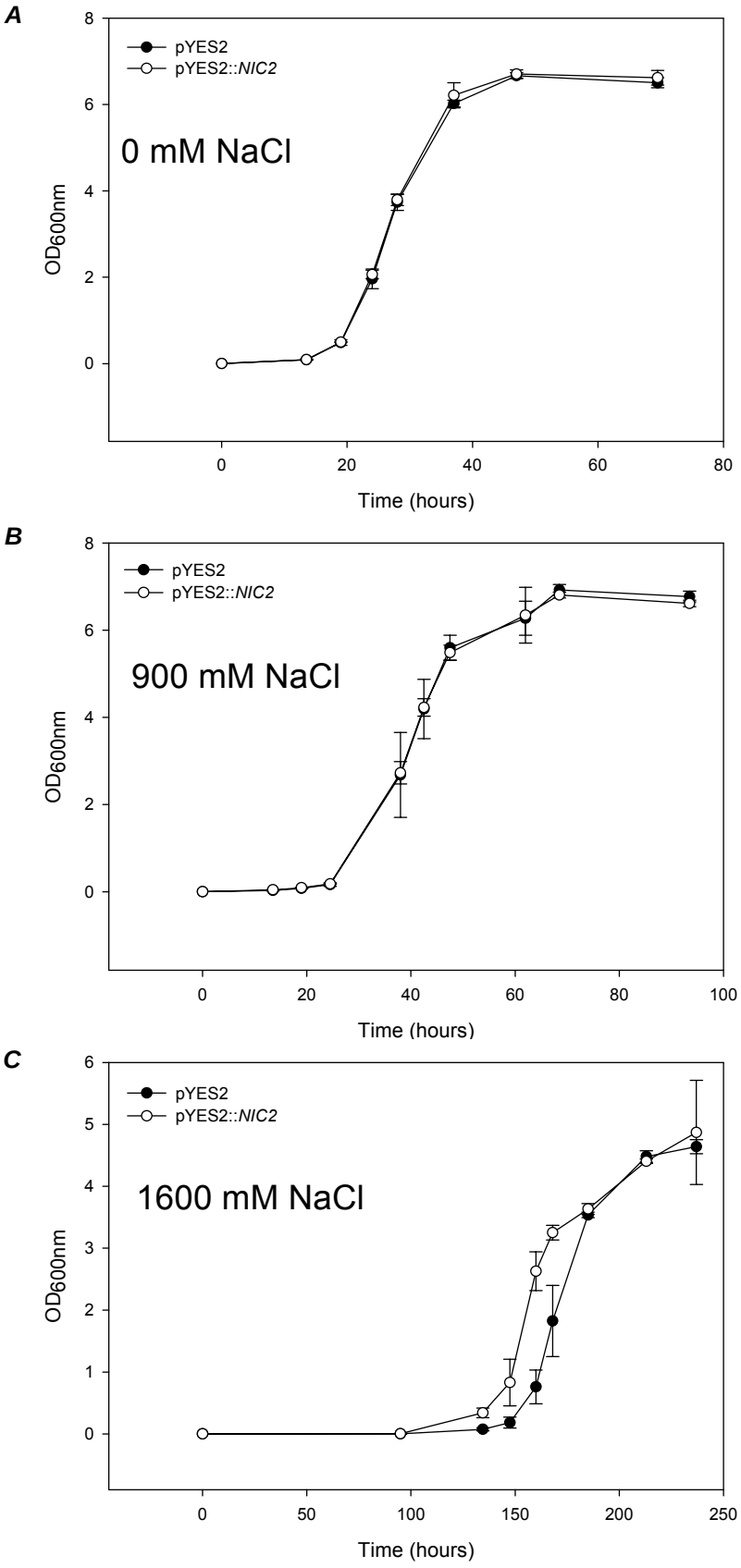

Figure 16. Yeast growth at increasing concentrations of NaCl. Growth responses to NaCl at concentrations of 0 mM (***A***), 900 mM (***B***) and 1600 mM (***C***) of the yeast cells transformed with the empty pYES2 vector or the vector pYES2::*NIC2*. Yeast cultures grew in SC-medium without uracil at 30°C. Each OD_{600nm} value was calculated from five independent measurements. Error bars represent means ± SD.

To quantify the effect of *NIC2* expression on lithium and sodium ion tolerance in yeast, the average values of all growth experiments (shown in **Fig. 15*A*** to **15*C*** and **Fig. 16*A*** to **16*C***) were determined and taken to calculate the time that was required to reach half-maximal optical density ($T_{1/2}$). The calculated values were normalised with the $T_{1/2}$ gained for the growth experiments of the reference cells carrying the empty pYES2 vector grown under the same conditions. At 0 mM LiCl, no $T_{1/2}$ difference was detectable between yeast cells expressing *NIC2* and the reference yeast cells. However, the increase of LiCl concentrations to 300 mM and then 600 mM led to a decrease of the $T_{1/2}$ value to maximal 21,9 % ± 0,4 at 600 mM LiCl for *NIC2* expressing yeast cells in comparison to the reference cells (**Fig. 17*A***). The time point of half-maximal optical density ($T_{1/2}$) was also determined for the growth of *NIC2* expressing yeast cells at 900 mM and 1600 mM NaCl (**Fig. 17*B***), and the maximum decrease of the $T_{1/2}$ value, which was observed at 1600 mM NaCl, was only 8,6 % ± 0,5 in comparison to the reference cells.

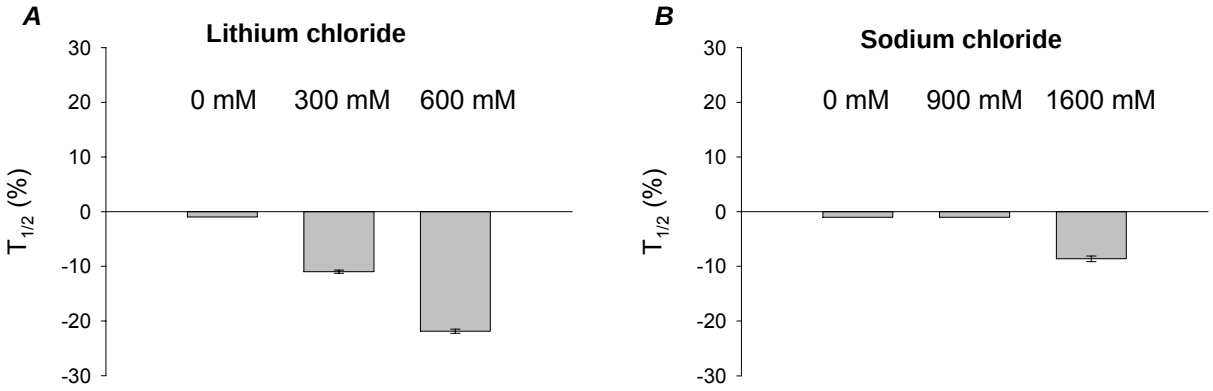

Figure 17. Li^+ and Na^+ concentration-dependent growth of yeast transformed with pYES2::*NIC2*. ***A***, Half-maximal optical density ($T_{1/2}$) growth values in the presence of 0 mM, 300 mM and 600 mM of LiCl. ***B***, Half-maximal optical density ($T_{1/2}$) growth values in the presence of 0 mM, 900 mM and 1600 mM of NaCl. All $T_{1/2}$ values were normalised with the $T_{1/2}$ gained for the growth experiments of the yeast carrying the empty pYES2 vector. Error bars represent means ± SD.

These results clearly indicate that expression of *NIC2* in yeast cells increases the tolerance towards lithium and slightly towards sodium ions.

- **$[Ca^{2+}]_{cyt}$ quantification in yeast cells expressing *NIC2* under hypertonic stress**

Hyperosmotic stress caused by high concentrations of LiCl and NaCl induces an immediate and short duration transient cytosolic Ca^{2+} increase in yeast (Matsumoto *et al*., 2002). Although the expression of *NIC2* did not increase the tolerance towards Ca^{2+} in yeast cells (see above; **Fig. 14*M*** to **14*P***), it increases the tolerance towards lithium and sodium ions. To test changes in Ca^{2+} signalling in yeast cells expressing *NIC2* after LiCl or NaCl stress, the Ca^{2+}-sensitive photoprotein AEQUORIN derived from a marine organism, the jellyfish *Aequorea victoria*, was used (Shimomura e*t al*., 1962; Blinks *et al.*, 1978). The *APOAEQUORIN* cDNA codes for the active product – APOAEQUORIN – and targets it to the cytoplasm. When transient cytosolic Ca^{+2} increases, this is detected by the luminescence of the Ca^{2+}-dependent AEQUORIN (Matsumoto *et at*., 2002). The *APOAEQUORIN* cDNA was subcloned into a pYES3/CT vector and co-transformed with the pYES2::*NIC2* plasmid into *Saccharomyces cerevisiae* yeast strain INVSc1. In addtion, other yeast cells were transformed with pYES3/CT::*APOAEQUORIN* and used as a negative control. Yeast cells were grown at 30°C overnight in liquid SC medium without uracil and tryptophane, additionally supplemented with 0.5 µM of hydrophobic prosthetic group coelenterazine, that, when bound to APOAEQUORIN, forms the active AEQUORIN. Using a custom-built luminometer, changes in the cytosolic Ca^{2+} level in refreshed yeast cells of an OD_{600nm} between 0.6 and 0.8 were examined. Application of LiCl at a final concentration of 1 M initiated an immediate and transient elevation of cytosolic Ca^{2+} with a delay of 10 sec and a duration of about 1 min (**Fig. 18*A***). The increase in the cytosolic Ca^{2+} level was significantly higher in the yeast cells transformed with pYES2::*NIC2* than in the control yeast cells. A similar Ca^{2+} transient profile, which appeared with a 10 sec of delay and had a duration of about 1 min, was also obtained after treatment of yeast cells with 1 M of NaCl and 1.6 M of sorbitol. The presence of NaCl caused the increase in the cytosolic Ca^{2+} level which was higher in the yeast cells transformed with pYES2::*NIC2* than in the control cells (**Fig. 18*B***). In the case of sorbitol, there was also a similar observation of an increased cytosolic Ca^{2+} level in the yeast cells transformed with pYES2::*NIC2* in comparison to the control cells (data not

shown). Based on these results, it is suggested that the increase in the cytosolic Ca^{2+} level was probably caused by hypertonic and not ionic stress, because similar Ca^{2+} transient profiles were obtained for LiCl, NaCl and sorbitol. Moreover, the observed 10 sec delay of the increase in the cytosolic Ca^{2+} level allows to speculate that Ca^{2+} entered into the cytoplasm from internal sources of the cells and not from the external solution. To test this hypothesis, the changes in the cytosolic Ca^{2+} level in the transformed yeast cells are currently tested in the presence of external calcium channel blocking agents like $GdCl_3$, $LaCl_3$. Yeast cells are incubated in media supplemented with 0.5 µM $GdCl_3$ or 50 µM $LaCl_3$ for 10 min before the application of LiCl, NaCl or sorbitol and subsequent measurements (data not shown).

These results confirm the hypothesis, that upon a hypertonic stress in the presence of NIC2, the increase in the cytosolic Ca^{2+} concentration is mainly due to release of Ca^{2+} from internal stores.

A

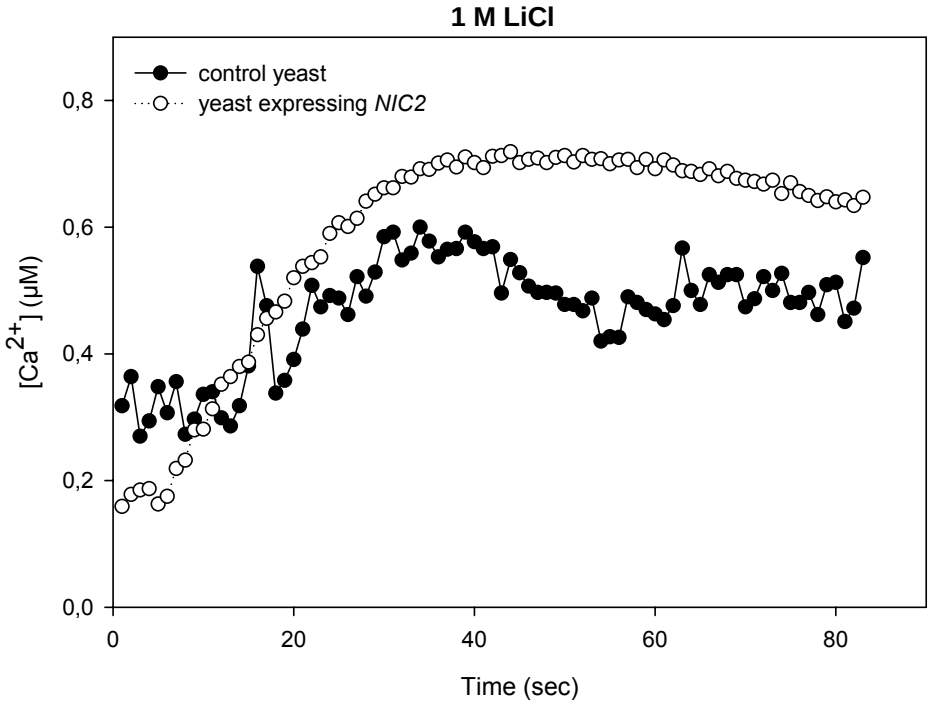

B

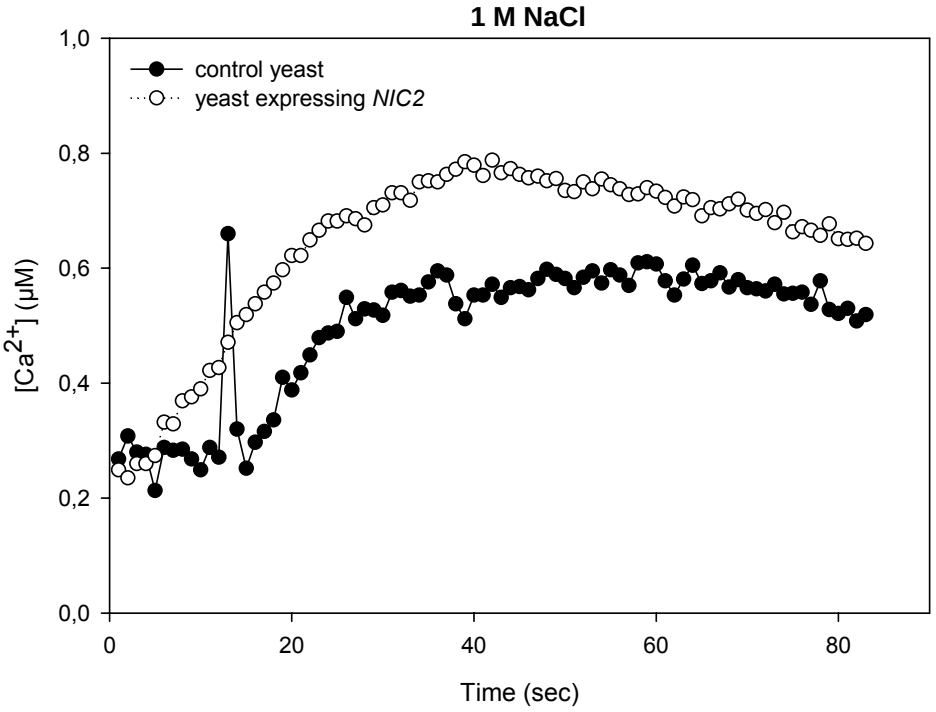

Figure 18. Transient increase in cytosolic Ca^{2+} concentration in yeast cells treated with a hypertonic shock. ***A***, LiCl-induced cytosolic Ca^{2+} increase in the control yeast and the yeast expressing *NIC2*. ***B***, NaCl-induced cytosolic Ca^{2+} increase in the control yeast and the yeast expressing *NIC2*. NaCl and LiCl at the final concentration of 1 M were added at the time point 0 sec. $[Ca^{2+}]$ were determined from aequorin luminescence measurements (for details see Materials and Methods).

4.1. Expression of *NIC2* in *Xenopus laevis* oocytes: ^{3}H-IAA uptake assay

The phenotypes of *Arabidopsis thaliana* plants where *NIC2* was overexpressed (presented in detail in the next chapter) suggested that the gene product might be responsible for auxin homeostasis. To determine whether NIC2 mediates the transport of IAA, uptake assay using *Xenopus laevis* oocytes was designed. In the assay, the time-dependent uptake of ^{3}H-labeled IAA was measured. As shown in **Fig. 19**, after each time point of incubation (10 min, 20 min, 30 min, 40 min, 50 min, and 60 min), the accumulation of ^{3}H-labeled IAA in control and *NIC2* expressing oocytes was at the same range. The experiment was repeated three times and during the time course of the measurements no difference in ^{3}H-IAA uptake was observed between the oocytes expressing *NIC2* and controls.

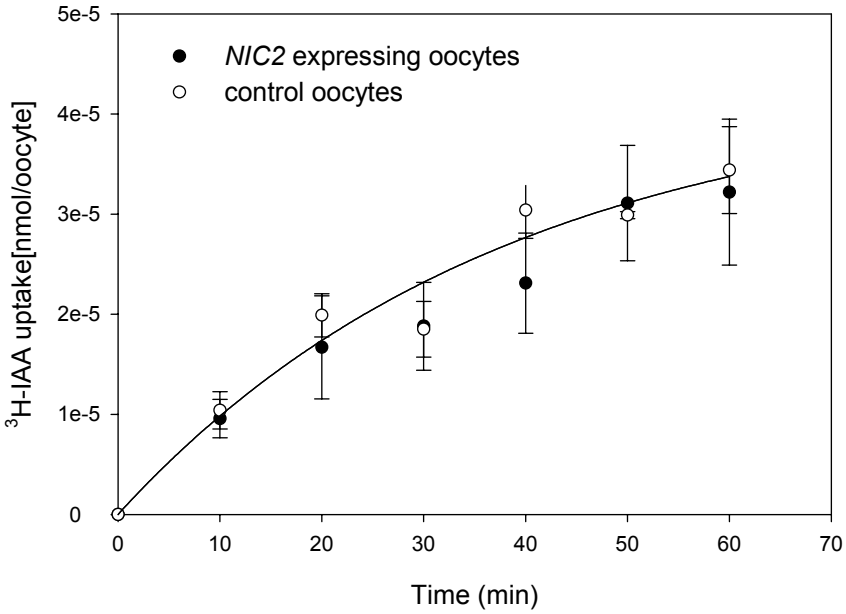

Figure 19. Time-dependent uptake of ^{3}H-IAA into oocytes. The avarages of ^{3}H-IAA uptake into *NIC2* expressing oocytes (black dots) and control oocytes (white dots) were calculated from 10 independent oocytes at each time point (10 min, 20 min, 30 min, 40 min, 50 min, and 60 min). Means ± SD.

5. Functional characterisation of *NIC2* in plants

Arabidopsis thaliana (L.) Heynh. C24 wild-type was used as an homologous expression system to elucidate the function and expression pattern of *NIC2* in plants.

5.1. Organ- and tissue-specific expression of *NIC2* in mature *Arabidopsis* plants

The pattern of *NIC2* expression in *Arabidopsis thaliana* was determined using real-time reverse transcription PCR. RNAs, isolated from primary and secondary roots, rosette leaves, inflorescence stems and flowers of 45-day-old *Arabidopsis* plants, were used as templates for cDNAs syntheses. For the detection of *NIC2* transcipt within the pool of different cDNAs, specifically designed primers, RT-*NIC2*for and RT-*NIC2*rev, that multiplied a 60 bp fragment of the transcipt, were used. As a control, specifically designed primers for the house-keeping gene, *UBQ10*, At4g05329for and At4g05329rev, were utilised. The calculated values from $2^{-\Delta C_T}$ reflect the level of *NIC2* expression (for more details see Material and methods). As shown in **Fig. 20**, *NIC2* was ubiquitously detected in all tested organs, but the expression was slightly stronger in roots and flowers compared to rosette leaves and inflorescence stems.

To define a spatial pattern of *NIC2* expression, a 1483 bp 5' genomic fragment upstream of the ATG start codon of *NIC2* was isolated, fused to the *E. coli* β-glucuronidase (*GUS*) reporter gene in the binary plasmid pBI101, and transformed into *Arabidopsis thaliana.* The analysis of transgenic lines indicated that the Pro_{NIC2}:*GUS* fusion gene was expressed in the vascular tissue of primary and secondary roots (**Fig. 21*A1***), rosette and cauline leaves (**Fig. 21*B1*** and **21*B4***), inflorescence stem (**Fig. 21*C1***), and flower (**Fig. 21*D1***), which was in agreement with *NIC2* expression determined by real-time reverse transcription PCR. Expression of Pro_{NIC2}:*GUS* was also detected in whole immature siliques (**Fig. 21*E1***) and in the abscission zone of mature siliques (**Fig. 21*E4***).

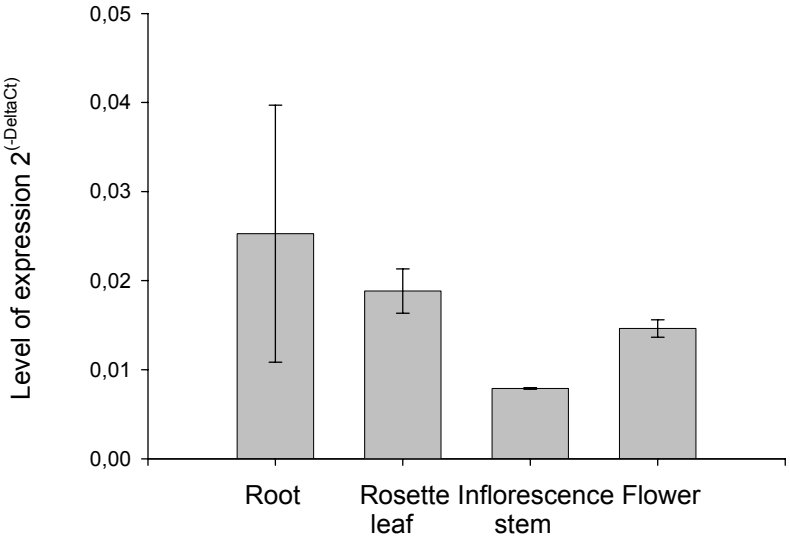

Figure 20. Organ-specific expression of *NIC2*. Real-time RT-PCR analysis indicated the level of *NIC2* expression in roots, rosette leaf, inflorescence stem and flower of 45-day-old *Arabidospis thaliana* (L.) Heynh. C24. The expression level of *NIC2* was calculated by subtracting the C_T value of *UBQ10* (house-keeping gene) from the C_T value of the *NIC2*, and ΔC_T value was used in $2^{-\Delta C}{}_T$ (for details see Materials and methods). Each $2^{-\Delta C}{}_T$ value was calculated from two independent measurements. Means ± SD.

In addition, a detailed analysis of primary roots revealed that the Pro_{NIC2}:*GUS* fusion gene was expressed in the stele of the root elongation zone of the root tip (**Fig. 21*A2***), and in the cells of the lateral root cap (**Fig. 21*A3***). The distribution of GUS activity in secondary (lateral) root exhibits the same pattern of expression (data not shown). GUS activity was also determined in 15 µm thick cross sections obtained from roots. Transverse cross sections taken through a root tip (**Fig. 21*A4***) and at some distance from the root tip, where the cells are fully differentiated, (**Fig. 21*A5***) showed that at the cellular level, GUS activity was present in pericycle cells (depicted as P in **Fig. 21*A4*** and **21*A5***). A detailed analysis of rosette leaves by longitudinal (**Fig. 21*B2***) and transverse (**Fig. 21*B3***) cross sections demonstrated, that the staining was present in xylem parenchyma cells (shown as XP). Xylem parenchyma were also stained in longitudinal inflorescence stem sections (**Fig. 21*C1*** and **21*C2***) as well as in longitudinal flower sections (**Fig. 21*D2***). Finally, transverse cross sections through immature siliques revealed that Pro_{NIC2}:*GUS* expression was present in the vascular tissue (**Fig. 21*E2***) and in the dehiscence zone of siliques (**Fig. 21*E3***).

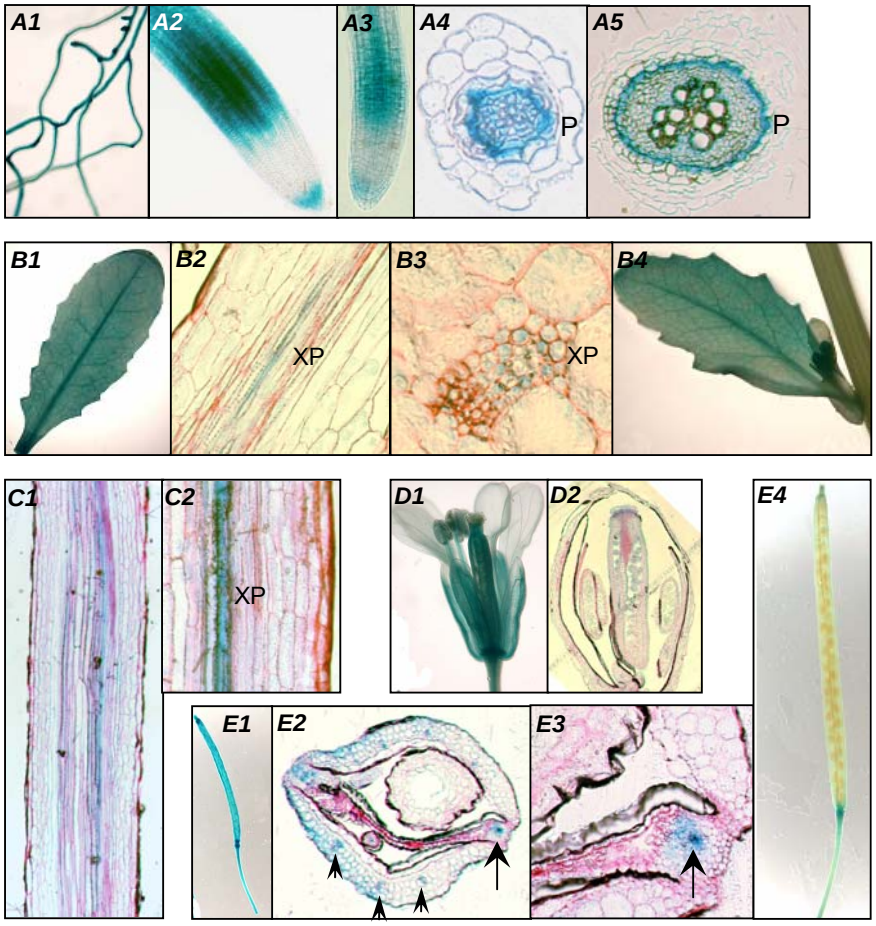

Figure 21. Analysis of GUS activity in mature *Arabidopsis* plants transformed with the Pro$_{NIC2}$:*GUS* fusion gene. Infiltrated plants were stained overnight at 37°C. GUS staining patterns were viewed in whole plant organs and in tissue cross-sections (15 µm) stained with 0.02% (w/v) Ruthenium Red. ***A1***, GUS staining was present in primary and secondary roots and ***A2***, more specifically occurred in the stele of the elongation zone and in the cells of the lateral root cap, ***A3***. Transverse cross sections through the root tip and at some distance above the root tip, ***A4*** and ***A5***, respectively, revealed strongest GUS activity in pericycle cells (depicted as P). In rosette and cauline leaves, ***B1*** and ***B4***, GUS activity was observed in the vascular tissue. Logitudinal, ***B2***, and transverse, ***B3***, cross sections through a rosette leaf, and longitudinal cross section through an inflorescence stem, ***C1*** and ***C2***, showed staining in xylem parenchyma cells (depicted as XP). ***D1***, GUS staining present in a mature flower. A longitudinal cross section, ***D2***, revealed specific localisation in vascular tissue. GUS staining was observed in immature siliques, ***E1***, which significantly decreased in mature siliques, ***E4***. Transverse cross sections, ***E2***, through the asbcission zone of an immature silique, and a higher magnification of this tissue, ***E3***, indicates intense activity in the vascular tissue (indicated by arrow heads) as well as in the dehiscence zone of siliques (indicated by arrows).

5.2. Expression of *NIC2* in the developing roots of *Arabidopsis* seedlings

To determine *NIC2* expression during development of roots in more detail, an analysis of transgenic *Arabidopsis* seedlings was performed. The Pro$_{NIC2}$:*GUS* fusion gene was invariably expressed in the roots of seedlings at 3 (**Fig. 22*A1***), 5 (**Fig. 22*B1***), 7 (**Fig. 22*C1***), 14 (**Fig. 22*D1***) and 30 days after germination (DAG) (**Fig. 22*E1***). A detailed analysis of

primary roots revealed in all cases the same expression pattern for Pro$_{NIC2}$:*GUS*, i.e., GUS activity was detected in the stele of the root elongation zone and the cells of the lateral root cap (**Fig. 22*A2***, **22*B2***, **22*C2***, **22*D2*** and **22*E2***). The distribution of GUS activity was also examined in lateral roots of different developmental stages. GUS staining was localised throughout lateral roots of the primordium stage (**Fig. 22*F***) and in developed secondary roots (**Fig. 22*G*** and **22*H***), which emerged from the primary root of seedlings 7 and 14 DAG, respectively. Subsequently, in secondary roots emerging from the primary root of 24 DAG seedlings, the GUS pattern changed. During further development, GUS activity disappeared from the vascular tissue of secondary roots close to the primary root (**Fig. 22*I*** and **22*J***), and appeared again, when a new lateral root primordium emerged from this secondary root (**Fig. 22*K***). Finally, the same expression pattern of Pro$_{NIC2}$:*GUS* was observed in the stele of the root elongation zone and in cells of the lateral root cap in a mature secondary root (**Fig. 22*L***), similar to the pattern observed in primary roots.

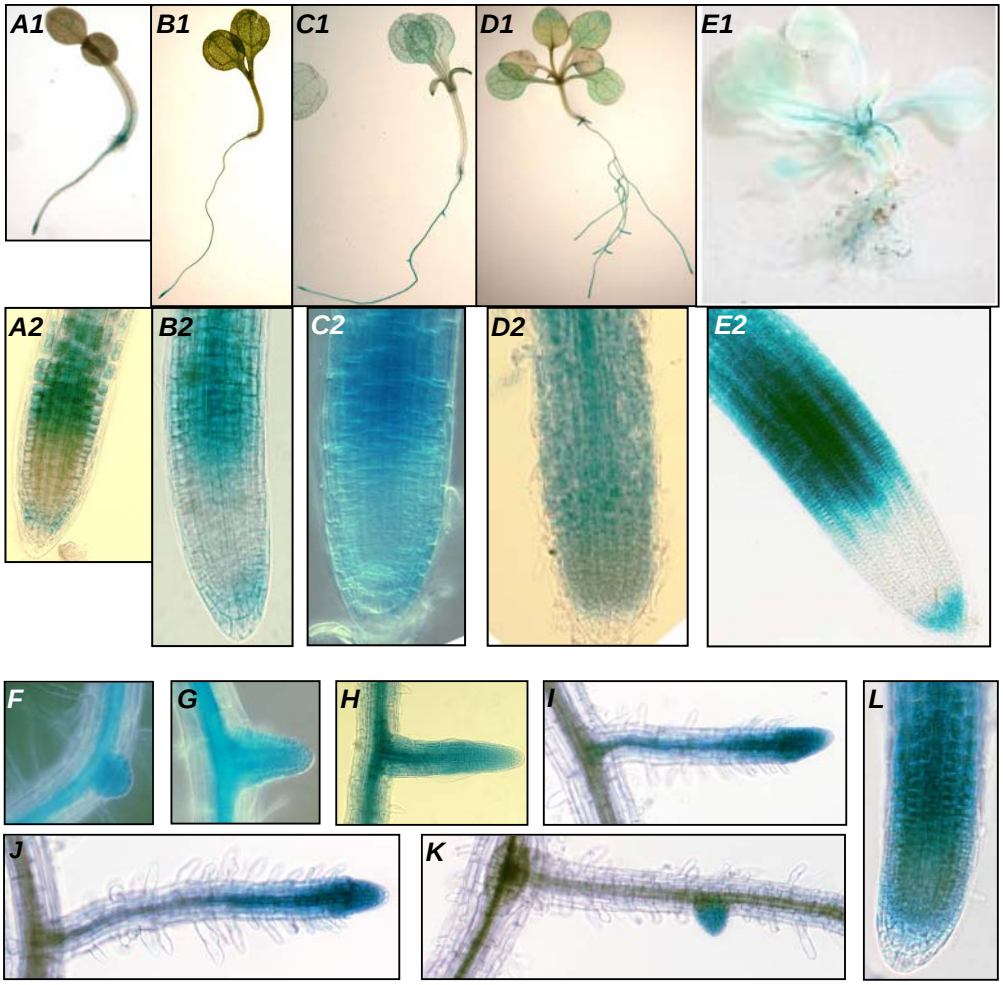

Figure 22. Analysis of Pro$_{NIC2}$:*GUS* activity in developing roots of *Arabidopsis* seedlings. Infiltrated seedlings were stained at 37°C for 2 to 4 h and GUS patterns were examined in the primary and secondary roots. GUS staining was observed in the primary roots of seedling 3 (***A1***), 5 (***B1***), 7 (***C1***), 14 (***D1***) and 30 DAG (***E1***). The detailed analysis of their root elongation zones and their root tips showed a similar GUS activity pattern (***A2***, ***B2***, ***C2***, ***D2*** and ***E2***, respectively). In different developmental stages of secondary roots, GUS staining was observed in lateral root primordia (***F***), in fully developed secondary roots emerging from the primary root of 7 (***G***) and 14 DAG (***H***) seedlings. GUS activity disappeared from the vascular tissue of secondary roots (***I*** and ***J***) emerging from a primary root of 24 DAG seedlings, but was again observed in a new lateral root primordium (***K***) which emerged from a secondary root. In mature secondary roots (***L***), GUS activity was observed in the stele of the root elongation zone and in cells of the lateral root cap.

The spatial and temporal pattern of *NIC2* expression in the developing roots of *Arabidopsis* seedlings is very similar to the pattern of auxin activity, which is a key regulator for lateral root development (Blakely *et al*., 1982; Laskowski *et al.*, 1995; Casimiro *et al*., 2001). Hence, it may be speculated that *NIC2* expression is influenced by auxin, which is indeed the case, as shown in chapter **5.7.**

5.3. Overexpression of *NIC2* in *Arabidopsis* changes the plant phenotype

To understand the possible role of *NIC2 in planta*, two different strategies were chosen, i.e., gene overexpression and gene silencing. For overexpression, the *NIC2* cDNA was subcloned downstream of the Cauliflower Mosaic Virus (CaMV) 35S promoter in the binary plasmid pGreen0229-35S and then transformed into *Arabidopsis thaliana* (L.) Heynh. C24 wild-type.

- **F1 generation**

Twenty-one transgenic lines (F1 generation) were obtained from two rounds of BASTA selection. As shown in **Fig. 23**, from the first set three independent lines (#1, #2, and #3) were grown to the stage of having siliques and seeds (**Fig. 23*B***, **23*C*** and **23*D***). The 50-day-old transgenic plants showed significantly altered plant structure compared to wild-type plants (**Fig. 23*A*** and **23*E***). In the second set, 18 independent lines were selected and some of them are shown as examples in **Fig. 23**. The lines #4, #8, #13, #16, #17 and #19 also exhibited an altered phenotype at the age of 30 days (**Fig. 23*F1***, **23*G1***, **23*H1***, **23*I1***, **23*J1*** and **23*K1***), but more dramatic changes in plant structure became apparent after an additional 15 days of growth (**Fig. 23*F2***, **23*G2***, **23*H2***, **23*I2***, **23*J2*** and **23*K2***). From these transgenic lines, only four were able to reach a growth stage of having siliques and seeds (#4, #13, #17 and #19), while the remaining lines including also those which are displayed (#8 and #16) died because of very early senescence which first appeared in rosette leaves and subsequently in short flower stalks and flowers. The majority of transgenic plants had an extremely bushy phenotype with almost no apical dominance, reflected by three to five times more lateral flowering shoots developed in comparison to the wild-type plants. The amount of flowers per plant was also higher (2-3 fold) as was the number of rosette leaves (2-2.5 fold), although the leaves and siliques of transgenic plants were much smaller than those of the wild-type. In addition, the constitutive overexpression of *NIC2* caused an earlier senescence of rosette leaves at an age of around 45 days, while in the wild-type plants this process was either hardly visible or not detected at this age.

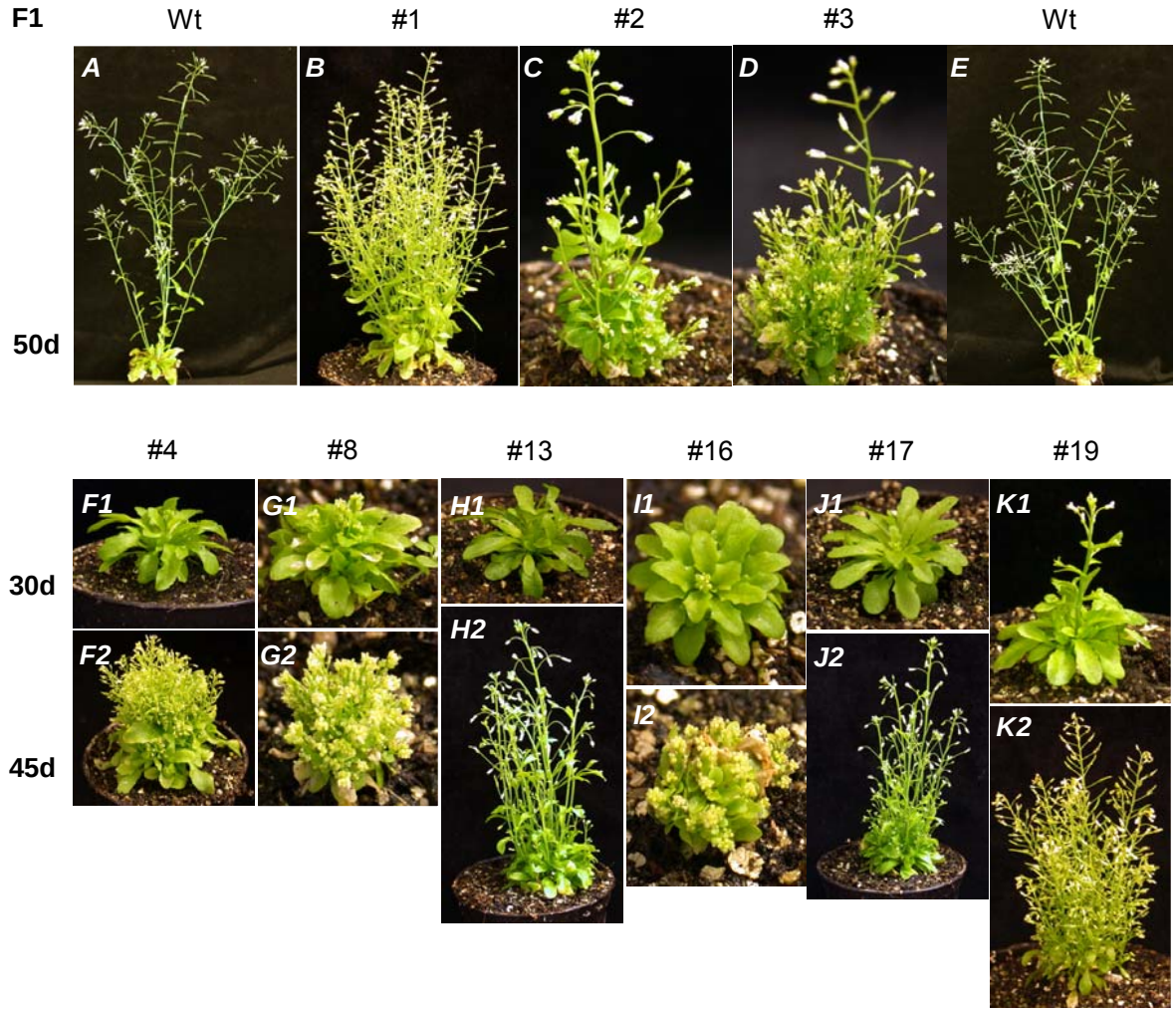

Figure 23. Phenotypes of transgenic *Arabidopsis* plants transformed with the *35S*:*NIC2* construct. F1 generation phenotypes of mature (50-day-old) *Arabidopsis* wild-type plants (Wt), ***A*** and ***E***. The first set of transgenic lines, ***B*** (#1), ***C*** (#2) and ***D*** (#3), grown in soil, showed dramatically changed plant structures. The examples of transgenic lines from the second set, ***F1*** (#4), ***G1*** (#8), ***H1*** (#13), ***I1*** (#16), ***J1*** (#17) and ***K1*** (#19) presented slight differences at day 30 of growth compared to the wild-type, however, after additional 15 days drastical changes in plant structures appeared, ***F2***, ***G2***, ***H2***, ***I2***, ***J2*** and ***K2***, respectively. F2 generation seeds were obtained from the following transgenic lines: #1, #2, #3, #4, #13, #17, and #19.

To test for the overexpression of *NIC2*, all shown transgenic lines (#1, #2, #3, #4, #8, #13, #16, #17, and #19) were examined using real-time reverse transcription PCR. RNA was isolated from rosette leaves, inflorescence stems and flowers of 45- to 50-day-old plants. *NIC2* transcipt was detected in a mixture of different cDNAs using specific primers, i.e., RT-*NIC2*for and RT-*NIC2*rev, which amplified a 60 bp fragment. As shown in **Fig. 24*A***, the expression level of *NIC2* in the parts grown above the ground was very similar to the level of *NIC2* expression in the wild-type. However, in the transgenic lines #1, #2 and #19, gene

expression was slightly higher. To calculate the quantity of the *NIC2* transcript in the transgenic lines, the values of its expression level ($2^{-\Delta Ct}$) were subtracted from the values of the *NIC2* expression level in the wild-type, which was taken as a reference (for details see Materials and methods). Three of the transgenic plants (#1, #2, and #19) showed slightly higher quantities of *NIC2* transcript (**Fig. 24*B***). However, with respect to the gene expression driven by the strong constitutive CaMV 35S promoter and the obtained phenotypes, these quantities correspond to surprisingly low amounts of the *NIC2* transcript in the transgenic plants.

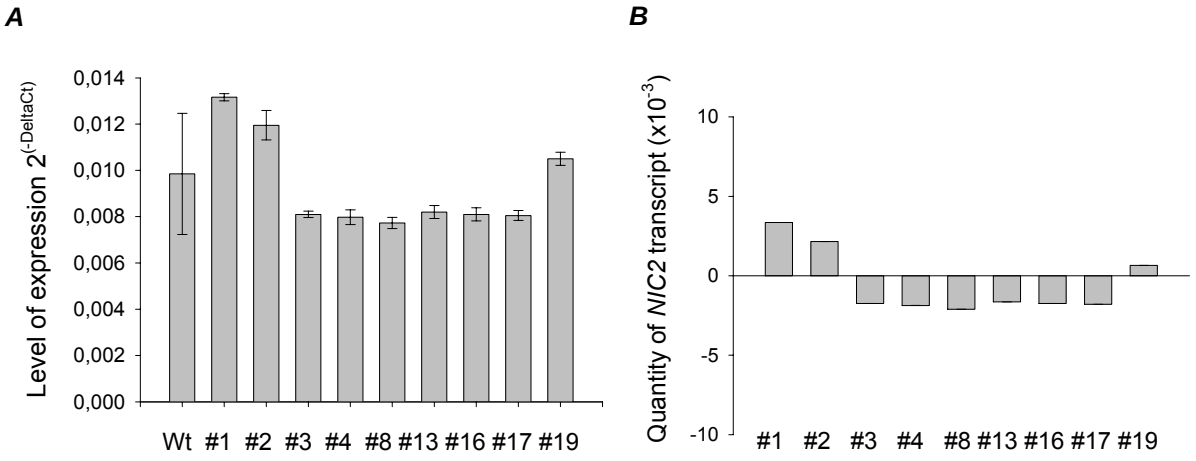

Figure 24. Real-time RT-PCR analysis of *NIC2* expression in the transgenic lines and wild-type. ***A***, Real-time RT-PCR analysis showing the levels of *NIC2* expression in above-ground tissues including rosette leaves, inflorescence stems and flowers of 9 independent transgenic lines (#1 to #19) and wild-type (Wt). Each value was calculated from two independent real-time RT-PCR measurements. Means ± SD. ***B***, The quantity of *NIC2* transcript in #1 to #19 independent transgenic lines was calculated by comparing its expression level in the wild-type (as a subtracted reference) with that in the transgenic plants. For details see Materials and methods.

- **F2 generation**

F2 generation seeds were obtained from 7 transgenic lines (#1, #2, #3, #4, #13, #17, #19). During germination seedlings were sprayed with BASTA. The obtained plant phenotypes from selected transgenic lines were closely similar to the phenotypes of the parental F1 generation (data not shown), and again, only some plants produced siliques and seeds.

- **F3 generation**

Finally, F3 plants were obtained from three transgenic lines (#1, #13 and #17). As shown in **Fig. 25**, 30-day-old transgenic plants (**Fig. 25*B***, **25*C*** and **25*D***) had dramatically changed phenotypes and flowered ~5 days earlier compared to the wild-type (**Fig. 25*A***). After additional 10 days of growth, their phenotypes resembled the phenotypes described above and shown in **Fig. 23**. Because *NIC2* was not highly expressed in rosette leaves, inflorescence stems and flowers, its expression was analysed in the root system including primary and secondary roots. RNA was isolated from roots of 30-day-old F3 generation transgenic lines (**Fig. 25**) and *NIC2* transcript level was analysed by real-time RT-PCR. As shown in **Fig. 25*E***, the expression level of *NIC2* in roots of transgenic lines was similar to that of the wild-type. The following calculation of *NIC2* transcript quantity in the transgenic lines (#1, #13 and #19) emphesised a slightly higher amount of the transcript (**Fig. 25*F***). However, with respect to the gene expression driven by the strong constitutive CaMV 35S promoter and the obtained phenotypes, these quantities again correspond to surprisingly low amounts of the *NIC2* transcript in the transgenic plants, indicating that already minor changes in NIC2 transcript level had a strong impact on plant development.

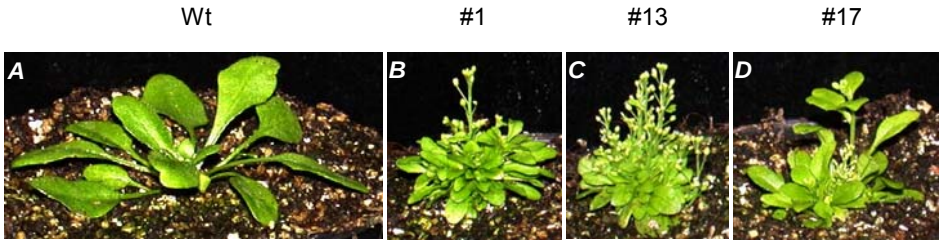

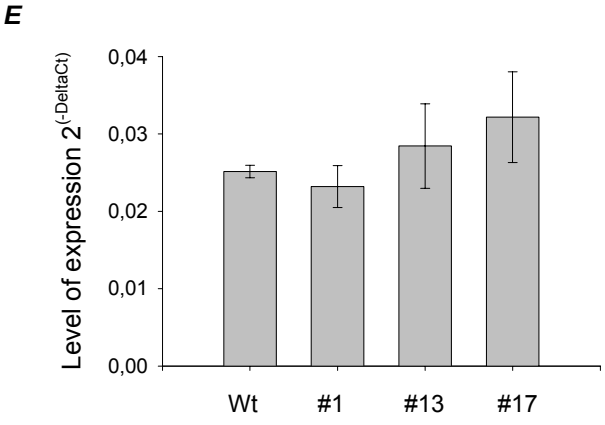

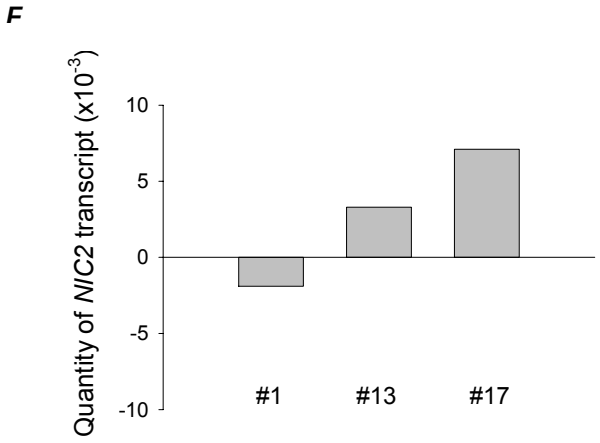

Figure 25. Analysis of transgenic *Arabidopsis* plants transformed with the *35S:NIC2* construct (F3 generation). 30-day-old transgenic lines, ***B*** (#1), ***C*** (#13) and ***D*** (#17) exhibited dramatically changed phenotypes and early flowering copmared to the wild-type (Wt), ***A***. Level of *NIC2* expression in roots of the transgenic lines #1, #13, and #17 and wild-type (Wt) as obtained by real-time RT-PCR, ***E***. Each value was calculated from four independent measurements. Means ± SD are indicated. The quantity of *NIC2* transcript in the transgenic lines #1, #13 to #17 was calculated by comparing its expression level in the wild-type (as a subtracted reference) with that in the transgenic plants, ***F***. For details see Materials and methods.

Furthermore, a light microscopic analysis of rosette leaves, flowers and seeds from the F3 generation transgenic lines (#1, #13, and #17) was carried out (**Fig. 26**). The vascular tissue pattern in blades of rosette leaves from 30-day-old plants showed slight changes. These differences were observed at the border of leaf blades and petioles in transgenic plants (**Fig. 26*B***, **26*C***, and **26*D***). These vascular tissues did not grow equally along the petiole causing a slight change of the pattern on one side (**Fig. 26*A*** and **26*E***). A detailed analysis of the flowers showed no visible changes in their structure, but some of flowers from the transgenic lines opened a few days later (~2-4) than the wild-type (data not shown). A light microscopic comparison of seeds revealed that seeds from transgenic lines (**Fig. 26*G***, **26*H*** and **26*I***) were more transparent than seeds of the wild-type (**Fig. 26*F***), but they had the same shape and a similar size.

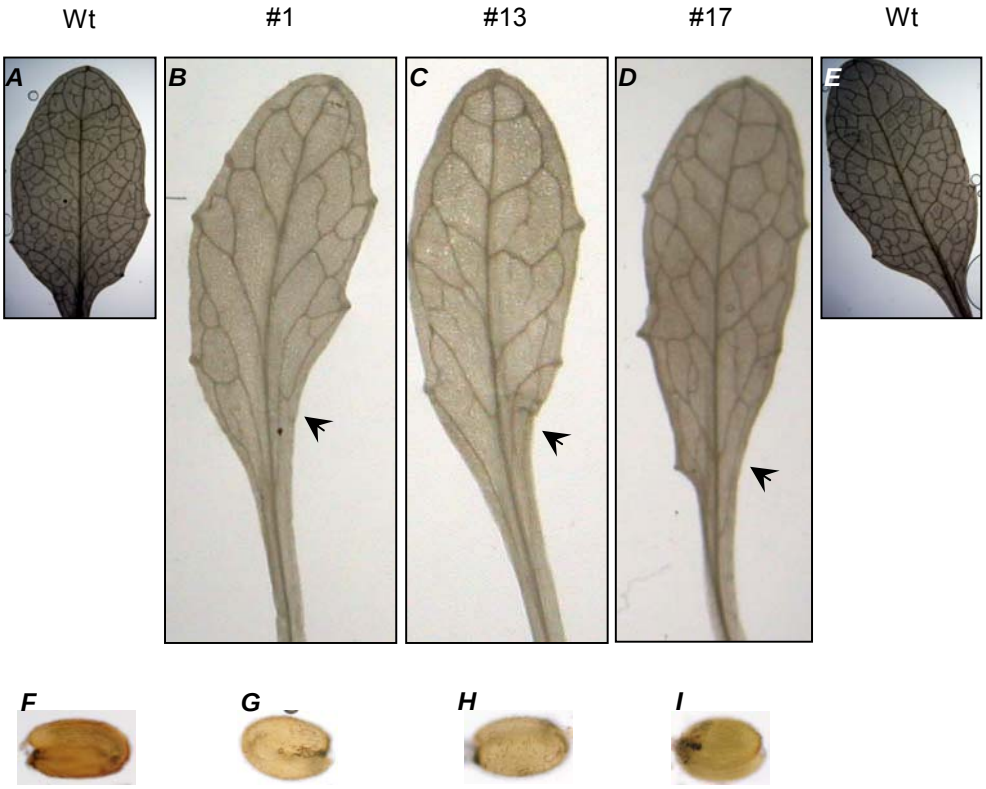

Figure 26. Comparison of rosette leaves and seeds from the *35S:NIC2* transgenic plants and wild-type. Rosette leaves of 30-day-old transgenic plants (F3 generation), i.e., lines #1 (***B***), #13 (***C***) and #17 (***D***), exhibited slight differences in their vascular tissue pattern when compared with leaves of wild-type plants (***A*** and ***E***). These differences were observed at the border of leaf blades and petioles in transgenic lines depicted by arrow heads. Rosette leaves were two times magnified in comparison to the wild-type for better view. Wild-type seeds (***F***) were less transparent than seeds from transgenic lines #1 (***G***), #13 (***H***) and #17 (***I***).

5.4. Silencing of *NIC2* expression in *Arabidopsis* also changes plant structure

To further investigate the function of *NIC2* in *Arabidopsis thaliana*, the gene was silenced using the intron-spliced hairpin RNA technology, called RNA interference (Smith *et al.*, 2000; Waterhouse and Helliwell, 2003). Nine indepenedent transgenic lines (F1 generation) were identified through BASTA selection, and a detailed analysis was performed with plants of the F2 and F3 generations.

- **F2 generation**

Examples #1 to #7, from the F2 generation of transgenic lines, showed varying phenotypes (**Fig. 27**). At day 50 of growth, some of the transgenic lines resembled the wild-type plant (**Fig. 27*A***), having a number of inflorescence stems, flowers and mature siliques (**Fig. 27*B***,

27*E* and **27*H***). Other plants exhibited a significantly different phenotype when compared to the wild-type, having either one or two curving inflorescence stems with a few flowers (**Fig. 27*C***, **27*D*** and **27*G***) or an inflorescence stem that had not yet been produced (**Fig. 27*F***). To examine whether the observed phenotypes were caused by silencing of *NIC2*, the shown transgenic plants were analysed using real-time RT-PCR. RNA was isolated from rosette leaves of 50-day-old transgenic plants and transcript was detected using *NIC2*-specific primers. As shown in **Fig. 27*I***, the expression level of *NIC2* in rosette leaves from transgenic lines was slightly different from the level of its expression in the wild-type. The following calculation, where the expression level of *NIC2* in the wild-type was taken as a subtracted reference, showed the expected lower quantities of *NIC2* transcripts in three transgenic lines (4-7; #5, 4-11; #6 and 8-3; #7) (**Fig. 27*J***). However, these quantities did not differ strongly from that of the wild-type.

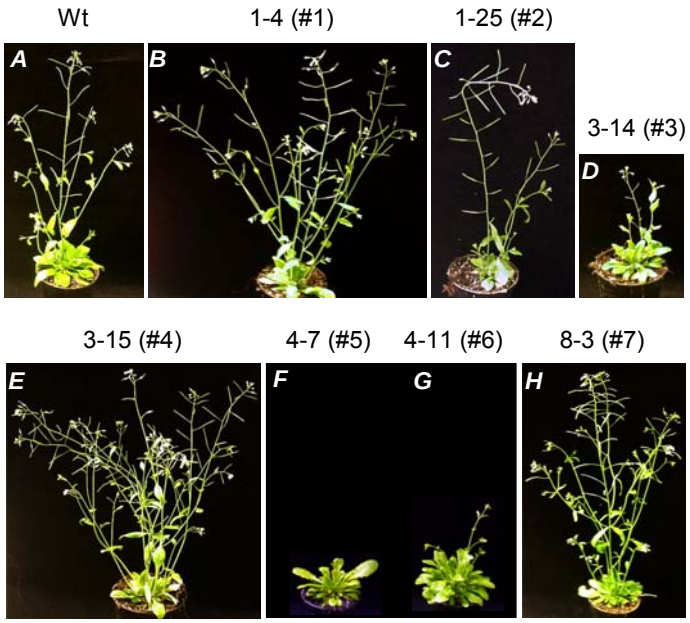

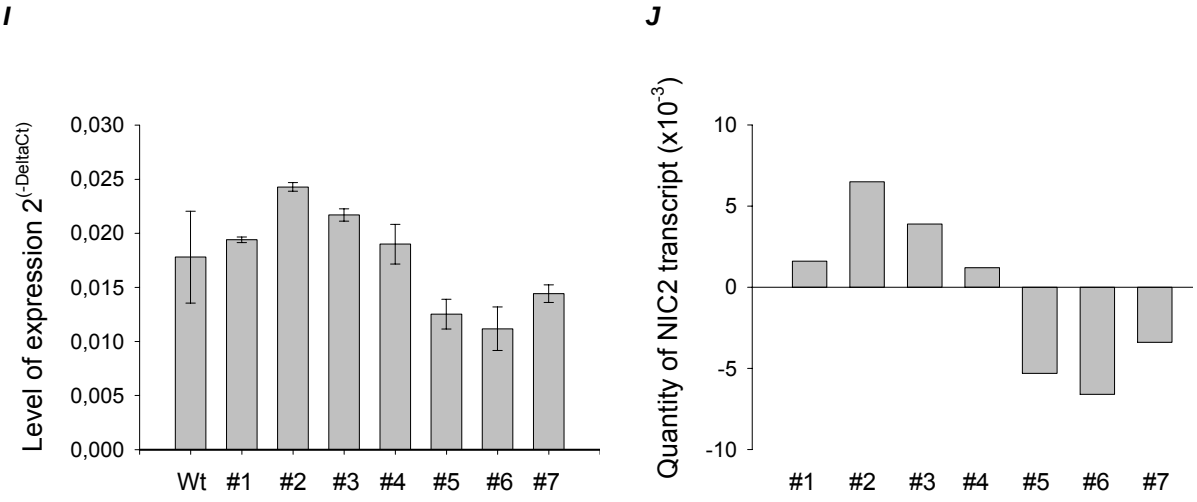

Figure 27. Analysis of transgenic *Arabidopsis NIC2*-RNAi lines (F2 generation). Phenotypes of 50-day-old transgenic lines, ***B*** (1-4; #1)*,* ***C*** (1-25; #2), ***D*** (3-14; #3), ***E*** (3-15; #4), ***F*** (4-7; #5), ***G*** (4-11; #6) and ***H*** (8-3; #7), and the wild-type plant (Wt), ***A***. Level of *NIC2* expression in rosette leaves of transgenic lines (#1,#2, #3, #4, #5, #6 and #7) and the wild-type (Wt) as determined by real-time RT-PCR analysis, ***I***. Each value was taken from two independent measurements. Means ± SD are indicated. The quantity of *NIC2* transcript in transgenic lines was calculated by comparing its expression level in the wild-type (as a subtracted reference) with that in the transgenic plants, ***J***. For details see Materials and methods.

- **F3 generation**

Plants of the F3 generation of BASTA resistant transgenic lines were also analysed. Expectedly, soil-grown adult *NIC2*-silenced plants were distinguishable from wild-type plants. Differences were observed in plant development and flowering time. As shown in **Fig. 28**, 40-day-old transgenic lines (1-4; #1, 1-25; #2, 3-14; #3, 3-15; #4, 4-7; #5, 4-11; #6 and 8-3; #7 in **Fig. 28*B*** to **28*H***, respectively) exhibited a markedly modified plant structure when compared to the wild-type (**Fig. 28*A***). The transgenic plants produced primary inforescence stems that were either longer (**Fig. 28*B***, **28*C***, **28*D*** and **28*H***) or of similar size (**Fig. 28*E*** to **28*G***) when compared with the wild-type parent. Despite their lengths, all stems were around 50 % thinner in diameter than the wild-type (data not shown). During the entire growth period they were bending towards the ground and then laid on the ground instead of growing upwards. Moreover, some of the transgenic lines had already fully developed secondary inflorescence stems with flowers which in the wild-type were still small. These stems grew in two different ways. When they developed from the base of the shoot system, they grew upwards like wild-type stems and did not bend towards the ground. But when they originated from the primary

inflorescence stems, they bent and laid on the ground, behaving like the primary stems. At this developmental stage, wild-type plants had in total from 4 to 6, mostly immature, siliques, whereas transgenic lines possessed in total between 10 to 20 siliques, and 60 to 70 % of them were already mature.

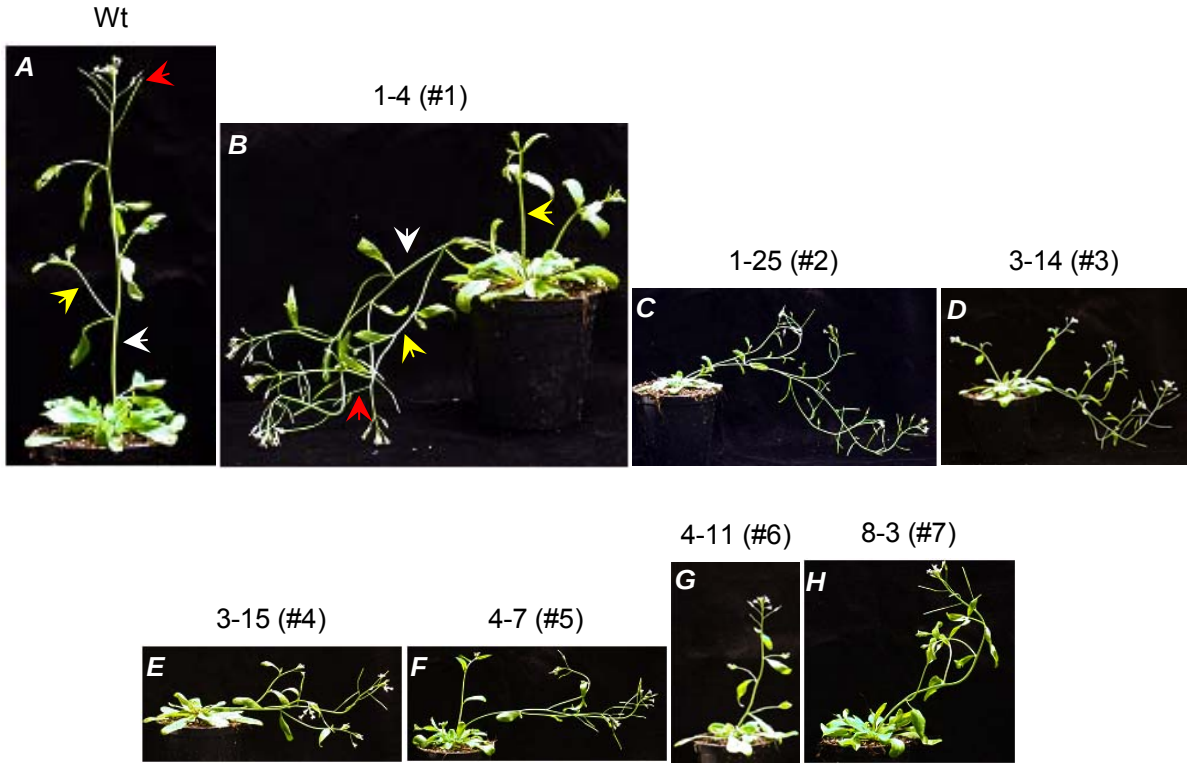

Figure 28. Phenotypes of transgenic *Arabidopsis NIC2*-RNAi lines (F3 generation). Phenotypes of 40-day-old *Arabidopsis thaliana* transgenic lines, ***B*** (1-4, #1), ***C*** (1-25; #2), ***D*** (3-14; #3), ***E*** (3-15; #4), ***F*** (4-7; #5), ***G*** (4-11; #6) and ***H*** (8-3; #7), grown in soil, showed dramatically changed plant structures compared to the wild-type (Wt), ***A***. The differences were observed during the development of the primary (white arrow heads) and secondary inflorescence stems (yellow arrow heads), and with respect to the total number of siliques (red arrow heads), in the transgenic (***B***) and wild-type plants (***A***). The wild-type plant and the transgenic line 1-4 (#1) were two times magnified in comparison to the remaining transgenic lines for better view.

RNA was isolated from the root system incuding primary and secondary roots of 40-day-old transgenic lines to investigate *NIC2* expression in the F3 lines shown in **Fig. 28**. *NIC2* transcript level was determined using real time reverse transcription PCR with *NIC2*-specific primers. As shown in **Fig. 29*A***, the expression level of *NIC2* in roots of the transgenic lines #1 to #7 was not largely different from its level in the wild-type. However, a quantitative calculation revealed the expected lower *NIC2* transcript numbers in all transgenic lines (**Fig. 29*B***).

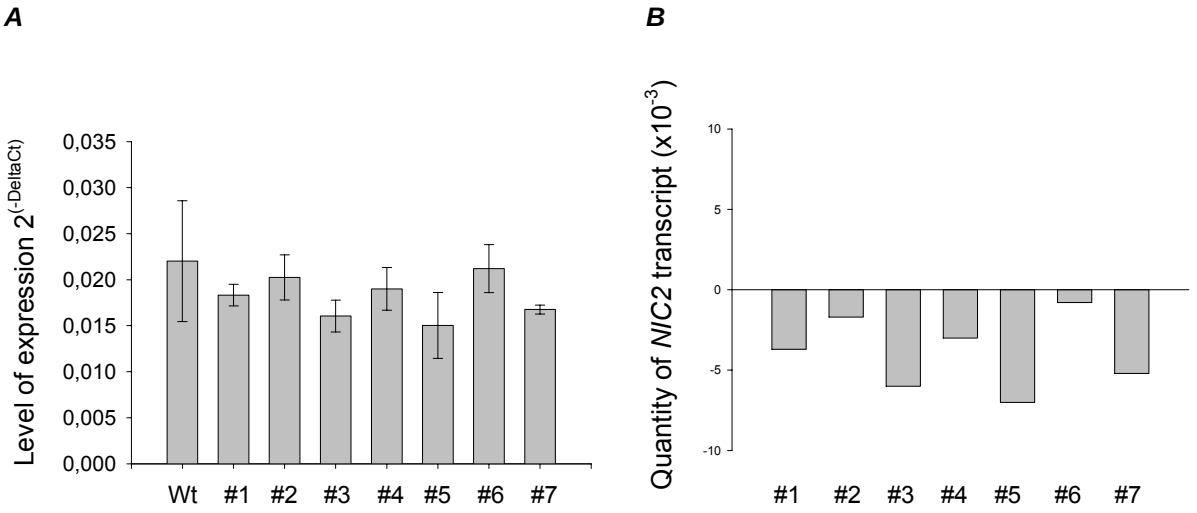

Figure 29. **Real-time RT-PCR analysis of *NIC2* expression in the transgenic *NIC2*-RNAi lines and wild-type.** ***A***, Real-time RT-PCR analysis showing the level of *NIC2* expression in roots of F3 generation transgenic lines (#1 to #7) and the wild-type (Wt). Each value was calculated from two independent measurements. Means ± SD are indicated. ***B***, The quantity of *NIC2* transcript in transgenic lines was calculated by comparing its expression level in the wild-type (as a subtracted reference) with that in the transgenic plants. For details see Materials and methods.

Furthermore, a light microscopic analysis of rosette leaves, flowers and seeds from the transgenic lines of the F3 generation was performed. The vascular tissue pattern in leaf blades and petioles of 40-day-old plants did not change. A detailed analysis of flowers showed also no visible changes in their structure. In addition, a light microscopic comparison of seeds from the transgenic plants showed similarities in their transparency to the wild-type seeds (data not shown).

In the F4 generation, all transgenic lines exhibited very similar phenotypes, having the characteristic features during their entire lifetime (data not shown).

5.5. Analysis of transgenic *35S*:*NIC2* and *NIC2* RNAi plants

To examine roots from the *NIC2* overexpression and the *NIC2* RNAi lines, an analysis of selected seedlings was performed.

- ***NIC2* overexpression and *NIC2* RNAi seedlings exhibit a modified root system**

Seedlings of *NIC2* overexpression lines #1, #13 and #17 (F4 generation) were grown on axenic medium in a vertical position for 8 days and roots were analysed. Compared to the primary root of wild-type plants which exhibit a gravitropic response due to gravistimulation under these conditions (**Fig. 30*A***), roots of the *NIC2* overexpression seedlings (**Fig. 30*B*** to **30*D***) slanted to the left of the vertical stimulus during their entire growth. However, they were not agravitropic (data not shown). Transgenic roots were 40 % longer than roots of the wild-type and a few lateral roots had already formed whereas wild-type roots generally lacked lateral roots at 8 DAG. This difference was even more evident after 11 days of growth when lateral and adventitious roots markedly increased in amount and size in the transgenic seedlings #1 (**Fig. 30*F***), #13 (**Fig. 30*G***) and #17 (**Fig. 30*H***), when compared to the wild-type (**Fig. 30*E***). In addition, among all tested *NIC2* overexpression seedlings, 10 to 20 % exhibited a different phenotype than described above. Instead of one primary root like in the wild-type, two or three short roots including one primary and two secondary roots with a similar length developed (data not shown).

The root system of *NIC2* RNAi plants was also examined. F4 generation seedlings of the selected lines (1-4; #1, 1-25; #2, 3-14; #3, 3-15; #4, 4-7; #5 and 4-11; #6) were grown on axenic medium in a vertical position for 11 days. Gravitropic responses of the transgenic roots were not altered (**Fig. 30*J*** to **30*O***), but similar to the response of wild-type seedlings (**Fig. 30*I***), which was in contrast to the roots of *NIC2* overexpression lines. At the 11th day of growth wild-type seedlings showed little outgrowth of lateral root primordia originating from the primary root, and one or two very small lateral roots that form at the root-shoot junction (**Fig. 30*I***). In the transgenic seedlings, many lateral roots developed from the primary root as

well as from the root-shoot junction (**Fig. 30*J*** to **30*O***). Although the lateral roots were relatively long at this developmental stage, the primary roots were still distinguishable in the transgenic seedlings. In addition, some of *NIC2* RNAi seedlings had 30-40 % longer roots than the wid-type, while the others exhibited either the same or shorter length of about 15-20 %.

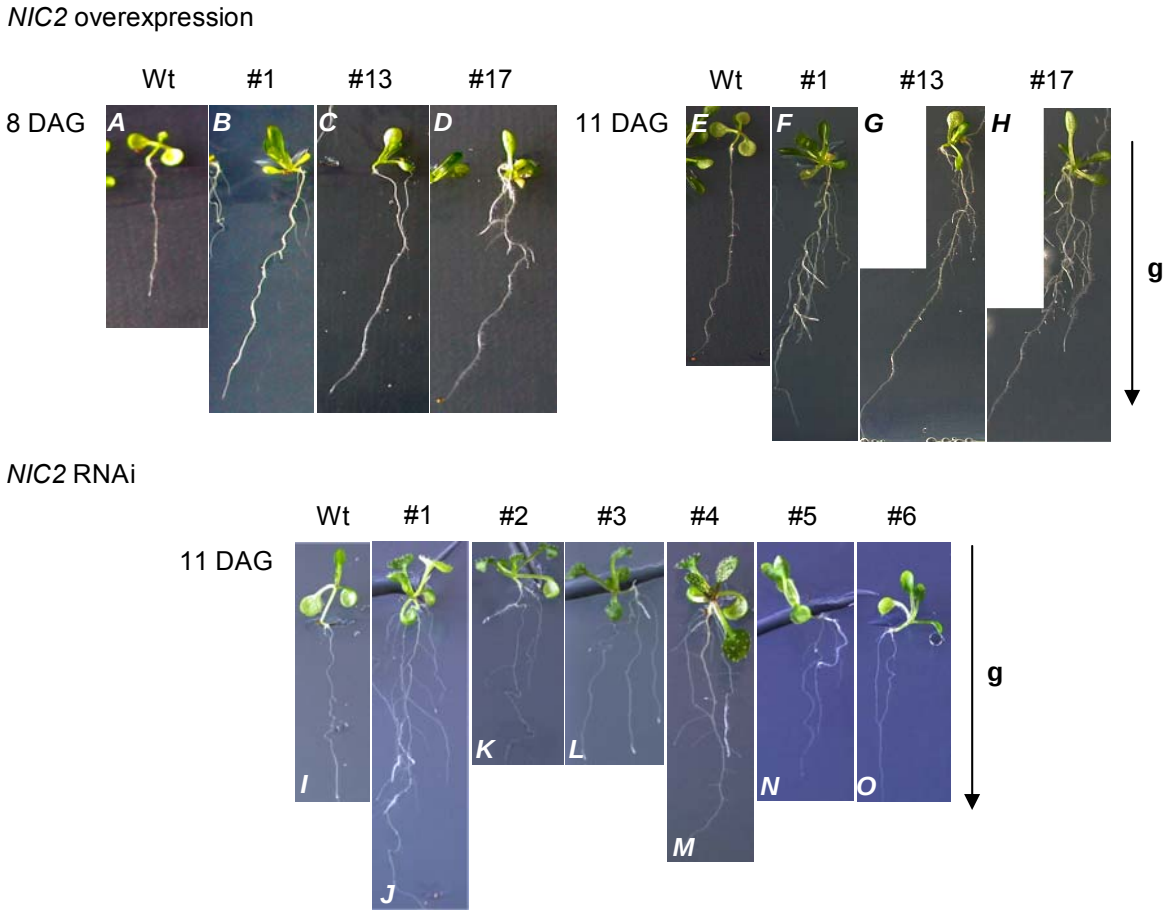

Figure 30. Phenotypes of transgenic *Arabidopsis* seedlings transformed with the *35S*:*NIC2* and *NIC2* RNAi constructs (F4 generation). 8-day-old *NIC2* overexpression seedlings, ***B*** (#1), ***C*** (#13) and ***D*** (#17), exhibit markedly different lengths and growth directions of the primary roots compared to the wild-type, ***A***. The difference is more evident after 11 days. Lateral and adventitious roots increase in amount and size in the transgenic seedlings, ***F*** (#1), ***G*** (#13) and ***H*** (#17) in comparison to the wild-type, ***E***. 11-day-old *NIC2* RNAi seedlings show also a changed root structure, ***J*** (1-4; #1), ***K*** (1-25; #2), ***L*** (3-14; #3), ***M*** (3-15; #4), ***N*** (4-7; #5) and ***O*** (4-11, #6), including the presence of lateral roots and their increased length compared to the wild-type, ***I***. The direction of gravistimulation (**g**) is indicated by arrows.

Auxin is a key regulator for lateral root development (Blakely *et al*., 1982; Laskowski *et al*., 1995; Casimiro *et al*., 2001). The decrease of auxin in roots corresponds to the reduction in the number of emerging lateral roots (Casimiro *et al*., 2001), whereas auxin overproduction causes the development of excess adventitious and lateral roots (Boerjan *et al*., 1995).

Hence, it is speculated that the phenotypes of *NIC2* overexpression and *NIC2* RNAi seedlings are likely evoked by decreased and increased amounts of auxin, respectively.

- **Gravitropic response of roots from *NIC2* overexpression seedlings**

During vertical growth the roots of seedlings that overexpress *NIC2* had a tendency to slant to the left of a vertical stimulus (see above). To analyse their gravitropic response, 7-day-old F4 generation transgenic seedlings (#1, #13 and #17) were grown vertically and then a gravistimulation was applied for 0 h, 2 h, 4 h, 6 h and 23 h by turning them by 90°. As shown in **Fig. 31**, at time 0 h roots of the wild-type (**Fig. 31*A1***) as well as the transgenic seedlings (**Fig. 31*B1*** to **31*D1***) exhibited growth following the previous gravistimulation. After 2 h, only roots of the wild-type responded to the gravistimulus (**Fig. 31*A2***), while roots of the transgenic seedlings did not (**Fig. 31*B2*** to **31*D2***). The first weak responses of roots from transgenic seedlings were observed after addtional 2 h (**Fig. 31*B3*** to **31*D3***), when roots started to reorientate in the direction of the applied gravistimulus. Their responses were much more significant after 6 h (**Fig. 31*B4*** to **31*D4***), following the response of the wild-type roots (**Fig. 31*A4***). At 23 h after gravistimulation, no differences in the response between the wild-type (**Fig. 31*A5***) and the transgenic seedlings (**Fig. 31*B5*** to **31*D5***) were observed, although the newly reorientated roots of the wild-type were much longer than the roots of the transgenic seedlings.

The behaviour of roots from the transgenic seedlings showed that they were not agravitropic, but their responses to the gravistimulus were delayed by 2 to 4 h compared to the wild-type.

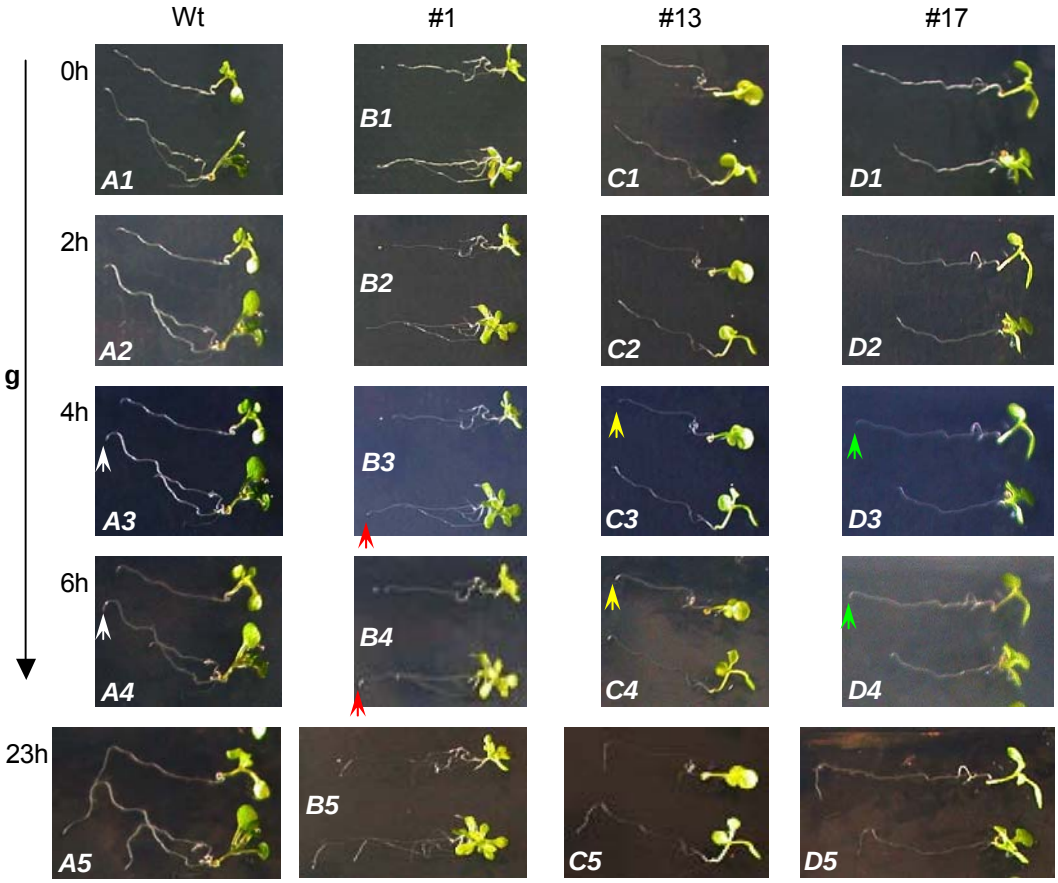

Figure 31. Gravitropic responses of transgenic *Arabidopsis* seedlings transformed with the *35S*:*NIC2* construct (F4 generation). Vertically grown 7-day-old *NIC2* overexpression seedlings (#1, #13 and #17) and wild-type were gravistimulated for 0 h, 2 h, 4 h, 6 h and 23 h. At 0 h time all examined seedlings (***A1*** to ***D1***) were grown following the previous gravistimulation. After 2 h, wild-type roots significantly reorientated (depicted by the arrow head in ***A2***), while roots of the transgenic seedlings showed no responses (***B2*** to ***D2***). At 4 h, delayed and weak reorientations of the transgenic roots were observed (depicted by the arrow heads in ***B3*** to ***D3***), which after additional 2 h became much more evident (depicted by the arrow heads in ***B4*** and ***D4***) compared to the wild-type (depicted by the arrow heads in ***A3*** and ***A4***), respectively. No differences in the response to gravistimulus between the wild-type (***A5***) and the transgenic seedlings (***B5*** to ***D5***) were observed after 23 h of growth. The direction of the gravistimulus (**g**) is indicated by the arrow.

5.6. Roots of *NIC2* overexpression seedlings exhibit auxin-resistant growth

Apical dominance, inflorescence stem elongation, primary and lateral root development as well as gravitropism were changed in *NIC2* overexpression plants or seedlings. The same processes are influenced by the plant hormone, auxin (Went and Thimann, 1937; Davis, 1995) and fluctuations in auxin concentrations induce changes in plant structure (Swarup *et al.*, 2002). Therefore, the overexpression of *NIC2* might have modified the endogenous level of auxin. To assess quantitatively the level of either resistance or sensitivity to auxins, the root growth of F4 generation *NIC2* overexpression seedlings was tested on different concentrations of various auxins. The transgenic lines #1, #13 and #17 were grown on

axenic medium in a vertical position for 17 days in the presence of either 5 µM IAA or 50 µM IBA. Compared to wild-type root growth (**Fig. 32*A***), roots of the transgenic seedlings (**Fig. 32*B*** to **32*D***) were found to be more resistant to 5 µM IAA, having larger numbers of lateral and adventitious roots. Roots of transgenic seedligs were also more resistant to 50 µM IBA (**Fig. 32*F*** to **32*H***) than the wild-type (**Fig. 32*A***), again showing many lateral roots. These results indicate that overexpression of *NIC2* leads to auxin resistance.

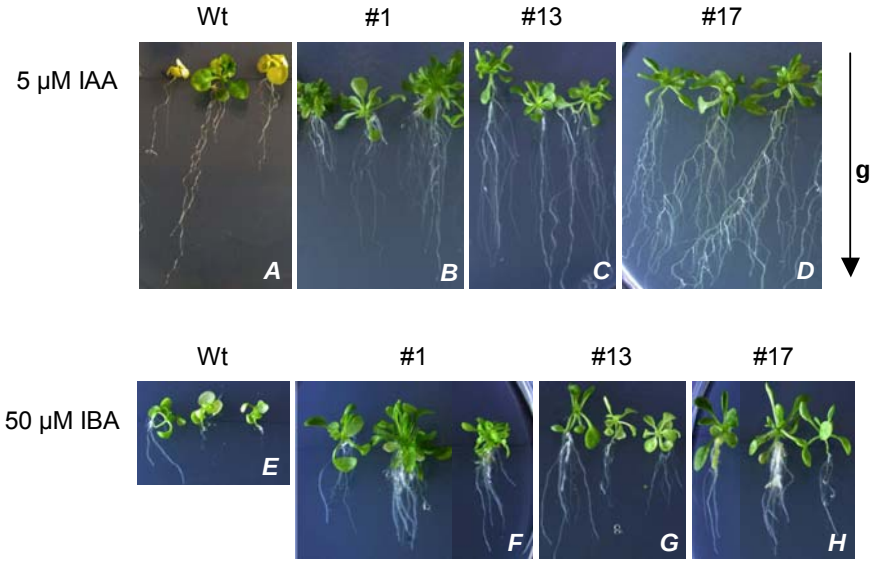

Figure 32. Auxin-resistant growth of *NIC2* overexpression seedlings. 17-day-old roots from *NIC2* overexpression seedlings showed significant growth resistance to 5 µM IAA, ***B*** (#1), ***C*** (#13) and ***D*** (#17), compared to wild-type root growth, ***A***. Growth resistance to 50 µM IBA was also observed for roots from transgenic seedlings, ***F*** (#1), ***G*** (#13) and ***H*** (#17), which developed more lateral roots than the wild-type, ***E***. The direction of the gravistimulus (**g**) is indicated by the arrow.

5.7. Analysis of Pro$_{NIC2}$:*GUS* activity upon various stimuli

The phenotypes of *NIC2* overexpression transgenic plants indicated that the gene might be involved in regulating auxin levels. Therefore, the promoter region of *NIC2*, a 1483-bp 5' genomic fragment upstream of the ATG start codon of the gene, was analysed using the PlantCare program (http://sphinx.rug.ac.be:8080/PlantCARE/) to identify potential auxin-response elements known from the literature (Ulmasov *et al.*, 1995; Hagen and Guilfoyle, 2002). One inverted auxin-response element, GAGACA, was found between 1199-1204 bp of the *NIC2* promoter which was localised 279 bp upstream of the ATG start codon (not shown).

- **Auxins**

To investigate the effect of auxin on *NIC2* expression, a detailed analysis of the primary roots of small transgenic seedlings carrying the Pro$_{NIC2}$:*GUS* construct was peformed (**Fig. 33**). Seedlings were grown horizontally for 5 days on sterile medium containing various auxins and then incubated for 4 h at 37°C in GUS staining solution. Seedlings that grew without application of auxin were used as a control (**Fig. 33*A***). After incubation they were weakly stained in the lateral root cap and in the stele of the elongation zone (inset in **Fig. 33*A***). Significantly higher GUS staining was observed in the roots of seedlings which grew on auxin containing medium (**Fig. 33*B*** to **33*D***). Seedlings that grew on 100 nM synthetic auxin, 2,4-dichlorophenoxy-acetic acid (2,4-D), had the most strongly increased GUS staining in a lateral root cap and in the shortened stele of the elongation zone (inset in **Fig. 33*B***). Lower GUS activity was observed in seedlings, which grew on 300 nM natural auxin, indole-3-acetic acid (IAA; inset in **Fig. 33*C***), and 100 nM synthetic auxin, naphthalene-1-acetic acid (NAA; inset in **Fig. 33*D***). Pro$_{NIC2}$:*GUS* activities were highly dependent on the applied auxins and their concentrations. The intensity of GUS staining in the root tips decreased according to 2,4-D > IAA > NAA application. Furthermore, the analysis of Pro$_{NIC2}$:*GUS* activity was performed with 6-day-old seedlings which were grown on medium containing 300 nM indole-3-butyric acid (IBA). IBA, besides IAA, is a further naturally occurring auxin in *A. thaliana* (Ludwig-Mueller *et al*., 1993). As shown in **Fig. 33*E***, control seedlings, that grew for 6 days without application of IBA, after 2 h at 37°C were weakly stained in the stele of the elongation zone as well as in the lateral root cap (inset in **Fig. 33*E***), while seedlings which were grown on 300 nM IBA exhibited increased GUS activity (**Fig. 33*F***) in the lateral root cap and in the stele of the elongation zone (inset in **Fig. 33*F***).

- **Flavonoids**

The activity of Pro$_{NIC2}$:*GUS* in the primary roots of transgenic seedlings was also studied under flavonoid treatment because flavonoids change the intracellular auxin level by negative regulation of auxin carriers in *A. thaliana* (Murphy *et. al*., 2000; Brown *et al*., 2001). Five-day-

old seedlings were grown horizontally on sterile medium containing either 1 nM naringenin (**Fig. 33*G***), 10 nM kaempferol (**Fig. 33*H***) or 1 nM quercetin (**Fig. 33*I***) and then incubated for 4 h at 37°C. None of the applied flavonoids changed the intensity of GUS staining in roots (insets in **Fig. 33*G*** to **33*I***, respectively) compared to the control (**Fig. 33*A***), which suggests that at the transcriptional level expression of *NIC2* was not altered by flavonoids.

- **Lithium and sodium chloride**

Based on the results obtained from the yeast experiments which showed a higher tolerance for LiCl and NaCl in the cells expressing *NIC2*, the activity of Pro_{NIC2}:*GUS* in the transgenic seedlings was also tested under salt treatment. Five-day-old seedlings were grown horizontally on medium containing either no salt (**Fig. 33*J***), 5 mM LiCl (**Fig. 33*K***) or 20 mM NaCl (**Fig. 33*L***) and then incubated for 4 h at 37°C. Compared to the primary root of the control seedling (inset in **Fig. 33*J***), the presence of LiCl and NaCl caused a slight increase in GUS activity in the root tips as well as in the steles of the elengation zones in the primary roots (insets in **Fig. 33*K*** and **33*L***, respectively). Similar GUS intensity was observed in 4 to 6 transgenic seedlings which were tested under each salt treatment.

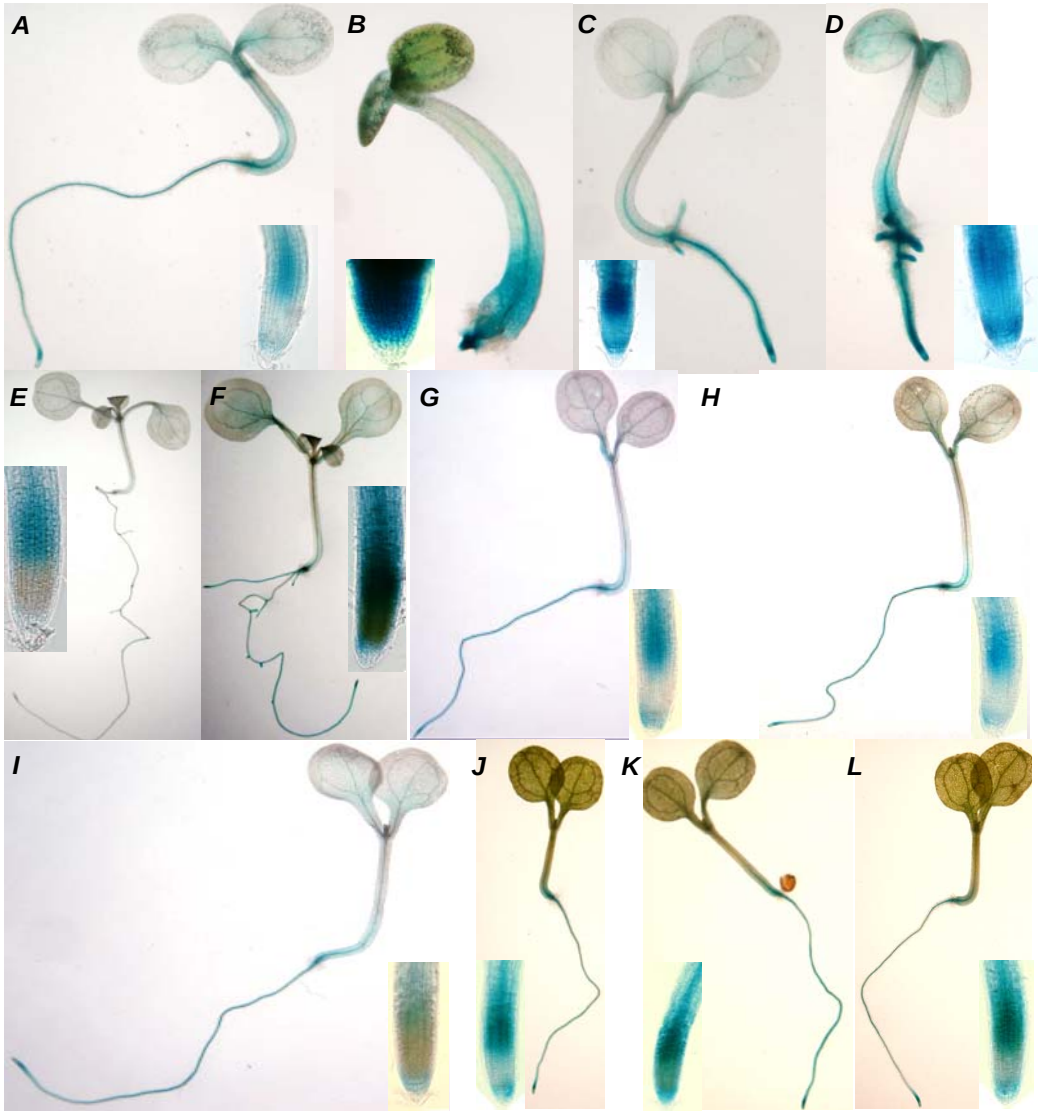

Figure 33. GUS activity driven by the *NIC2* promoter in the primary roots of 5-6 DAG seedlings after treatment with various auxins, flavonoids and salts. ***A***, GUS activity in the primary root of an untreated 5-day-old seedling (inset in ***A***) was weaker than GUS activity in primary roots of seedlings grown on 100 nM 2,4-D, ***B***, 300 nM IAA, ***C***, and 100 nM NAA, ***D***. The intensity of staining in the root tips (insets in ***B***, ***C*** and ***D***, respectively) was dependent on auxin application according to 2,4-D > IAA > NAA. The GUS activity was also stronger in 6-day-old seedlings grown on 300 nM IBA (***E***) than in the control (***F***), especially in the root caps (insets in ***E*** and ***F***). The activities of GUS in the primary roots (insets) in the presence of upon 1 nM naringenin, ***G***, 10 nM kaempferol, ***H***, and 1 nM quercetin, ***I***. In 5 day-old-seedligs, after growth in the presence of 5 mM LiCl, ***K***, and 20 mM NaCl, ***L***, the GUS staining was slightly higher in the root tips and steles of elonagtion zones of the primary roots (insets in ***K*** an ***L***) compared to the control, ***J***.

- **Gravitropism**

The presence of Pro$_{NIC2}$:*GUS* activity in the lateral root cap and the stele of the root elongation zone as well as its dependence on auxin pointed towards a correlation between *NIC2* expression and gravitropism. To investigate a gravitropic effect on *NIC2* expression in the root cap, a gravistimulation assay was performed. The Pro$_{NIC2}$:*GUS* transgenic

Arabidopsis seedlings were grown vertically for 5 days and then turned by 90° for 0 min, 60 min, and 120 min. At each time-point seedlings were collected and incubated in GUS staining solution for 4 h at 37°C. As shown in **Fig. 34*A***, at time point 0 min GUS activity was similar at the lower and upper sides of the lateral root caps in root tips. After 60 min of gravistimulation, the distribution of GUS staining changed slightly and started to accumulate at the lower side of the root tip (data not shown). After 120 min of gravistimulation, the changed intensity of the GUS staining was observed at the upper side of the root tip, while at the lower side of the root tip the GUS staining stayed unchanged (**Fig. 34*B***). Gravistimulation results in the formation of an auxin gradient across the root tip, where more auxins accumulate at the bottom than at the top of the root cap (Chen *et al*., 1999). It can be speculated that this increased level of auxins at the lower side of the root tip induces Pro_{NIC2}:*GUS* expression.

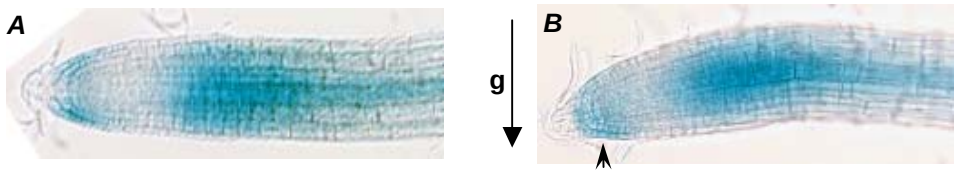

Figure 34. GUS activity driven by the *NIC2* promoter in primary roots of 5 DAG seedlings after a gravistimulation treatment. Before gravistimulation the GUS staining intensity was similar at the upper and the lower sides of the lateral root cap in the roop tip, ***A***. After 120 min of gravistimulation (by 90°), the activity changed and was higher at the lower side of the lateral root cap depicted by the arrow head, ***B***. The direction of the gravistimulation (**g**) is indicated by the arrow.

5.8. Peroxisomal localisation of NIC2 in *Nicotiana tabacum* BY2 protoplasts

In silico analysis of NIC2 indicated that the protein might be embedded in the cell membrane. To determine NIC2 subcellular localisation, the 3' end of the *NIC2* open reading frame was fused to the green fluorescent protein (*GFP*) gene and transiently introduced *via* the construct, pA7-*35S*-*NIC2*-*GFP*, into *Nicotiana tabacum* BY2 protoplasts. Initial results from two independent transformations indicated that the NIC2-GFP fusion protein was localised in small, round organelles inside BY2 protoplasts (data not shown). To elucidate the proper localisation of NIC2-GFP fusion protein, tobacco BY2 protoplasts were transformed with two control plasmids, pA7-*35S*-*GFP*, to label the cytoplasm and the nucleus, and pOL-*35S*-*SKL*-*DsRED*, to label peroxisomes (kindly provided by Hélène Barbier-Brygoo, Gif-sur-Yvette, France). BY2 protoplasts were also co-transformed with pA7-*35S*-*NIC2*-*GFP* and pOL-*35S*-*SKL*-*DsRED*. After 40 h of incubation, the transformed protoplasts (**Fig. 35*A*** to **35*C***) were viewed under the fluorescent microscope equipped with green fluorescence filter settings for the detection of GFP protein and NIC2-GFP fusion protein, and with rhodamine filter settings to detect SKL-DsRED protein. As shown in **Fig. 35*D*** and **35*E***, control GFP was localised in the nucleus and cytoplasm, whereas the control SKL-DsRED was located in the peroxisomes of BY2 protoplasts. In the co-transformed BY2 protoplasts, the localisation of NIC2-GFP fusion protein was identical (**Fig. 35*G***) to the localisation of SKL-DsRED (**Fig. 35*F***). Both proteins undoubtedly co-localised in the same peroxisomes, as is shown with a higher magnification in **Fig. 35*H*** and **35*I***, respectively.

- **Localisation of a peroxisomal targeting sequence**

As shown above, the *in silico* analysis recognised no targeting sequences in NIC2 for peroxisomes. In order to identify protein parts responsible for a peroxisomal localisation, two different constructs were generated. In the first construct, pA7-*35S*-(174 bp)-*NIC2*-*GFP*, the *NIC2* cDNA was shortened by 174 bp at the 5' end which corresponded to 58 amino acid residues at the N-terminus of the protein. In the second construct, pA7-*35S*-(1089 bp)-*NIC2*-*GFP*, the central part of 1089 bp from *NIC2* cDNA was cut out, which corresponded to 363

amino acid residues in the protein. The remaining *NIC2* cDNA parts were re-ligated, constructing protein that consisted of the N-terminal (58 amino acid residues) and the C-terminal (90 amino acid residues) parts. The 3' ends of the truncated *NIC2* cDNAs were fused to the green fluorescent protein (*GFP*) gene and transiently co-transformed with pOL-*35S-SKL-DsRED* into *Nicotiana tabacum* BY2 protoplasts. After 40 h of incubation, the transformed protoplasts (**Fig. 35*J*** and **35*M***) were viewed under the fluorescent microscope. The co-transformed BY2 protoplasts still showed peroxisomal localisations for NIC2-GFP fusion proteins. As shown in **Fig. 35*L***, the N-terminally truncated NIC2-GFP fusion protein co-localised with SKL-DsRED in peroxisomes (**Fig. 35*K***). NIC2-GFP fusion protein, that was deleted for the central part of NIC2, also co-localised in peroxisomes (**Fig. 35*O***), together with SKL-DsRED (**Fig. 35*N***).

The results indicated that the peroxisomal targeting sequence was located at the C-terminal part of NIC2, which was present in all constructs used for expression in BY2 protoplasts.

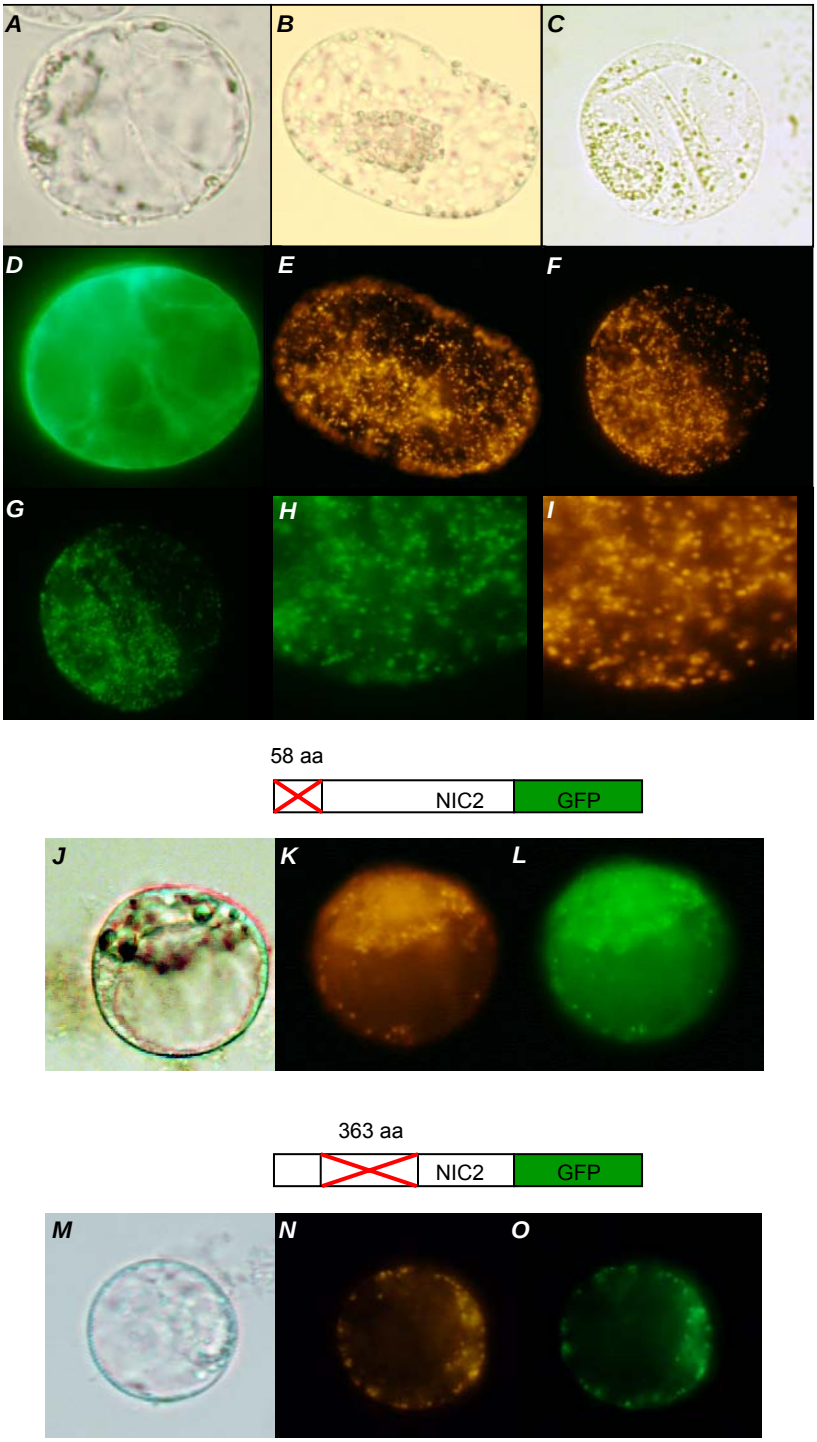

Figure 35. Subcellular localisation of NIC2-GFP fusion protein in *Nicotiana tabacum* BY2 protoplasts. After 40 hours of incubation, control GFP showed nuclear and cytoplasmic localisation, ***D*** and control SKL-DsRED was localised in peroxisomes, ***E***. Co-expression of SKL-DsRED and NIC2-GFP fusion protein indicates peroxisomal localisation of NIC2, ***F*** and ***G***, shown also in magnified images in ***H*** and ***I***, respectively. Localisation of the N-terminally truncated NIC2-GFP fusion protein was also peroxisomal, ***L***, compared to co-localised SKL-DsRED, ***K***. Deletion of the central part of the protein did not change the peroxisomal localisation of NIC2-GFP fusion protein, ***O***, which co-localised with SKL-DsRED, ***N***. The two deletion constructs are schematically presented above the microscopic images. ***A***, ***B***, ***C***, ***J*** and ***M*** light microscopic and ***D*** to ***I***, ***K***, ***L***, ***N*** and ***O*** fluorescence images of *Nicotiana tabacum* BY2 protoplasts.

Discussion

The *NIC2* gene encoding the putative novel ion carrier 2 was isolated from the *Arabidopsis thaliana* genome. Together with *NIC1* it was clustered with six additional genes (*NIC3*-*NIC8*) in one family, which was named the NIC family. After the complete sequencing of the *Arabidopsis thaliana* genome (Arabidopsis Genome Initiative, 2000), the subsequent *in silico* analysis revealed that the NIC family together with 48 further genes found in the genome encode putative transporter proteins. They were classified as members of the multidrug and toxic compounds extrusion family defined by Brown *et. al*. (1999). Accordingly, a putatvie multidrug efflux carrier encoded by *NIC2* shows homologies with the bacterial and yeast MATE carriers. Using heterologous and homologous expression systems, it has been shown that NIC2 likely possesses polyspecific features in transporting exogenous multidrug and toxic compounds to protect the *E. coli* and *S. cerevisiae* cells and in transporting endogenous substrate(s) in *A. thaliana*.

1. *NIC2* confers resistance of *E. coli* KAM3 towards TEACl, TMACl and F-IAA

Like several multidrug efflux transporters from various bacteria and *AtDTX1* from *A. thaliana*, *NIC2* was functionally characterised in a model expression system, i.e. the *E. coli* KAM3 mutant. In order to show *NIC2* properties in transporting diverse multidrug and toxic compounds, the gene was expressed in KAM3 cells using the IPTG-inducible system and grown in the presence of selected drugs and toxins typically used to characterise MATE carriers (Morita *et al*., 1998 and 2000; Nishino and Yamaguchi, 2001; Yang *et al*., 2003). KAM3 cells were not complemented by the expression of *NIC2* when grown on media supplemented with IPTG and Norfloxacin, Acriflavine, Ethidium bromide, Berberine, TEACl or TMACl. To reduce the probable effect of protein toxicity on cell growth, due to high expression level, the experiment was also performed without the application of IPTG. The obtained results were, however, identical to the ones observed before. As a positive control for the expression and the complementation of KAM3 cells the *E. coli* MATE gene, *YDHE*/*NORE* was used. In contrast to the literature, IPTG-induced expression of

YDHE/*NORE* did not complement KAM3 growth with Norfloxacin, Acriflavine or Ethidium bromide (Nishino and Yamaguchi, 2001). The high amount of the host protein encoded by the IPTG-inducible gene likely occurred to be toxic to the bacterial cells, which generally has a relatively low expression in *E. coli* (Allen *et al*., 2000; Gerdes *et al*., 2003; The *E. coli* Genome Project; http://www.genome.wisc.edu/). Moreover, the experiment was performed one more time with the same toxic compounds, but without an application of IPTG. Due to the leakiness of *lac*-derived promoters (Baneyx, 1999), its expression should have occurred at a low level. Nevertheless, YDHE/NORE was still toxic to the bacterial cells. On the other hand, according to the literature (Morita *et al*., 1998), KAM3 growth was partly complemented in the presence of Berberine, and additionally, slightly complemented in the presence of TEACl and TMACl. Upon induction with IPTG, bacterial cells showed retarded growth, while in the absence of the inducer they grew significantly better. The bacterial cells grew because less harmful toxins (i.e. Berberine, TEACl and TMACl) were used with these experiments (Morita *et al.*, 1998). The lack of KAM3 complementation by expression of *NIC2* could have had a similar reason. The foreign membrane protein encoded by *NIC2* probably exhibits adverse effects when synthesised, independent of the presence of IPTG or toxic compounds. These data are in accordance with the general observation that bacterial cells have to keep the synthesis of membrane proteins at a very low level, e.g. at around 0.1 % of the cellular proteins (Henderson *et al*., 2000), otherwise the overexpression of either native or foreign membrane proteins can be lethal.

To overcome the leakiness, and hence protein toxicity, and to better control *NIC2* as well as *YDHE*/*NORE* expression, both genes were in a second experiment directed by the 856 bp upstream flanking sequence of the *YDHE*/*NORE* to control the expression level of both genes by the supply of drug or toxic compounds (Morita *et al*., 1998 and 2000; Yang *et al*., 2003). The data showed that expression of *YDHE*/*NORE* increased resistance of KAM3 cells only to Norfloxacin. The lack of KAM3 complementation with Acriflavine, Berberine and Ethidium bromide disagrees with the literature (Morita *et al*., 1998 and 2000; Yang *et al*., 2003). Since YDHE/NORE confers resistance to these compounds, the obtained data

suggest that its expression driven by the upstream flanking sequence of *YDHE*/*NORE* was probably not dependent on these toxic compounds and, therefore, not enough protein was synthesised to mediate drug efflux. Moreover, *YDHE*/*NORE* did also not complement KAM3 cells supplied with TEACl, TMACl or F-IAA, but these compounds have never been tested before.

The expression of *NIC2*, when driven by the upstream flanking sequence of *YDHE*/*NORE*, did not complement KAM3 growth in the presence of Acriflavine, Berberine, Ethidium bromide and Norfloxacin, simiar to the previous experimental data for *NIC2*. On the other hand, KAM3 cells could be complemented when grown in the presence of TEACl, TMACl and F-IAA. The results allow to speculate about the substrate specificity of NIC2, which makes TMACl and the structurally similar molecule TEACl good candidates for the extrusion. The recently characterised *Arabidopsis* MATE carrier, ALF5, when expressed in yeast *S. cerevisiae*, also increased resistance to TMACl (Diener *et al*., 2001), showing a similar substrate specificity like NIC2, while resistance to TEACl mediated by ALF5 has not been reported. Another good candidate for the extrusion by NIC2 is a toxic analogue of the potential precursor of indole-3-acetic acid (IAA), 5-fluoro-indole-3-acetic acid (F-IAA) (Bartel, 1997). Similar to *NIC2* expression in *E. coli* KAM3, ethylene insensitive root 1 (*EIR1*) expression in *S. cerevisiae* mutant yeast strain *gef1* confers resistance to fluorinated indolic compounds, like F-IAA, preventing their toxicities. EIR1 is a root-specific protein, involved in auxin transport and, therefore, is required for gravitropism in *A. thaliana* (Luschnig *et al*., 1998). The chemical structural diversities of TEACl, TMACl and F-IAA suggest that NIC2 likely possesses properties to transport a broad range of drugs and toxins, however, this needs further investigation.

2. *NIC2* increases lithium and sodium tolerance in the wild-type yeast *S. cerevisiae*

Due to the presence of two MATE carriers in the yeast *S. cerevisiae*, YDR338C and ERC1, the yeast single mutants *ydr338c* and *erc1* as well as the double mutant *ydr338c erc1* were subjected to functional characterisation in order to create an eukaryotic sensitive tool, similar

to *E. coli* KAM3. While the overexpression of *YDR338C* was never tested for resistance to any toxic compound, Shiomi *et al*. (1991 and 1995) showed that overexpression of *ERC1* confers resistance to a methionine toxic analogue, DL-ethionine. Supported by these data and because YDR338C and ERC1 share high sequence similarity, the growth of yeast mutant strains *ydr338c*, *erc1*, and *ydr338c erc1* was tested in the presence of various concentrations (0.5 mM to 1.5 mM) of DL-ethionine. None of the yeast mutant strains exhibited growth sensitivity to this toxic compound. The yeast mutant strains were also tested for susceptibilities towards other drug and toxic compounds (summarised in **Table 3** in the Results part), but again no differential growth was detected. Although the mechanism of the ERC1-mediated resistance has not been established thus far, it has been proposed that ERC1 transports DL-ethionine from the cytoplasm to mitochondria, where ERC1 is putatively localised (Comprehensive Yeast Genome Database; http://mips.gsf.de/desc/yeast/). The function of YDR338C remains unknown, but one of the possible subcellular localisations for YDR338C indicated by the TargetP database (http://www.cbs.dtu.dk/services/TargetP/) are also mitochondria. Hence, while mitochondrially localised proteins can be functionally characterised, when overexpressed, like in the case of e.g. ERC1 (Shiomi *et al*., 1991 and 1995), their absence, due to mutations in the genes, make their functional characterisation difficult. The creation of a sensitive eukaryotic tool therefore failed and the subsequent characterisation of *NIC2* was performed in the parental *S. cerevisiae* strain BY4741.

The driving force of the antiport mechanism of MATE carriers is based on a Na^+ or H^+ gradient across the plasma membrane (Morita *et al*., 1998 and 2000; Li *et al*., 2002; He *et al*., 2004). To emphasise the conceivable transport of ions, which is a part of the antiport mechanism, yeast cells expressing *NIC2* were grown in a non-physiological excess of various inorganic salts. Drop test experiments showed that the expression of *NIC2* in the wild-type yeast *S. cerevisiae* confers ion tolerance. LiCl tolerance became apparent at 150 mM LiCl, and then continued through 300 mM, 450 mM and 600 mM. According to Rodriguez-Navarro and Asensio (1977) and Dichtl *et al*. (1997), wild-type yeast exhibits relatively high tolerance towards LiCl (up to 200 mM). Therefore, expression of *NIC2* in the

wild-type yeast increased tolerance to a three-fold higher concentration of LiCl. This tolerance was observed in liquid growth experiments. Accordingly, expression of *NIC2* in wild-type *S. cerevisiae* confers tolerance towards 300 mM and 600 mM LiCl. At 600 mM LiCl, the time required to reach half-maximal optical density ($T_{1/2}$) significantly decreased. In contrast, independent of the concentration used (1000 mM to 1500 mM), a difference in the tolerance towards NaCl was not observed in the drop test experiments. These data are in agreement with those obtained by Prior *et al*. (1996), which showed that wild-type yeast tolerates NaCl up to a concentration of 1500 mM. However, as a less toxic analogue of lithium (Jia *et al*., 1993), sodium was further tested in the liquid growth experiment. As expected, at 900 mM NaCl, yeast expressing *NIC2* and the control yeast show no difference in growth, but at 1600 mM a slightly increased tolerance appeared in yeast expressing *NIC2*. Although various concentrations of chloride were used in the both experiments, it is assumed that the growth differences were not caused by this anion. Hence, it is postulated that the tolerance of yeast *S. cerevisiae*, confered by NIC2, is towards lithium and sodium. Whether the tolerance is due to a transport mediated by NIC2, is still unknown. To test this hypothesis further experimental approaches, such as a measurement of Li^+/Na^+ antiport activity, have to be undertaken.

The above data are in accordance with other data reported in the literature (Morita *et al*., 1998 and 2000; Li *et al*., 2002; He *et al*., 2004). They highlight the probablility that lithium can also be involved in antiport mechanisms mediated by MATE carriers. This led to the additional consideration of the monovalent cation potassium, and the divalent cation calcium as potential antiport ions. However, the expression of *NIC2* in yeast did not confer tolerance to KCl to $CaCl_2$, independent on their concentrations.

3. *NIC2* causes a transient cytosolic Ca^{2+} increase in wild-type yeast after hyperosmotic stress

As shown above, the expression of *NIC2* increases tolerance of wild-type yeast towards lithium and sodium. The high concentrations of both ions (600 mM LiCl and 1600 mM NaCl)

also cause a hypertonic shock, which according to Matsumoto *et al*. (2002) induces an immediate and short-duration transient cytosolic Ca^{2+} increase. Using the Ca^{2+}-sensitive photoprotein AEQUORIN (Shimomura e*t al*., 1962; Blinks *et al*., 1978), targeted to the cytoplasm (Matsumoto *et at*., 2002), LiCl- and NaCl-induced changes in cytosolic Ca^{2+} concentrations were analysed in the wild-type yeast and yeast expressing *NIC2*. The application of either LiCl or NaCl at a final concentration of 1 M initiated an immediate and transient elevation of cytosolic [Ca^{2+}], which increases to higher levels in the yeast expressing *NIC2* when compared to the control yeast. Additionally, these elevations of cytosolic [Ca^{2+}] occured with a delay of 10 sec and lasted about 1 min in duration. To elucidate whether the observed increases in cytosolic [Ca^{2+}] are due to an ionic or osmotic shock, 1.6 M sorbitol was also tested. Because similar [Ca^{2+}] transient profiles appear with a 10 sec of delay and a duration of about 1 min thereafter, it can be assumed that this increase of cytosolic [Ca^{2+}] in the wild-type yeast expressing *NIC2* is caused by hyperosmotic, and not by ionic stress. Matsumoto *et al*. (2002) reported that in *S. cerevisiae*, the hyperosmotic stress initially induces a short Ca^{2+} influx from the extracellular space through a complex of the L-type voltage-gated Ca^{2+} channel-like protein CCH1 and the Ca^{2+}-permeable stretch-activated nonselective cation channel MID1, which then causes the activation of the vacuolar membrane localised TRP channel-like protein YVC1. YVC1 mediates an internal Ca^{2+} release, increasing its concentration in the cytoplasm (Denis and Cyert, 2002). Accordingly, the hyperosmotically stressed cytosolic Ca^{2+} elevation in the control yeast would be solely due to the action of CCH1, MID1 and YVC1 like-channels, while in the yeast expressing *NIC2*, cytosolic [Ca^{2+}] increases to higher levels because of the additional action of NIC2. Moreover, in the yeast expressing *NIC2*, a 10 sec delay observed after hyperosmotic shock leads to the suggestion that Ca^{2+} enters the cytoplasm from internal Ca^{2+} sources and not from the external solution. Since expression of *NIC2* did not confer tolerance towards high concentration of $CaCl_2$, it is speculated that NIC2 does not mediate Ca^{2+} release by itself from the internal sources such as a vacuole, which is the major site of intracellular Ca^{2+} storage, the Golgi apparatus or mitochondria which also play significant roles in maintaining

Ca^{2+} homeostasis (Jung *et al*., 1997; Miseta *et al*., 1999; Foerster and Kane, 2000; Jung *et al*., 2004). Furthermore, if Ca^{2+} release is not mediated by NIC2, it could be possible that during hyperosmotic stress NIC2 interacts with a yeast protein or a set of proteins which possess features to release Ca^{2+} from its internal sources. Further studies involving protein-protein interaction studies may shed light on it.

Based on the characterisations accomplished using the heterologous expression systems, it appears that NIC2 performs multidrug and toxic resistance towards TEACl, TMACl and F-IAA, and toxic levels of sodium and lithium. These transporting features highlight the polyspecificity of NIC2. However, the molecules transported *in vivo* by NIC2 need to be identified.

4. *NIC2* overexpression and *NIC2* RNAi change the phenotype of *Arabidopsis thaliana*

The expression pattern of *NIC2* in *Arabidopsis thaliana* determined by real-time RT-PCR shows that *NIC2* is ubiquitously expressed in primary and secondary roots, rosette leaves, inflorescence stems and flowers. Its expression level is, however, sligthly higher in roots in comparison to the remaining organs. To understand the role of *NIC2*, two different strategies were chosen, involving *NIC2* overexpression and gene silencing. *Arabidopsis* plants transformed with the *35S*:*NIC2* construct, which causes *NIC2* overexpression, exhibit morphologically altered phenotypes during their entire growth. Most of the 30-day-old transgenic plants possess many small inflorescence stems and 2-2.5 fold more rosette leaves, with vascular tissue patterns at the border of leaf blades and petioles sligthly differing from that of wild-type leaves, showing uneven growth along the petiole. Fourty-five-day-old and 50-day-old transgenic plants have extremely bushy phenotypes with no apical dominance, which is reflected by 3-5 fold higher number of much smaller lateral flowering shoots than flowering shoots in the wild-type. Skoog and Miller (1957) have established that exposing callus cultures to a low auxin-cytokinin ratio results in shoot development, while Wickson and Thimann (1958) demonstrated that auxin is required for apical dominance, and

for cytokinin promotion of lateral bud formation. The altered apical dominance phenotype of *Arabidopsis* auxin and cytokinin mutant supports this model. *axr1* plants are deficient in their auxin response and feature increased lateral bud formation without an apical dominance (Strinberg *et al*., 1999). Moreover, Romano *et al*. (1991) have demonstrated that the expression of *IAAL* results in reduced hypocotyl length in *Arabidopsis* plants due to the lowered endogenous auxin level. The fact that auxins promote *Arabidopsis* hypocotyl growth, together with gibberellic acid (GA), is also confirmed by other literature data (Smalle *et al*., 1997; Richards *et al*., 2001). Hence, the bushy phenotypes with no apical dominance reflected by many smaller inflorescence stems in comparison to the wild-type may account for the first evidence that the auxin level is likely changed in the transgenic plants due to the overexpression of *NIC2.* Furthermore, the slightly different vascular tissue pattern observed in leaves of the transgenic plants also suggests that the auxin level is changed there, which is in agreement with the model that auxin induces vascular differentiation as well (Lyndon, 1990; Mattsson *et al*., 1999). However, this interpretation needs further detailed investigation. Fourty-five-day-old and 50-day-old transgenic plants produce more flowers (2-3 fold) and accompanying siliques with smaller seed sizes and more transparent seeds than in the wild-type. This leads to the speculation that the possibly reduced auxin level in the transgenic plants may inhibit the full development of the siliques, because proper parthenocarpic fruit development depends on auxin and GA, which act together (Vivian-Smith and Koltunov, 1999). Additionally, the senescence of rosette leaves and inflorescence stems which occur much earlier in the transgenic plants than in the wild-type, therefore, leading to the death of most of the *NIC2* overexpression plants, may also indicate a reduced auxin level, according to Beyer and Morgan (1971). They demonstrated a correlation between ethylene-promoted leaf abscission and closely associated senescence and reduced polar auxin transport. Although the endogenous level of auxins has not been established, based on these data and on the literature, it is speculated that the phenotypes of the *NIC2* overexpression plants are likely due to a decreased auxin level.

The intron-spliced hairpin RNA technology (abbrev. RNAi) for gene silencing was used to further investigate the function of *NIC2*. *Arabidopsis* plants transformed with a *NIC2* RNAi construct also exhibit markedly modified phenotypes during their entire growth. In comparison with the wild-type, most of the 40-day-old transgenic plants produce much longer primary inflorescence stems. Due to their fast developmental growth, these inflorescence stems are 50 % thinner and, therefore, at first bend towards the ground and then lay on the ground, instead of growing upwards. The same behaviour is observed for secondary inflorescence stems which outgrow from the primary inflorescence stems. However, secondary inflorescence stems which develop from the base of the shoot system, grow upwards similar to stems of the wild-type. Romano *et al*. (1995) have shown that transgenic plants expressing the *IAAM* have an elevated auxin level and, therefore, longer hypocotyls. Leyser *et al*. (1996) and Cline *et al*. (2001) also provided data showing that the development of an enhanced apical dominance phenotype in *axr3* mutant plants is mainly caused by an increased response to auxin. In addition, Ross *et al*. (2000) established that stem elongation requires auxins which maintain normal levels of bio-active GA in the elongating stem tissues. Hence, the lengthened inflorescence stems, including primary and secondary ones, in *NIC2* RNAi transgenic plants are likely due to an increased auxin level. As shown, the *NIC2* RNAi transgenic plants also possess many already mature siliques, whereas the wild-type plants have a few, mostly immature ones. Since auxin and auxin-dependent biosynthesis of GA both regulate parthenocarpic fruit development (Vivian-Smith and Koltunov, 1999), the earlier maturation of siliques in the transgenic plants may also be triggered by an increased level of auxin. The seeds obtained from these plants have a similar transparency to those of the wild-type seeds. Like *NIC2* overexpression plants, the endogenous level of auxins has not been established in *NIC2* RNAi plants, but again the phenotypes of the *NIC2* RNAi plants are consistent with a changed, this time possibly increased, auxin level.

5. *NIC2* overexpression seedlings exhibit a modified root system with a delay in gravitropic response and auxin resistant growth

Additional data from the investigation of the root system of the *NIC2* overexpression seedlings are consistant with the proposed auxin hypothesis resulting from a decreased auxin level. Primary roots from 8-day-old transgenic seedlings are 40 % longer than wild-type. According to Rahman *et al*. (2001), auxin is a positive regulator for ethylene-induced inhibition in root elongation. Hence, the reduction of the intracellular level of auxin in the transgenic seedlings may cause their resistance to ethylene and, therefore, trigger further elongation of primary roots. Moreover, 8-day-old *NIC2* overexpression seedlings have a few lateral roots already formed, whereas the wild-type has not. These data may be in contrast with the proposed auxin hypothesis. Casimiro *et al*. (2001) have revealed that lateral root initiation requires polar auxin transport, however, the amount of auxin to initiate lateral root development still remains unknown. Whereas primary roots of the wild-type seedlings exhibit a proper gravitropic response resulting from gravistimulation, roots of *NIC2* overexpression seedlings slant to the left when viewed from above the agar surface. Rutherford and Masson (1996), and Migliaccio *et al*. (2000) have presented data where roots of wild-type *A. thaliana* seedlings in the Wassilewskija (WS) and Landsberg erecta (Ler) ecotypes often grow aslant on vertical agar surfaces. Slanted root growth always occurs to the right of the gravity vector when the root is viewed through the agar surface (or to the left when viewed from above the agar surface), and is not observed in the Columbia ecotype. Although the wild-type *Arabidopsis* C24 ecotype has not been tested in this respect, it is suggested that the slanting response which occurred in the roots of the transgenic seedlings may be due to an interaction between roots and the agar medium itself, effects of gravitropism and movements of *Arabidopsis* roots (Okada and Shimura, 1990; Simmons *et al*., 1995), and not due to the overexpression of *NIC2*. Moreover, roots from *NIC2* overexpression lines are not agravitropic. During the time-dependent vertical growth their responses to the gravitropic stimulus are delayed by 2 to 4 h in comparison to the wild-type. Auxin also plays a central role in tropic responses such as gravitropism (Went and Thimann, 1937; Davis *et al*., 1995).

Hence, it is spectulated that the delayed gravitropic response is likely due to a decreased auxin level in roots of the *NIC2* overexpression seedlings, although the endogenous level of auxins has not been determined yet. Furthermore, to assess the level of resistance or sensitivity to auxins, the roots of *NIC2* overexpression seedlings were tested in the presence of 5 µM indole-3-actetic acid (IAA) or 50 µM indole-3-butyric acid (IBA), which, besides IAA, is the second naturally occurring auxin in *A. thaliana* (Ludwig-Mueller *et al*., 1993). Compared to wild-type root growth, roots of the transgenic seedlings are much more resistant to both exogenously applied auxins, exhibiting a large number of adventitious and lateral roots, indicating that overexpression of *NIC2* leads to auxin resistance.

6. *NIC2* RNAi seedlings also display a modified root system

The root system of *NIC2* RNAi seedlings was also examined. They exhibit many lateral roots which outgrow from the primary root as well as from the root-shoot junction. Blakely *et al*. (1982) and Laskowski *et al*. (1995) have demonstrated that auxin represents a key regulator of lateral root development, which has been confirmed by Casimiro *et al*. (2001) and Bhalerao *et al.* (2002), who showed that shoot-derived auxin promotes *Arabidopsis* lateral root initiation. The altered root phenotype of *Arabidopsis* auxin mutants support this model. *superroot1* (*sur1*) and *superroot2* (*sur2*) plants display several abnormalities reminiscent of auxin effects, including the development of excess adventitious and lateral roots, which ultimately occur to be caused by increased levels of either both free and conjugated auxin or only free auxin (Boerjan *et al*., 1995; Delarue *et al*., 1998). Despite the fact, that endogenous level of auxins has not been determined yet, it is suggested that the root phenotypes of *NIC2* RNAi seedlings are due to an increased auxin level.

7. Organ- and tissue-specific expression of *NIC2* correlates with sites of auxin action in mature *Arabidopsis* plants

To define the spatial pattern of *NIC2* expression, *Arabidopsis* plants were transformed with the Pro_{NIC2}:*GUS* construct, which consists of the 1483 bp promoter region of *NIC2* fused to

the *E. coli β-glucuronidase* (*GUS*) gene. Based on the results obtained for the Pro_{NIC2}:*GUS* fusion, *NIC2* is expressed in the vascular tissue of the primary and secondary roots, rosette and cauline leaves, inflorescence stems and flowers. It is also expressed throughout whole immature siliques and then in the abscission zone of mature siliques. The subsequent detailed analysis revealed that the organ- and tissue-specific expression of *NIC2* reflects various sites of auxin action.

Firstly, the analysis of the primary roots revealed that the stele of the elongation zone and the lateral root cap in the root tip are the sites of *NIC2* expression. It is well established, that auxin plays an important role in gravitropism being mediated by cellular influx and efflux carriers (Marchant *et al*., 1999; Friml and Palme, 2002). In a gravistimulated root, the activation of the gravity signal transduction pathway occurs in columella cells and is transmitted to the lateral root cap cells, which then results in the formation of an auxin gradient across the root tip (Ottenschlager *et al*., 2003). Consequently, more auxin accumulates at the bottom than at the top of the root. After transmission of the auxin gradient into the elongation zone, it promotes a differential rate of cell growth on opposite flanks, which is resposible for the root curvature (Chen *et al*., 1999, Blancaflor and Masson, 2003).

Secondly, the transverse cross-sections through the primary root tip show that at the cellular level, *NIC2* is expressed in the pericycle cells, which is the layer just inside the endodermis surrounding the vascular tissue of the root. In addition, the analysis of the secondary (lateral) roots exhibits that the expression of *NIC2* is changing there and depends on the definite developmental stage. At the primordium stage, *NIC2* is expressed throughout the whole emerging secondary roots. During further development, its expression changes, disappearing from the vascular tissue of secondary roots which is close to the primary root, but appears again, when a new root primordium emerges from this secondary root. Finally, in the mature secondary root, the stele of the elongation zone and the lateral root caps are the sites of *NIC2* expression, which resembles the site of *NIC2* expression in the primary root. It has been shown many times, that auxin is a key regulator for lateral root development, the formation of which consists of two major steps, i.e. the cell cycle reactivation in the pericycle

cells and establishment of a new meristem (Blakely *et al*., 1982; Laskowski *et al.*, 1995; Beeckman *et al*., 2001; Himanen *et al*., 2002). The lateral roots are initiated by a certain amount of free endogenous auxin, which activates pericycle initial cell divisions at the xylem poles. Accordingly, the application of exogenous auxin, 1-naphthalene acetic acid (NAA), induces pericycle activation, but the frequency and position of lateral root initiation occur independently of control mechanisms from the surrounding tissues (Himanen *et al*., 2002). In contrast, the local application of the polar auxin transport inhibitor, N-1-naphthylphthalamic acid (NPA), results in a decrease of free auxin in roots with a corresponding reduction in the number of emerging lateral roots (Casimiro *et al*., 2001; Himanen *et al*., 2002). Hence, the amount of auxin seems to determine the frequency and position of lateral root initiation from the pericycle cells, where expression of *NIC2* has been found.

Thirdly, a detailed analysis of rosette leaves and inflorescence stems demonstrates that *NIC2* is also expressed in xylem parenchyma cells, which are part of vascular tissues in these organs. Auxin supply is believed to initiate the formation of xylem, a water-conducting tissue (Fukuda, 1996). A specific signal transduction pathway which is initiated by auxin specifies the vascular fate of young procambial initials into xylem parenchyma cells and of these parenchyma cells into tracheary elements. This cell formation represents a specialised form of programmed cell death (PCD) (Fukuda, 1996; Roberts and McCann, 2000; Nieminen *et al*., 2004). These two different processes can probably be regulated by an auxin gradient across the cambial zone. This radial distribution pattern of endogenous auxin exhibits a peak level in the cambial zone where cell division takes place, and then steeply decreases towards the mature xylem and phloem (Uggla *et al*., 1996). It indicates that a high amount of auxin may act as a positional signal to regulate the area of cell divisions in the cambial zone (Uggla *et al.*, 1996; Mellerowicz *et al*., 2001; Schrader *et al*., 2003), while a lower amount of auxin may trigger the parenchyma cell fate, but this is only a speculation at the moment.

Fourthly, the transverse cross-sections through immature siliques demonstrate that the expression of *NIC2* is specific to the vascular tissue running along the silique as well as in the dehiscence zone of the silique, where the cells undergo cell wall breakdown in the

process of separation. Although little work has been carried out to determine which hormonal ligands may trigger dehiscence, auxins have been proposed to play a role in the regulation and timing of pod dehiscence (Chauvaux *et al*., 1997; Roberts *et al*., 2002). A decline in auxin concentration in the dehiscence zone (DZ) may be the trigger that elevates cell wall degrading enzyme activity, which is then necessary for dehiscence to take place, however, other factors may also be important (Chauvaux *et al*., 1997).

Fifthly, the expression of *NIC2* is also detected in the abscission zone of mature siliques. Auxin is the principal endogenous regulator for abscission and closely associated senescence (Beyer and Morgan, 1971; Roberts *et al*., 2002). Auxin gradient across the abscission zone regulates onset and rate of abscission. According to Addicot *et al*. (1955), abscission does not occur with auxin gradients characteristic for healthy, mature tissues with high auxin distal to the abscission zone and low auxin proximal to the abscission zone. It occurs after a fall in the ratio of distal to proximal auxin. Recently, Patterson (2001) and Roberts *et al*. (2002) demonstrated that this phenomenon is controlled by ethylene. Ethylene influences and controls the abscission through the inhibition of auxin supply to the cell *via* an effect on the basipetal auxin transport capacity, but not the velocity, and perhaps on auxin destruction and synthesis as well.

In conclusion, the organ- and tissue-specific expression of *NIC2* correlates to several places of auxin action, where the auxin gradient seems to be very important for the cell fate. Therefore, an increase or a decrease of active auxin must be precise and this depends on either transport or catabolism, in which NIC2 as the MATE carrier may be involved.

8. Expression of *NIC2* in the root tip is induced by auxins, slightly induced by salts and not altered by flavonoids

In silico analysis has revealed an inverted auxin-response element (AuxRE), GAGACA, in the promoter region of *NIC2* (Ulmasow *et al*., 1995; Guilfoyle *et al*., 1998). It is localised 279 bp upstream of the ATG start codon. Guilfoyle *et al*. (1998) have demonstrated that the activity of an AuxRE is not dependent on its orientation within a promoter, but it must occur

as direct repeats that are spaced by 5 bp. Although a second AuxRE is not present in the *NIC2* promoter, the exogenously applied auxins induce activity of Pro_{NIC2}:*GUS* in the stele of the elongation zone and the lateral root cap in the root tip compared to the control. Five-day-old seedlings that grow on 100 nM synthetic auxin, 2,4-dichlorophenoxy-acetic acid (2,4-D), have the most strongly increased GUS staining. Comparably lower GUS activities are observed in seedlings grown on 300 nM natural auxin, indole-3-acetic acid (IAA), and 100 nM synthetic auxin, naphthalene-1-acetic acid (NAA). 300 nM indole-3-butyric acid (IBA), the second naturally occurring auxin in *A. thaliana* (Ludwig-Mueller *et al*., 1993), also induces GUS staining in 6-day-old seedlings. Delbarre *et al*. (1996) and Yamamoto and Yamamoto (1998) have demonstrated that NAA enters cells by passive diffusion and its accumulation level is controlled by efflux carriers. By contrast, 2,4-D uptake is mostly ensured by influx carriers and is not secreted by the efflux carriers, while IAA and IBA enter cells using influx and efflux carriers (Friml and Palme, 2002; Rashotte *et al*., 2003). As a result 2,4-D can reach a high concentration in cells, whereas IAA, IBA and NAA accumulate to much lower levels. Considering this, the diverse GUS activities observed in the root tip of the transgenic seedlings are due to the transport features of the applied auxins. Therefore, the GUS staining decreases following the series 2,4-D > IAA/IBA ≥ NAA. Based on these results, it can be concluded that *NIC2* is an auxin-inducible gene.

The activity of Pro_{NIC2}:*GUS* has also been tested under salt treatment. Compared to the primary root of the control seedlings, the presence of 5 mM LiCl and 20 mM NaCl causes only a slight increase in the GUS activity. An in *silico* analysis of the *NIC2* promoter using the PLACE database, which is a database of plant *cis*-acting regulatory DNA elements (http://www.dna.affrc.go.jp/PLACE/signalscan.html), did not reveal any of the known *cis*-elements responsive for enviromental stresses (data not shown). Also the experimental data originating from the Genevestigator database (https://www.genevestigator.ethz.ch/) demonstrate an unchanged expression level of *NIC2* after salt stress in comparison to the control.

Because NIC2 may be involved in the regulation of the endogenous level of auxin, the activity of Pro_{NIC2}:*GUS* was also studied after flavonoid treatment. Murphy *et al*. (2000) and Brown *et al*. (2001) have shown that flavonoids such as naringenin, keampferol and quercetin can change the intracellular auxin level by the negative regulation of auxin carriers in *A. thaliana*. However, in comparison to the control none of these flavonoids have changed the GUS intensity in the transgenic seedlings. Although the results apparently suggest that at the transcriptional level expression of *NIC2* is not altered by flavonoids, there is still an unanswered question about their interaction with NIC2.

9. Gravitropism markedly changes the expression site of *NIC2* in the root tip

The localisation of *NIC2* expression in the lateral root cap was also analysed after a gravitropic stimulus. After 120 min of gravistimulation, the changed intensity of the GUS staining was observed at the upper side of the root tip, while at the lower side the GUS staining stayed unchanged. It is well known that gravistimulation results in the formation of an endogenous auxin gradient across the root tip, where more auxin accumulates at the bottom than at the top of the lateral root cap (Chen *et al*., 1999; Chen *et al*., 2002; Blancaflor and Masson, 2003; Ottenschlager *et al*., 2003). Therefore, it is suggested that the increased expression of *NIC2* takes place when the amount of endogenous auxin also increases due to the gravistimulation. This highlights the correlation of the high auxin level and the increased expression of *NIC2* and also confirms that *NIC2* is probably an auxin-inducible gene.

10. IAA uptake assay demonstrates no transport activity of NIC2

To determine whether NIC2 mediates the transport of the most characterised endogenous auxin, IAA, an uptake assay using *Xenopus laevis* oocytes was designed. However, no differences in the accumulation of ^{3}H-labelled IAA in the control and *NIC2* expressing oocytes were detected. Since no transport activity could be shown for NIC2, it is possible that the localisation of NIC2 in oocytes is not in the plasma membrane. *In silico* analyses seem to

confirm this hypothesis, providing no clear evidence for subcellular localisation of NIC2 at the plasma membrane. However, it is also well possible that NIC2 is not an auxin transporter.

11. At the subcellular level NIC2 is localised in peroxisomes

The localisation pattern observed in *Nicotiana tabacum* BY2 protoplasts revealed that NIC2-GFP fusion protein is localised in peroxisomes. Since the protein contains 11 predicted transmembrane spanning regions, it is likely that NIC2 is situated in the peroxisomal membrane rather than in the peroxisomal matrix. The mechanisms controlling protein targeting and import are well understood for peroxisomal matrix proteins. They contain one of two different peroxisomal targeting signals (PTS) either at the C-terminus (tripeptide motif: SKL) or at the N-terminus (nonapeptide motif: -R-X_6-H/Q-A/L/F) (Mullen, 2002; Murphy *et al*., 2003). In comparison, much less is known about the targeting and insertion/assembly of peroxisomal membrane proteins (PMP). The consensus motif of a prototypic membrane peroxisomal targeting signal (mPTS) has not been reached, because they can vary from a short stretch of three to six positively charged amino acid residues to large nonoverlapping segments localised in transmembrane domains (Trelease, 2002; Murphy *et al*., 2003). Despite of that, the analysis of the two truncated NIC2-GFP fusion proteins in BY2 protoplasts allows to identify a part of the protein which is probably responsible for its peroxisomal localisation. The targeting sequence is likely located at the C-terminus of NIC2. The results describe here demonstrate that the first truncated NIC2-GFP protein fusion lacking 58 amino acid residues of the N-terminus, and the second truncated NIC2-GFP protein fusion lacking 363 central amino acid residues, are still targeted to peroxisomes. However, this result does not exlude the possibility that also the nonoverlapping segments of the remaining transmembrane domains take part in the peroxisomal targeting of NIC2.

12. Auxins, peroxisomes and hypothetical function of NIC*2* in *A. thaliana*

Although the majority of research has focused on the primary free auxin, IAA, Ludwig-Mueller *et al*. (1993) have demonstrated another abundant auxin in plants, IBA. It is not very clear

whether IBA and IAA can act and move by similar mechanims, but it has been shown that IBA can be interconverted to IAA in plant peroxisomes (Bartel *et al*., 2001), which led to the suggestion that IBA may act as a precursor to IAA (**Fig. 36**). Recent progress using *Arabidopsis* mutants has suggested that plant peroxisomes, besides the pivotal role in three metabolic pathways: lipid breakdown *via* β-oxidation, photorespiration and H_2O_2-detoxification (van den Bosch *et al*., 1992), are also a source and sensor of molecules that can effect plant growth and development in profound ways (Hayashi and Nishimura, 2003). The signal molecule to be considered is IBA, which *via* the peroxisomal β-oxidation pathway can supply plants with free IAA (Zolman *et al*., 2000 and 2001). IAA is a phytohormone that is involved in mediating a number of essential plant growth and developmental processes (Davis, 1995). As a hormone with such important functions, its steady state level and fluctuations must be determined by the inputs to and outputs from the IAA pool (Slovin *et al*., 1999). The current knowledge about the inputs of the IAA pool includes *de novo* biosynthesis, hydrolysis of IAA-conjugates and IBA-β-oxidation (Slovin *et al*., 1999; Bartel *et al*., 2001). The known outputs from the IAA pool contain either its transport in conjugation with sugars, amino acids or peptides away from that site and storage (Cohen and Bandurski, 1992; Bartel *et al*., 2001; Ljung *et al*., 2002), or conjugation into an inactive form and oxidative destruction (Slovin *et al*., 1999; Ljung *et al*., 2002). *Arabidopsis* conjugates include IAA-Ala, IAA-Leu (Barlier *et al*., 2000), IAA-Asp, IAA-Glu, IAA-glucose (Tam *et al*., 2000) and an IAA-peptide (Walz *et al*., 2002). While IAA-Ala, IAA-Leu and an IAA-peptide are the storage and transport conjugations that can provide free IAA (Bartel *et al*., 2001; Ljung *et al*., 2002), IAA-Asp, IAA-Glu and IAA-glucose represent the catabolic conjugations (Tam *et al*., 2000). Therefore, it has been suggested that the conjugated moiety indicates the fate of the attached IAA for storage, transport, or degradation. To date, little work has been carried out to determine where exactly IAA is degradaded within a cell. It is thought that it may occur through the action of oxidases (Normanly *et al*., 1995 and 1997), based on the evidence that *in vitro* plant peroxidases can degradate IAA *via* a decarboxylation pathway (Östin *et al*., 1995). However, in *Arabidopsis* a non-decarboxylative oxidation pathway seems to be the

major IAA catabolic pathway (Östin *et al*., 1998), which due to the specific conditions may also occur in plant peroxisomes, although this has not been experimentally tested (**Fig. 36**). According to the chemiosmotic model (Lomax *et al*., 1995), auxin enters the cell either directly in its protonated form or through the action of a saturable auxin uptake carrier. Hence, the protonated forms of auxin such as IAAH-conjugates and IAAH can be also preferable for the transport into peroxisome *via* auxin carriers. Since the subcellular localisation of NIC2 occurs in peroxisomes, its hypothetical function in *A. thaliana* can be considered. As an efflux transporter (efflux from the cytoplasm into the peroxisome) NIC2 may act at sites of auxin action such as the lateral root cap, where the auxin level increases during gravitropism and then likely decreases, otherwise the response of the root would be disturbed. Moreover, NIC2 may also act as an efflux transporter at the sites where the auxin level must be lowered to trigger the subsequent processes, like the formation of the water-conducting tissue, xylem, from the xylem parenchyma cells, dehiscence in the dehiscence zone of the mature silique, and abscission in the abscission zone of mature siliques. Therefore, considering all the experimental results obtained for NIC2, together with the information about auxins and plant peroxisomes presented above, it is speculated that the hypothetical function of NIC2 is the efflux transport which takes part in the auxin homeostasis in certain plant tissues, probably by removing auxin conjugates, e.g. IAA-Asp or IAA-Glu, from the cytoplasm into peroxisomes (**Fig. 36**).

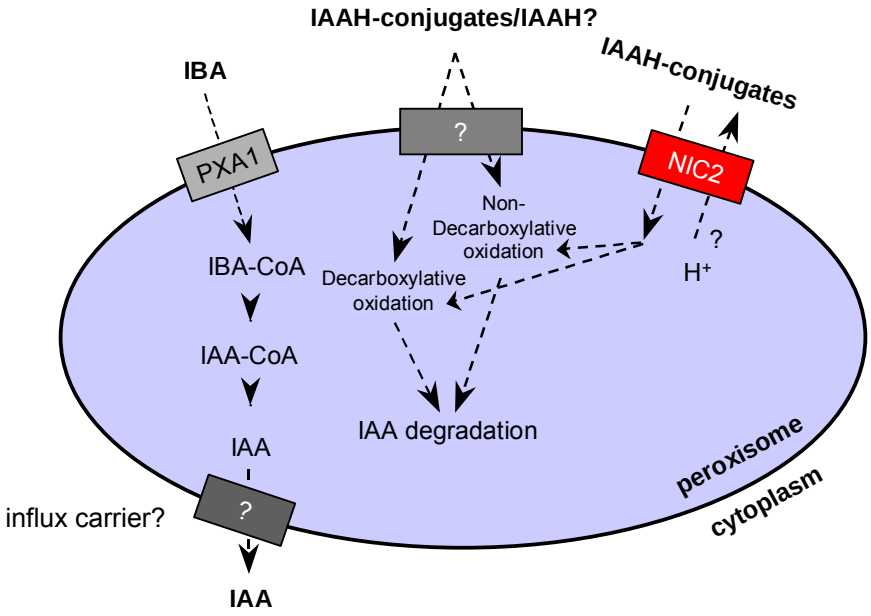

Figure 36. Hypothetical function of NIC2 in *Arabidopsis thaliana* peroxisomes. IBA is likely imported to the matrix of peroxisomes by the ABC-transporter-like protein PXA1 (Zolman *et al*., 2001), where it is converted to IAA in a process that parallels fatty acid β-oxidation. The transporter that influxes IAA from the peroxisomes to the cytoplasm remains to be identified. IAA-conjugates and probably IAA are oxidised in peroxisomes *via* decarboxylative oxidation or *via* non-decarboxylative oxidation pathway. Both lead to IAA degradation. The proposed hypothetical function of NIC2 is the transport of IAA-conjugates from the cytoplasm into the peroxisomes which may be elicited by a probable influx of H^+ from the peroxisomes.

To the best of the knowledge, neither Na^+ nor Li^+ are stored in plant peroxisomes, which could elicit the transport of IAA-conjugates by NIC2. Since no experiment has been done for H^+, it still remains unknown whether at the same time H^+ is influxed by NIC2 from peroxisomes, while protonated IAA-conjugates (IAAH-conjugates) are effluxed. Hence, further studies involving an IAA uptake assay in isolated plant peroxisomes coupled with a H^+ transport may address these unsolved questions.

References

Addicot, F.T., Lynch, R.S., Carns, H.R. (1955) Auxin gradient Theory of Abscission Regulation. Science **121**, 644.

Allen, T.E., Herrgard, M.J, Liu, M., Qiu, Y., Glasner, J.D., Blattner, F.R., Palsson, B.O. (2003) Genome-scale analysis of the uses of the *Escherichia coli* genome: model-driven analysis of heterogeneous data sets. J Bacteriol. **185,** 6392-9.

***Arabidopsis* Genome Initiative.** (2000) Analysis of the genome sequence of the flowering plant *Arabidopsis thaliana*. Nature **408**,796-815.

Baneyx, F. (1999) Recombinant protein expression in *Escherichia coli*. Curr Opin Biotechnol. **10**, 411-21.

Barlier, I., Kowalczyk, M., Marchant, A., Ljung, K., Bhalerao, R., Bennett, M., Sandberg, G., Bellini, C. (2000). The *SUR2* gene of *Arabidopsis thaliana* encodes the cytochrome P450 CYP83B1, a modulator of auxin homeostasis. Proc. Natl. Acad. Sci. USA **97**, 14819–14824.

Bartel, B. (1997) Auxin biosynthesis. Annu. Rev. Plant Physiol. Plant Mol. Biol. **48**, 51-66.

Bartel, B., LeClere, Sh., Magidin, M., Zolman, K.. (2001) Inputs to the Active Indole-3-Acetic Acid Pool: *De Novo* Synthesis, Conjugate Hydrolysis, and Indole-3-Butyric Acid β-Oxidation J Plant Growth Regul **20**, 198–216.

Beeckman, T., Burssens, S., Inze, D. (2001) The peri-cell-cycle in *Arabidopsis*. J. Exp. Bot. **52,** 403-11.

Beyer, E.B., Morgan, P. (1971) The Role of Ethylene Modification of Auxin Transport. Plant Physiol. **48**, 208–212.

Bhalerao, R.P., Eklof, J., Ljung, K., Marchant, A., Bennett, M., Sandberg, G. (2002) Shoot-derived auxin is essential for early lateral root emergence in *Arabidopsis* seedlings. Plant J. **29**, 325-32.

Bill, RM. (2001) Yeast--a panacea for the structure-function analysis of membrane proteins? Curr Genet. **40**, 157-71.

Blakely, L.M., Durham, M., Evans, T.A., Blakely, R.M.. (1982) Experimental studies on lateral root formation in radish seedlings roots. I. General methods, developmental stages, and spontaneous formation of laterals. Bot. Gaz, **143**, 341-352.

Blancaflor, E.B., Masson, P.H., (2003) Plant gravitropism. Unraveling the ups and downs of a complex process. Plant Physiol. **133**, 1677-90.

Blinks, J.R., Mattingly, P.H., Jewell, B.R., van Leeuwen, M., Harrer, G.C., and Allen, D.G.. (1978) Practical aspects of the use of aequorin as a calcium indicator: Assay, preparation, microinjection, and interpretation of signals. Methods Enzymol. **57,** 292-328.

Boerjan, W., Cervera, M.T., Delarue, M., Beeckman, T., Dewitte, W., Bellini, C., Caboche, M., Van Onckelen, H., Van Montagu, M., Inze, D. (1995) Superroot, a recessive mutation in *Arabidopsis*, confers auxin overproduction. Plant Cell. **7**, 1405-19.

Borges-Walmsley, M.I., Walmsley, A.R. (2001) The structure and function of drug pumps. Trends Microbiol. **9,** 71-9.

Borges-Walmsley, M.I., McKeegan, K.S., Walmsley, A.R., (2003) Structure and function of efflux pumps that confer resistance to drugs. Biochem. J. **1,** 313-38.

van den Bosch, H., Schutgens, R.B., Wanders, R.J., Tager, J.M., (1992) Biochemistry of peroxisomes**.** Annu. Rev. Biochem. **61,** 157-97.

Braibant, M., Guilloteau, L., Zygmunt, M.S. (2002) Functional characterization of Brucella melitensis NorMI, an efflux pump belonging to the multidrug and toxic compound extrusion family. Antimicrob. Agents Chemother. **46,** 3050-3.

Brown, M.H., Paulsen, I.T., and Skurray, R.A. (1999). The multidrug efflux protein NorM is a prototype of a new family of transporters. Mol. Microbiol. **31**, 394-5.

Brown, D.E., Rashotte, A.M., Murphy, A.S., Normanly, J., Tague, B.W., Peer, W.A., Taiz, L., Muday, G.K. (2001) Flavonoids act as negative regulators of auxin transport in vivo in *Arabidopsis*. Plant Physiol. **126,** 524-35.

Buchanan, B., Gruissem, W., Jones, R.L. (2000) Biochemistry and Molecular Biology of Plants 1st edition. American Society of Plant Physiologists Rockville, Maryland.

Casimiro, I., Marchant, A., Bhalerao, R.P., Beeckman, T., Dhooge, S., Swarup, R., Graham, N., Inze, D., Sandberg, G., Casero, P.J., Bennett, M. (2001) Auxin transport promotes *Arabidopsis* lateral root initiation. Plant Cell. **13**, 843-52.

Chauvaux, N., Child, R., John, K., Ulvskov, P., Borkhard, V., Prinsen, E., Van Onckelen, H. (1997) The role of auxin in cell separation in the dehiscence zone of oilseed rape pods J. Exp. Bot. **48,** 1423-1429.

Chen, R., Guan, C., Boonsirichai, K., Masson, P.H. (2002) Complex physiological and molecular processes underlying root gravitropism. Plant Mol. Biol. **49,** 305-17.

Chen, J., Morita, Y., Huda, M.N., Kuroda, T., Mizushima, T., Tsuchiya, T. (2002) VmrA, a member of a novel class of Na(+)-coupled multidrug efflux pumps from Vibrio parahaemolyticus. J. Bacteriol. **184,** 572-6.

Chen, R., Rosen, E., Masson, P.H. (1999) Gravitropism in higher plants. Plant Physiol. **120**, 343-50.

Chung, Y.J., Saier, M.H. (2001) SMR-type multidrug resistance pumps. Curr. Opin. Drug Discov. Devel. **4,** 237-45.

Cline, G.M., Chatfield, S.P., Leyser, O. (2001) NAA Restores Apical Dominance in the *axr3-1* Mutant of *Arabidopsis thaliana*. Annals of Botany **87,** 61-65.

Clough, S.J., Bent, A.F., (1998) Floral dip: a simplified method for *Agrobacterium*-mediated transformation of *Arabidopsis thaliana*. Plant J. **16,** 735-43.

Cohen, J.D., Bandurski, R.S., (1982) The chemistry and physiology of the bound auxins. Annual Review of Plant Physiology. **33,** 403-430.

Cregg, J. M., Lin, Cereghino, J., Shi, J., Higgins, D. R. (2000) Recombinant protein expression in *Pichia pastoris*. Mol. Biotechnol. **16,** 23-52.

Czechowski, T., Bari, R.P., Stitt, M., Scheible, W.R., Udvardi, M.K., (2004) Real-time RT-PCR profiling of over 1400 *Arabidopsis* transcription factors: unprecedented sensitivity reveals novel root- and shoot-specific genes. Plant J. **38,** 366-79.

Davis, P.J. (1995) *Plant Hormones.* Kluwer Academic Publishers, Dordrecht, The Netherlands.

Davies, J. (1994) Inactivation of antibiotics and the dissemination of resistance genes. Science **264,** 375-82.

Debeaujon, I., Peeters, A.J., Kloosterziel K.M., Koornneef, M. (2001) The TRANSPARENT TESTA12 gene of *Arabidopsis* encodes a multidrug secondary transporter-like protein required for flavonoid sequestration in vacuoles of the seed coat endothelium. Plant Cell. **13,** 853-71.

Delaney, T.P., Friedrich, L., Ryals, J.A., (1995) *Arabidopsis* signal transduction mutant defective in chemically and biologically induced disease resistance. Proc. Natl. Acad. Sci. U S A. **92,** 6602-6.

Delarue, M., Prinsen, E., Onckelen, H.V., Caboche, M., Bellini, C. (1998) Sur2 mutations of *Arabidopsis thaliana* define a new locus involved in the control of auxin homeostasis Plant J. **14,** 603-11.

Delbarre, A., Muller, P., Imhoff, V., Guern, J. (1996) Comparison of mechanisms controlling uptake and accumulation of 2,4-dichlorophenoxy acetic acid, naphthalene-1-acetic acid, and indole-3-acetic acid in suspension-cultured tobacco cells. PLANTA **198,** 532-541.

Denis, V., Cyert, M.S. (2002) Internal Ca2_release in yeast is triggered by hypertonic shock and mediated by a TRP channel homologue. J. Cell Biol. **156,** 29–34.

Dichtl, B., Stevens, A., Tollervey, D. (1997) Lithium toxicity in yeast is due to the inhibition of RNA processing enzymes.. EMBO J. **16,** 7184-95.

Diener, A.C., Gaxiola, R.A., Fink, G.R. (2001) *Arabidopsis* ALF5, a multidrug efflux transporter gene family member, confers resistance to toxins. Plant Cell. **13,** 1625-38.

Dinh, T., Paulsen, I.T., Saier, M.H. (1994) A family of extracytoplasmic proteins that allow transport of large molecules across the outer membranes of gram-negative bacteria. J. Bacteriol. **176,** 3825-31.

Dixon, D.P., Cummins, L., Cole, D.J., Edwards, R. (1998) Glutathione-mediated detoxification systems in plants. Curr. Opin. Plant Biol. **1,** 258-266.

Dolniak Blazej (2001) NIC2 – Isolation and characterisation of the second member of the NIC family from *Arabidopsis thaliana*. Master thesis. University of Wroclaw, Poland.

Dreyer, I., Poree, F., Schneider, A., Mittelstadt, J., Bertl, A., Sentenac, H., Thibaud, J., Mueller-Roeber, B. (2004) Assembly of plant Shaker-like K(out) channels requires two distinct sites of the channel alpha-subunit. B. Biophys J. **87,** 858-72.

Eckart, M.R., Bussineau, C.M. (1996) Quality and authenticity of heterologous proteins synthesized in yeast. Curr. Opin. Biotechnol. **7,** 525-30.

Friml, J., Palme, K. (2002) Polar auxin transport--old questions and new concepts? Plant Mol Biol. **49,** 273-84.

Forster, C., Kane, M. (2000) Cytosolic Ca2 Homeostasis Is a Constitutive Function of the V-ATPase in *Saccharomyces cerevisiae*. J. Biol. Chem. **275,** 38245–38253.

Fukuda, H. (1996) Xylogenesis: Initiation, Progression, and Cell Death. Annu. Rev. Plant Physiol. Plant Mol. Biol. **47,** 299-325.

Gerdes, S.Y., Scholle, M.D., Campbell, J.W., Balazsi, G., Ravasz, E., Daugherty, M.D., Somera, A.L., Kyrpides, N.C., Anderson, I., Gelfand, M.S., Bhattacharya, A., Kapatral, V., D'Souza, M., Baev, M.V., Grechkin, Y., Mseeh, F., Fonstein, M.Y., Overbeek, R., Barabasi, A.L., Oltvai, Z.N., Osterman, A.L. (2003) Experimental determination and system level analysis of essential genes in *Escherichia coli* MG1655. J. Bacteriol. **185,** 5673-84.

Gietz, R.D., Schiestl, R.H., Willems, A.R., Woods, R.A. (1995) Studies on the transformation of intact yeast cells by the LiAc/SS-DNA/PEG procedure. Yeast. **11,** 355-60

Green, L.S., Rogers, E.E. (2004) FRD3 controls iron localization in *Arabidopsis*. Plant Physiol. **136,** 2523-31.

Guilfoyle, T., Hagen, G., Ulmasov, T., Murfett, J. (1998) How does auxin turn on genes? Plant Physiol. **118,** 341-7.

Hagen, G., Guilfoyle, T. (2002) Auxin-responsive gene expression: genes, promoters and regulatory factors. Plant Mol. Biol. **49,** 373-85.

Hayashi, M., Nishimura, M. (2003) Entering a new era of research on plant peroxisomes. Curr. Opin. Plant Biol. **6,** 577-82.

He, G.X., Kuroda, T., Mima, T., Morita, Y., Mizushima, T., Tsuchiya, T. (2004) An H(+)-coupled multidrug efflux pump, PmpM, a member of the MATE family of transporters, from *Pseudomonas aeruginosa*. J. Bacteriol. **186,** 262-5.

Henderson, P.J., Hoyle, C.K., Ward, A. (2000) Expression, purification and properties of multidrug efflux proteins. Biochem. Soc. Trans. **28,** 513-7.

Higgins, C.F. (1992) ABC transporters: from micro-organisms to man. Annu. Rev. Cell Biol. 8, 67-113.

Himanen, K., Boucheron, E., Vanneste, S., de Almeida-Engler, J., Inze, D., Beeckman, T. (2002) Auxin-mediated cell cycle activation during early lateral root initiation. Plant Cell. **14,** 2339-51.

Hogue, D.L., Kerby, L., Ling, V. (1999) A mammalian lysosomal membrane protein confers multidrug resistance upon expression in *Saccharomyces cerevisiae* J. Biol. Chem. **274,** 12877-82.

Hvorup, R.N., Winnen, B., Chang, A.B., Jiang, Y., Zouh, X.F, Saier, M.H. (2003) The multidrug/oligosaccharidyl-lipid/polysaccharide (MOP) exporter superfamily Europ. J. Biochem. **270,** 799.

Huda, M.N., Morita, Y., Kuroda, T., Mizushima, T., Tsuchiya, T. (2001) Na+-driven multidrug efflux pump VcmA from *Vibrio cholerae* non-O1, a non-halophilic bacterium. FEMS Microbiol. Lett. **203,** 235-9.

Jia, Z.P., McCullough, N., Martel, R., Hemmingsen, S., Young, P.G. (1992) Gene amplification at a locus encoding a putative Na+/H+ antiporter confers sodium and lithium tolerance in fission yeast. EMBO J. **11,** 1631-40.

Jung, D.W., Bradshaw, P.C., Pfeiffer, D.R. (1997) Properties of a cyclosporin-insensitive permeability transition pore in yeast mitochondria. J. Biol. Chem. **272,** 21104-12.

Jung, D.W., Bradshaw, P.C., Litsky, M., Pfeiffer, D.R. (2004) Ca2+ transport in mitochondria from yeast expressing recombinant aequorin. Anal. Biochem. **324,** 258-68.

Kron, S.J., Gow, N.A. (1995) Budding yeast morphogenesis: signalling, cytoskeleton and cell cycle. Curr. Opin. Cell Biol. **7,** 845-55.

Laskowski, M.J., Williams, M.E., Nusbaum, H.C., Sussex, I.M. (1995) Formation of lateral root meristems is a two-stage process. Development. **121,** 3303-10.

Leyser, H.M., Pickett, F.B., Dharmasiri, S., Estelle, M. (1996) Mutations in the AXR3 gene of *Arabidopsis* result in altered auxin response including ectopic expression from the SAUR-AC1 promoter. Plant J. **10,** 403-13.

Li, L., He, Z., Pandey, G.K., Tsuchiya, T., Luan, S. (2002) Functional cloning and characterization of a plant efflux carrier for multidrug and heavy metal detoxification. J. Biol. Chem. **277,** 5360-8.

Liman, E.R., Tytgat, J., Hess, P. (1992) Subunit stoichiometry of a mammalian K+ channel determined by construction of multimeric cDNAs. Neuron **9,** 861-871.

Ljung, K., Hull, A.K., Kowalczyk, M., Marchant, A., Celenza, J., Cohen, J.D., Sandberg, G. (2002) Biosynthesis, conjugation, catabolism and homeostasis of indole-3-acetic acid in *Arabidopsis thaliana*. Plant Mol. Biol. **49,** 249-72.

Lomax, T., Muday, G., Rubery, P. (1995) Auxin transport. In: PJ Davies, Editor, Plant Hormones: Physiology, Biochemistry and Molecular Biology, Kluwer Academic Publishers, London pp. 509–530.

Ludwig-Mueller, J., Sass, S., Sutter, E.G., Wodner, M., Epstein, E. (1993) Indole-3-butyric acid in *Arabidopsis thaliana*. I. Identification and quantification. Plant Growth Regul. **13,** 179-187.

Luschnig, C., Gaxiola, R.A., Grisafi, P., Fink, GR. (1998) EIR1, a root-specific protein involved in auxin transport, is required for gravitropism in *Arabidopsis thaliana*. Genes Dev. **12,** 2175-87.

Lyndon, R. F. (1990). Plant Development, The Cellular Basis. Boston, MA:Unwin Hyman.

Ma, D., Cook, D.N., Alberti, M., Pon, N.G., Nikaido, H., Hearst, J.E. (1995) Genes acrA and acrB encode a stress-induced efflux system of *Escherichia coli*. Mol. Microbiol. **16,** 45-55.

Marchant, A., Kargul, J., May, S.T., Muller, P., Delbarre, A., Perrot-Rechenmann, C., Bennett, M.J. (1999) AUX1 regulates root gravitropism in *Arabidopsis* by facilitating auxin uptake within root apical tissues. EMBO J. **18,** 2066-73.

Martinoia, E., Klein, M., Geisler, M., Sánchez-Fernández, R., Rea, P.A. (2000) Vacuolar transport of secondary metabolites and xenobiotics. In: Robinson DG, Rogers JC (eds) Vacuolar compartments. Annual plant reviews. Academic Press, Sheffield. **5,** 221-253.

Matsumoto, T.K., Ellsmore, A.J., Cessna, S.G., Low, P.S., Pardo, J.M., Bressan, R.A., Hasegawa, P.M. (2002) An osmotically induced cytosolic Ca2+ transient activates calcineurin signaling to mediate ion homeostasis and salt tolerance of *Saccharomyces cerevisiae*. J. Biol. Chem. **277,** 33075-80.

Mattsson, J., Sung, Z.R., Berleth, T. (1999) Responses of plant vascular systems to auxin transport inhibition. Development **126,** 2979-91.

Mellerowicz, E.J., Baucher, M., Sundberg, B., Boerjan, W. (2001) Unravelling cell wall formation in the woody dicot stem. Plant Mol. Biol. **47,** 239-74.

Migliaccio, F., Piconese, S., Tronelli, G. (2000) The right-handed slanting of *Arabidopsis thaliana* roots is due to the combined effects of positive gravitropism, circumnutation and thigmotropism. J. Gravit. Physiol. **7,** 1-6.

Miseta, A., Fu, L., Kellermayer, R., Buckley, J., Bedwell, D.M. (1999) The Golgi Apparatus Plays a Significant Role in the Maintenance of Ca21 Homeostasis in the *vps33*D Vacuolar Biogenesis Mutant of *Saccharomyces cerevisiae*. J. Biol. Chem. 274, 5939–5947.

Miyamae, S., Ueda, O., Yoshimura, F., Hwang, J., Tanaka, Y., Nikaido, H. (2001) A MATE family multidrug efflux transporter pumps out fluoroquinolones in *Bacteroides thetaiotaomicron*. Antimicrob. Agents Chemother. **45,** 3341-6.

Morita, Y., Kataoka, A., Shiota, S., Mizushima, T., Tsuchiya, T. (2000) NorM of *Vibrio parahaemolyticus* is an Na(+)-driven multidrug efflux pump. J. Bacteriol. **182,** 6694-7.

Morita, Y., Kodama, K., Shiota, S., Mine, T., Kataoka, A., Mizushima, T., Tsuchiya, T. (1998) NorM, a putative multidrug efflux protein, of *Vibrio parahaemolyticus* and its homolog in *Escherichia coli*. Antimicrob. Agents Chemother. **42,** 1778-82.

Mullen, R.T. (2002) Targeting and import of matrix proteins into peroxisomes. In A Baker, I Graham, eds, Plant Peroxisomes: Biochemistry, Cell Biology and Biotechnological Applications. Kluwer Academic Publishers, Dordrecht, The Netherlands, 339–385.

Murashige, T., & Skoog, F. (1962) Physiol. Plant. **15,** 473-97.

Murphy, M.A., Phillipson, B.A., Baker, A., Mullen, R.T. (2003) Characterization of the targeting signal of the *Arabidopsis* 22-kD integral peroxisomal membrane protein. Plant Physiol. **133,** 813-28.

Murphy, A., Peer, W.A., Taiz, L. (2000) Regulation of auxin transport by aminopeptidases and endogenous flavonoids. Planta. **211,** 315-24.

Nawrath, C., Heck, S., Parinthawong, N., Metraux, J.P. (2002) EDS5, an essential component of salicylic acid-dependent signaling for disease resistance in *Arabidopsis*, is a member of the MATE transporter family. Plant Cell. **14,** 275-86.

Nawrath, C., Metraux, J.P. (1999) Salicylic acid induction-deficient mutants of *Arabidopsis* express PR-2 and PR-5 and accumulate high levels of camalexin after pathogen inoculation. Plant Cell. **11,** 1393-404.

Nieminen, K.M., Kauppinen, L., Helariutta, Y. (2004) A weed for wood? *Arabidopsis* as a genetic model for xylem development. Plant Physiol.;**135,** 653-9.

Nikaido, H. (1996) Multidrug efflux pumps of gram-negative bacteria. J Bacteriol. **178,** 5853-9.

Nikaido, H. (1989) Outer membrane barrier as a mechanism of antimicrobial resistance**.** Antimicrob Agents Chemother. **33,** 1831-6.

Nikaido, H., Vaara, M. (1985) Molecular basis of bacterial outer membrane permeability Microbiol Rev. **49,** 1-32.

Nikaido, H., Zgurskaya, H.I. (2001) AcrAB and related multidrug efflux pumps of *Escherichia coli*. J Mol. Microbiol. Biotechnol. **3,** 215-8.

Nishino, K., Yamaguchi, A. (2001) Analysis of a complete library of putative drug transporter genes in *Escherichia coli*. J. Bacteriol. **183,** 5803-12.

Normanly, J., Slovin, J.P., Cohen, J.D. (1995) Rethinking Auxin Biosynthesis and Metabolism. Plant Physiol. **107,** 323-329.

Normanly, J. (1997) Auxin Metabolism. Physiologia Plantarum **100,** 431-442.

Okada, K., Shimura, Y. (1990) Reversible root tip rotation in *Arabidopsis* seedlings induced by obstacle-touching stimulus. Science **250,** 274-276.

Östin, A., Kowalyczyk, M., Bhalerao, R., Sandberg, G. (1998). Metabolism of indole-3-acetic acid in *Arabidopsis*. Plant Physiol. **118,** 285–296.

Östin, A. (1995) Metabolism of indole-3-acetic acid in plants with emphasis on non-decarboxylative catabolism. Dissertation. Swedish University of Agricultural Sciences, Umeå

Ottenschlager, I., Wolff, P., Wolverton, C., Bhalerao, R.P., Sandberg, G., Ishikawa, H., Evans, M., Palme, K. (2003) Gravity-regulated differential auxin transport from columella to lateral root cap cells. Proc. Natl. Acad. Sci. U S A. **100,** 2987-91.

Patterson, S.E. (2001) Cutting Loose. Abscission and Dehiscence in *Arabidopsis*. Plant Physiol. **126,** 494-500.

Pao, S.S., Paulsen, I.T., Saier, M.H. (1998) Major facilitator superfamily Microbiol. Mol. Biol. Rev. **62,** 1-34.

Paulsen, I.T., Skurray, R.A., Tam, R., Saier, M.H., Turner, R.J., Weiner, J.H., Goldberg, E.B., Grinius, L.L. (1996) The SMR family: a novel family of multidrug efflux proteins involved with the efflux of lipophilic drugs. Mol. Microbiol. **19,** 1167-75

Paulsen, I.T., Brown, M.H., Skurray, R.A. (1996) Proton-dependent multidrug efflux systems. Microbiol. Rev. **60,** 575-608.

Paulsen, I.T., Lewis, K. (2002) Microbial Multidrug Efflux, Horizon Scientific Press, Norfolk.

Pellengahr Klaus (2004) Charakterisierung von ausgewählten Protein-Phospahatsen und MATE-Proteinen aus *Arabidopsis thaliana*. PhD thesis. University of Potsdam, Germany.

Poree Fabien (2004) Functional Characterisation of NIC3 a member of the MATE transporter family from *Arabidopsis thaliana* (L.) Heynh. PhD thesis. University of Potsdam, Germany.

Prior, C., Potier, S., Souciet, J.L., Sychrova, H. (1996) Characterization of the NHA1 gene encoding a Na+/H+-antiporter of the yeast *Saccharomyces cerevisiae*. FEBS Lett. **387,** 89-93.
Putman, M., van Veen, H.W., Konings, W.N. (2000) Molecular properties of bacterial multidrug transporters. Microbiol. Mol. Biol. Rev. **64,** 672-93.

Rahman, A., Amakawa, T., Goto, N., Tsurumi, S. (2001) Auxin is a positive regulator for ethylene-mediated response in the growth of *Arabidopsis* roots. Plant Cell Physiol. **42,** 301-7.

Rashotte, A.M., Poupart, J., Waddell, C.S., Muday, G.K. (2003) Transport of the two natural auxins, indole-3-butyric acid and indole-3-acetic acid, in *Arabidopsis*. Plant Physiol. **133,** 761-72.

Richards, D.E., King K.E., Ait-ali, T., Harberd, N.P. (2001) A Molecular Genetic Analysis of Gibberellin Signaling. Annu. Rev. Plant Physiol. Plant Mol. Biol. **52,** 67-88.

Rivas, R., Vizcaino, N., Buey, R.M., Mateos, P.F., Martinez-Molina, E., Velazquez, E. (2001) An effective, rapid and simple method for total RNA extraction from bacteria and yeast. J. Microbiol. Methods. **47,** 59-63.

Roberts, K., McCann, M.C. (2000) Xylogenesis: the birth of a corpse. Curr. Opin. Plant Biol. **3,** 517-22.

Roberts, J.A., Elliott, K.A., Gonzalez-Carranza, Z.H. (2002) Abscission, dehiscence, and other cell separation processes. Annu. Rev. Plant Biol. **53,** 131-58.

Rodriguez-Navarro, A., Asensio, J. (1977) An efflux mechanism determines the low net entry of lithium in yeasts. FEBS Lett. **75,** 169-72.

Rogers, E.E., Ausubel, F.M. (1997) *Arabidopsis* enhanced disease susceptibility mutants exhibit enhanced susceptibility to several bacterial pathogens and alterations in PR-1 gene expression. Plant Cell. **9,** 305-16.

Rogers, E.E., Guerinot, M.L. (2002) FRD3, a member of the multidrug and toxin efflux family, controls iron deficiency responses in *Arabidopsis*. Plant Cell. **14,** 1787-99.

Romano, C.P., Robson, P.R., Smith, H., Estelle, M., Klee, H. (1995) Transgene-mediated auxin overproduction in *Arabidopsis*: hypocotyl elongation phenotype and interactions with the hy6-1 hypocotyl elongation and axr1 auxin-resistant mutants. Plant Mol. Biol. **27,** 1071-83.

Romano, C.P., Hein, M.B., Klee, H.J. (1991) Inactivation of auxin in tobacco transformed with the indoleacetic acid-lysine synthetase gene of *Pseudomonas savastanoi*. Genes Dev. **5,** 438-46.

Ross, J.J., O'Neill, D.P., Smith, J.J., Kerckhoffs, L.H., Elliott, R.C. (2000) Evidence that auxin promotes gibberellin A1 biosynthesis in pea. Plant J. **21,** 547-52.

Rutherford, R., Masson, P.H. (1996) *Arabidopsis thaliana* sku mutant seedlings show exaggerated surface-dependent alteration in root growth vector. Plant Physiol. Aug;111(4):987-98.

Sambrook, J., Fritsch, E. F., Maniatis, T. (1989) Molecular Cloning: A Laboratory Manual, 2nd Ed., Cold Spring Harbor Laboratory, Cold Spring Harbor, NY.

Saier, M.H., Tam, R., Reizer, A., Reizer, J. (1994) Two novel families of bacterial membrane proteins concerned with nodulation, cell division and transport. Mol. Microbiol. **11,** 841-7.

Saier, M.H., Beatty, J.T., Goffeau, A., Harley, K.T., Heijne, W.H., Huang, S.C., Jack, D.L., Jahn, P.S., Lew, K., Liu, J., Pao, S.S., Paulsen, I.T., Tseng, T.T., Virk, P.S. (2000) The major facilitator superfamily. J. Mol. Microbiol. Biotechnol. **2,** 255.

Saurin, W., Dassa, E. (1994) Sequence relationships between integral inner membrane proteins of binding protein dependent transport systems: evolution by recurrent gene duplications, Protein Sci. **3,** 325–44.

Schrader, J., Baba, K., May, S.T., Palme, K., Bennett, M., Bhalerao, R.P., Sandberg, G. (2003) Polar auxin transport in the wood-forming tissues of hybrid aspen is under simultaneous control of developmental and environmental signals. Proc. Natl. Acad. Sci. U S A. **100,** 10096-101.

Shimomura, O., Johnson, F.H., Saiga, Y. (1962) Extraction, purification and properties of aequorin, a bioluminescent protein from the luminous hydromedusen, *Aequorea.* J. Cell. Comp. Physiol. **59,** 223-39.

Shiomi, N., Fukuda, H., Murata, K., Kimura, A. (1995) Improvement of S-adenosylmethionine production by integration of the ethionine-resistance gene into chromosomes of the yeast *Saccharomyces cerevisiae*. Appl. Microbiol. Biotechnol. **42,** 730-3.

Shiomi, N., Fukuda, H., Fukuda, Y., Murata, K., Kimura, A. (1991). Nucleotide sequence and characterization of a gene conferring resistance to ethionine in yeast *Saccharomyces cerevisiae*. J. Ferment. Bioeng. **71,** 211–215.

Simmons, C., Soll, D., Migliaccio, F. (1995) Circumnutation and gravitropism cause root waving in *Arabidopsis thaliana.* Journal of Experimental Botany **46,** 143–150.

Skoog, F., Miller, C.O. (1957) Chemical regulation of growth and organ formation in plant tissues cultured in vitro. Symp. Soc. Exp. Biol. **54,** 118-30.

Slovin, J., Bandurski, R., Cohen, J. (1999) Auxin. In P Hooykaas, M Hall, K Libbenga, eds, Biochemistry and Molecular Biology of Plant Hormones. **33,** 115-140.

Smalle, J., Haegman, M., Kurepa, J., Van Montagu, M., Straeten, D.V. (1997) Ethylene can stimulate *Arabidopsis* hypocotyl elongation in the light. Proc. Natl. Acad. Sci. U S A. **94,** 2756-2761.

Smith, N.A., Singh, S.P., Wang, M.B., Stoutjesdijk, P.A., Green, A.G., Waterhouse, P.M. (2000) Total silencing by intron-spliced hairpin RNAs. Nature **407,** 19-20

Stirnberg, P., Chatfield, S.P., Leyser, H.M. (1999) AXR1 acts after lateral bud formation to inhibit lateral bud growth in *Arabidopsis*. Plant Physiol. **121,** 839-47.

Swarup, R., Parry, G., Graham, N., Allen, T., Bennett, M. (2002) Auxin cross-talk: integration of signalling pathways to control plant development Plant Mol. Biol. **49,** 411-26.

Tam, Y.Y., Epstein, E., Normanly, J. (2000) Characterization of auxin conjugates in *Arabidopsis*. Low steady-state levels of indole-3-acetyl-aspartate, indole-3-acetyl-glutamate, and indole-3-acetyl-glucose. Plant Physiol. **123,** 589–595.

Tam, R., Saier, M.H. (1993) Structural, functional, and evolutionary relationships among extracellular solute-binding receptors of bacteria. Microbiol Rev. **57,** 320–46.

Trelease, R.N. (2002) Peroxisomal biogenesis and acquisition of membrane proteins. In A Baker, I Graham, eds. Plant Peroxisomes: Biochemistry, Cell Biology and Biotechnological Applications. Kluwer Academic Publishers, Dordrecht, The Netherlands, 305–337.

Tseng, T.T., Gratwick, K.S., Kollman, J., Park, D., Nies, D.H., Goffeau, A., Saier, M.H. (1999) The RND permease superfamily: an ancient, ubiquitous and diverse family that includes human disease and development proteins. J. Mol. Microbiol. Biotechnol. **1,** 107-25.

Uggla, C., Moritz, T., Sandberg, G., Sundberg, B. (1996) Auxin as a positional signal in pattern formation in plants. Proc. Natl. Acad. Sci. U S A. **93,** 9282-6.

Ulmasov, T., Liu, Z.B., Hagen, G., Guilfoyle, T.J. (1995) Composite structure of auxin response elements. Plant Cell. **7,** 1611-23.

Vivian-Smith, A., Koltunow, A.M. (1999) Genetic analysis of growth-regulator-induced parthenocarpy in *Arabidopsis*. Plant Physiol. **121,** 437-51.
Weisblum, B. (1995) Erythromycin resistance by ribosome modification. Antimicrob. Agents Chemother. **39,** 577-85.

Walz, A., Park, S., Momonoki, Y.S., Slovin, J.P., Ludwig-Mueller, J., Cohen, J.D. (2002) A gene encoding a protein modified by the phytohormone indoleacetic acid. Proc. Natl. Acad. Sci. U S A. **99**, 1718-23.

Waterhouse, P.M., Helliwell, C.A. (2003) Exploring plant genomes by RNA-induced gene silencing. Nat. Rev. Genet. **4,** 29-38.

Went, F.W., Thimann, K.V. (1937) Phytohormones, Macmillian, New York

Wickson, M., Thimann, K.V. (1958) The antagonism of auxin and kinetin in apical dominance. Physiol. Plant **11,** 62–74.

Yamamoto, M., Yamamoto, K.T. (1998) Differential effects of 1-naphthaleneacetic acid, indole-3-acetic acid and 2,4-dichlorophenoxyacetic acid on the gravitropic response of roots in an auxin-resistant mutant of *Arabidopsis*, aux1. Plant Cell Physiol. **39,** 660-4.

Yang, S., Clayton, S.R., Zechiedrich, E.L. (2003) Relative contributions of the AcrAB, MdfA and NorE efflux pumps to quinolone resistance in *Escherichia coli*. J. Antimicrob. Chemother. **51,** 545-56.

Yelin, R., Rotem, D., Schuldiner, S. (1999) EmrE, a small *Escherichia coli* multidrug transporter, protects *Saccharomyces cerevisiae* from toxins by sequestration in the vacuole. J. Bacteriol. **181,** 949-56.

Zgurskaya, H.I., Nikaido, H. (2000) Multidrug resistance mechanisms: drug efflux across two membranes. Mol. Microbiol. **37,** 219-25.

Zolman, B.K., Yoder, A., Bartel, B. (2000) Genetic analysis of indole-3-butyric acid responses in *Arabidopsis thaliana* reveals four mutant classes. Genetics **156,** 1323-37.

Zolman, B.K., Silva, I.D., Bartel, B. (2001) The *Arabidopsis* pxa1 mutant is defective in an ATP-binding cassette transporter-like protein required for peroxisomal fatty acid beta-oxidation. Plant Physiol. **127,** 1266-78.

Summary

The multidrug and toxic compounds extrusion (MATE) family includes hundreds of functionally uncharacterised proteins from bacteria and all eukaryotic kingdoms except the animal kingdom, that function as drug/toxin::Na^+or H^+ antiporters. In *Arabidopsis thaliana* the MATE family comprises 56 members, one of which is NIC2 (Novel Ion Carrier 2). Using heterologous expression systems including *Escherichia coli* and *Saccharomyces cerevisiae*, and the homologous expression system of *Arabidopsis thaliana*, the functional characterisation of *NIC2* was performed. It has been demonstrated that NIC2 confers resistance of *E. coli* towards the chemically diverse compounds such as tetraethylammonium chloride (TEACl), tetramethylammonium chloride (TMACl) and a toxic analogue of indole-3-acetic acid, 5-fluoro-indole-acetic acid (F-IAA). Therefore, NIC2 may be able to transport a broad range of drug and toxic compounds. In wild-type yeast the expression of *NIC2* increased the tolerance towards lithium and sodium, but not towards potassium and calcium. In *A. thaliana*, the overexpression of *NIC2* led to strong phenotypic changes. Under normal growth condtions overexpression caused an extremely bushy phenotype with no apical dominance but an enhanced number of lateral flowering shoots. The amount of rossette leaves and flowers with accompanying siliques were also much higher than in wild-type plants and the senescence occurred earlier in the transgenic plants. In contrast, RNA interference (RNAi) used to silence *NIC2* expression, induced early flower stalk development and flowering compared with wild-type plants. In additon, the main flower stalks were not able to grow vertically, but instead had a strong tendency to bend towards the ground. While *NIC2* RNAi seedlings produced many lateral roots outgrowing from the primary root and the root-shoot junction, *NIC2* overexpression seedlings displayed longer primary roots that were characterised by a 2 to 4 h delay in the gravitropic response. In addition, these lines exhibited an enhanced resistance to exogenously applied auxins, i.e. indole-3-acetic acid (IAA) and indole-3-butyric acid (IBA) when compared with the wild-type roots. Based on these results, it is suggested that the *NIC2* overexpression and *NIC2* RNAi phenotypes were due to decreased or increased levels of auxin, respectively. The Pro_{NIC2}*:GUS* fusion gene

revealed that *NIC2* is expressed in the stele of the elongation zone, in the lateral root cap, in new lateral root primordia, and in pericycle cells of the root system. In the vascular tissue of rosette leaves and inflorescence stems, the expression was observed in the xylem parenchyma cells, while in siliques it was also in vascular tissue, but as well in the dehiscence and abscission zones. The organ- and tissue-specific expression sites of *NIC2* correlate with the sites of auxin action in mature *Arabidopsis* plants. Further experiments using Pro$_{NIC2}$:*GUS* indicated that *NIC2* is an auxin-inducible gene. Additionally, during the gravitropic response when an endogenous auxin gradient across the root tip forms, the GUS activity pattern of the Pro$_{NIC2}$:*GUS* fusion gene markedly changed at the upper side of the root tip, while at the lower side stayed unchanged. Finally, at the subcellular level NIC2-GFP fusion protein localised in the peroxisomes of *Nicotana tabacum* BY2 protoplasts. Considering the experimental results, it is proposed that the hypothetical function of NIC2 is the efflux transport which takes part in the auxin homeostasis in plant tissues probably by removing auxin conjugates from the cytoplasm into peroxisomes.